Diss. ETH No. 21535

Identification of critical source areas for herbicide transport to surface waters

A thesis submitted to attain the degree of
DOCTOR OF SCIENCES of ETH ZURICH
(Dr. sc. ETH Zurich)

presented by
TOBIAS MICHAEL DOPPLER
Dipl. Umwelt-Natw. ETH
born 08 October 1980
citizen of Bättwil SO

accepted on the recommendation of
Prof. Dr. Paolo Burlando, examiner
Dr. Christian Stamm, co-examiner
Prof. Dr. Jan Seibert, co-examiner

2013

Contents

Summary

In areas with mainly agricultural land use, the pollution of streams with herbicides remains a problem in many countries including Switzerland. The limit of a maximum concentration of $0.1\ \mu g\, L^{-1}$ per single compound in surface waters, fixed by Swiss law, can often not be achieved during the application periods. This leads to a threat for the aquatic ecosystems. Under Swiss (climatic) conditions, the main part of the herbicide pollution stems from diffuse sources when herbicides are washed off the fields and transported to the streams. Field studies have shown that herbicide losses can be generated on a relatively small proportion of a catchment. These areas are called *critical source* or *contributing areas*. This spatial heterogeneity offers the possibility for efficient mitigation measures to reduce diffuse pollution because actions on a small proportion of the area could significantly reduce the herbicide input to the stream.

This thesis aimed at assessing and improving the predictability of critical source areas for herbicides. More specifically, the goals were to:

1. improve the process understanding of herbicide mobilization and transport at catchment scale, especially in areas with artificial drainage;

2. quantify the spatial variability of herbicide losses in an agricultural test catchment at the scale of individual fields;

3. test the predictability of critical source areas with a dynamic, spatially distributed hydrological model.

Saturation excess overland flow was a major mobilization and transport process in previous studies in the Swiss Plateau. The spatial variability of soil water regimes was therefore the main driver for the spatial heterogeneity in herbicide transport to the stream. To increase the spatial data availability, we tested how one can make use of spatial data on the soil water regime that is contained in conventional soil maps to improve the prediction of CSAs. The approach we chose was a combination of field experiment and modeling. We performed

controlled herbicide applications and sampled the stream and the drainage system at several locations to quantify spatial differences in herbicide loss behavior. Simultaneously, we monitored different hydrological variables in the experimental catchment to relate soil water regimes to the observed herbicide loads. For the prediction of critical source areas we focused on the prediction of areas prone to saturation excess overland flow. We worked with a dynamic, spatially distributed hydrological model. The model has a lumped and conceptual representation of the unsaturated zone and a spatially distributed, process based representation of the saturated zone. To validate the spatial model predictions we estimated the duration of soil saturation based on soil morphological attributes. This approach allowed a judgement of the predictive capabilities of the model.

The field experiment showed that both, infiltration excess and saturation excess overland flow, can be important processes for herbicide mobilization and transport. Under the particular weather conditions of the study period, infiltration excess dominated the losses in absolute terms. Furthermore, our results showed that in areas with little surface connectivity - that is where surface runoff from the fields can not directly enter the stream but is retained in topographic depressions - maintenance manholes of the drainage system and road and farmyard storm drains can be relevant input pathways. In addition, our results demonstrated that sorption can influence herbicide transport through macropores despite the short residence time during fast transport. Stronger sorbing compounds were retained more during preferential flow than less sorbing compounds.

The observed spatial variability of herbicide loss rates was not as large as it was expected based on the large variabilitiy of soil water regimes in the catchment, thus suggesting that the spatial variability of herbicide losses is not the same everywhere. Even more important, the ranking of the losses from the fields was not the same in all the events. This means that the location of critical source areas is not necessarily temporally stable but that it can change with rain events. Site specific management makes sense only in areas with high variability, while area-wide mitigatin measures should rather be considered in areas with little variability.

A prediction of areas prone to saturation excess overland flow is nontheless still promising because the location of these areas is assumed to be more stable in time. The quantification of the frequency of soil saturation based on soil morphological attributes compares well with piezometric measurements. These estimates can be used as an additional spatially distributed data set on soil water regimes. The quantitative estimates were used as validation data for the spatial model predictions.

However, the model results of this study were not accurate enough for the predction of CSAs caused by saturation excess overland flow. Groundwater level dynamics and the

spatial pattern of soil saturation were not correctly reproduced by the model. There are indications that a more detailed representation of the coupling between the unsatureated and the saturated zone is needed. Furthermore, the spatial resolution and the representation of the drainage system seem to be crucial for an accurate groundwater level prediction especially in drained areas. By means of such such a more complex model it might be possible to accurately predict CSAs. However, while complex models are very useful for research, they may not be useful for practical applications due to the complexity of the model setup, the excessive data requirements and the high computational demand. And finally, small scale features, such as plowing direction and the properties of field edges, which can not be reasonably implemented into models often dominate the loss behavior.

Overall, this study provides a number of arguments why the CSA concept is difficult to implement successfully in practice. The spatial variability of herbicide loss rates can be too low; in such cases area-wide mitigation measures are more promising. Furthermore, the location of CSAs can change between rain events. In addition, a certain and accurate model prediction of CSAs only based on available data does not seem to be feasable due to the high data requirements of an accurate enough model and the uncertainty associated with its predictions.

Nevertheless, the extent of the results allows to derive a few recommendations for the reduction of diffuse pollution. Reductions can be achieved

1. by limiting the occurrece of infiltration excess overland flow by means of erosion control measures which are well established in agriculture.

2. by preventing overland flow from directly entering the stream or a shortcut to the stream (manholes, stormdrains). Land management should aim, for instance, at a soil path for all water before it enters the stream.

3. by site specific management, meaning that critical source areas are taken out of crop rotation or planted with less intensive crops. In this case the identification of critical source areas requires field visits by experts and communication with the local farmers. In this respect one can take advantage of maps that can help to identify potential risk zones, among which the most important are i) an erosion risk map, ii) a drainage map (including manhole and storm drain locations), iii) a map of surface connectivity, iv) a soil map (possibly with soil saturation duration estimates), and v) a map of the topographic wetness index.

Zusammenfassung

In Regionen mit mehrheitlich landwirtschaftlicher Landnutzung ist die Verschmutzung von Fliessgewässern mit Herbiziden auch in der Schweiz nach wie vor ein Problem. In den Applikationsperioden wird die gesetzlich festgelegte Maximalkonzentration von 0.1 μg L^{-1} pro Substanz häufig überschritten. Dies führt zu einer Gefährdung der aquatischen Ökosysteme.

Unter schweizer Bedingungen stammt die Gewässerbelastung mit Herbiziden hauptsächlich aus diffusen Quellen; d.h. die Herbizide werden während Regenereignissen von den Feldern weggewaschen und ins Gewässer transportiert. Frühere Felduntersuchungen haben gezeigt, dass der Grossteil der Herbizidbelastung von einem relativ kleinen Teil des Einzugsgebiets stammen kann. Diese Flächen werden *beitragende Flächen* oder *critical source areas* genannt. Diese räumliche Heterogenität ermöglicht effiziente Schutzmassnahmen, da Eingriffe auf einem kleinen Teil der Fläche die Herbizidbelastung im Gewässer signifikant reduzieren können.

Das Ziel dieser Arbeit war es die Vorhersagbarkeit von beitragenden Flächen zu beurteilen und zu verbessern. Die drei Hauptziele waren dabei:

1. die Prozesse bei der Mobilisierung und beim Transport von Herbiziden besser zu verstehen, speziell in künstlich entwässerten Gebieten;

2. die räumliche Variabilität der Herbizidverluste in einem Test-Gebiet auf Feld-Skala zu quantifizieren;

3. die Vorhersagbarkeit von beitragenden Flächen mit einem dynamischen, räumlich verteilten hydrologischen Modell zu testen.

In früheren Feldstudien im Schweizer Mittelland war Sättigungs-Oberflächenabfluss der wichtigste Mobilisierungs- und Transportprozess für Herbizide. Die räumliche Variabilität des Bodenwasserhaushalts war deshalb ein Hauptfaktor um die räumliche Verteilung des Herbizidtransports ins Fliessgewässer zu erklären. Konventionelle Bodenkarten enthalten Informationen zum Bodenwasserhaushalt. Wir haben untersucht inwiefern man diese

Information nutzen kann um die Verfügbarkeit räumlicher Daten zur Vorhersage von bei-
tragenden Flächen zu verbessern. Dazu haben wir eine Kombination aus Feldexperiment
und Modellstudie gewählt. In einem kleinen Einzugsgebiet wurden kontrolliert Herbizide
ausgebracht. Danach wurden an mehreren Stellen im Bach und im Drainagensystem Pro-
ben genommen um die räumlichen Unterschiede im Herbizidtransport zu quantifizieren.
Gleichzeitig wurden verschiedene hydrologische Grössen gemessen um den Bodenwasser-
Haushalt mit den beobachteten Herbizidverlusten in Beziehung zu setzen. Bei der Vor-
hersage von beitragenden Flächen haben wir uns auf die Vorhersage von Flächen konzen-
triet die zu Sättigungs-Oberflächenabfluss neigen. Wir arbeiteten mit einem dynamischen,
räumlich verteilten hydrologischen Modell. Die ungesättigte Zone wurde im Modell kon-
zeptuell und räumlich aggregiert dargestellt während die gesättige Zone räumlich verteilt
und prozessbasiert abgebildet wurde. Die räumlichen Modellvorhersagen wurden an, aus
der Bodenkarte geschätzten, Bodensättigungsdauern validiert.

Das Feldexperiment hat gezeigt, dass beide Mechanismen, Infiltrationsüberschuss- und
Sättigungs - Oberflächenabfluss, wichtige Mobilisierungs- und Transportprozesse für Her-
bizide sein können. Unter den Wetterbedingungen in der Studienperiode wurden die Herbi-
zidverluste von Infiltrationsüberschuss - Oberflächenabfluss dominiert. Ausserdem hat die
Feldstudie gezeigt, dass Schächte des Draingagensystems und Strassen- und Hofplatzent-
wässerungen wichtige Eintragswege sein können. Dies trifft insbesondere in Gebieten mit
geringer Oberflächenkonnektivität zu, d.h. in Regionen wo Oberflächenabfluss nicht direkt
ins Gewässer gelangt, sondern in topographischen Senken zurückgehalten wird. Die Resul-
tate zeigen ausserdem, dass das Sorptionsverhalten der Herbizide deren Transport durch
Makroporen beeinflusst. Trotz der kurzen Aufenthaltszeit während dem Transport durch
Makroporen wurden stärker sorbierende Substanzen stärker zurückgehalten als schwächer
sorbierende Substanzen.

Die beobachtete räumliche Variabilität der Herbizidverlustraten war deutlich geringer als
sie aufgrund der Heterogenität des Bodenwasserhaushalts erwartet wurde. Offensichtlich
ist die räumliche Variabilität der Herbizidverluste nicht in allen Regionen gleich gross.
Ausserdem waren die Felder mit den höchsten Verlustraten nicht in allen Regenereignis-
sen die gleichen; die Reihenfolge änderte sich mit den Regenereignissen. Das heisst, dass
die Lage von beitragenden Flächen zeitlich nicht konstant sein muss. Eine an den Standort
angepasste Bewirtschaftung zur Reduktion der Herbizidbelastung ist nur in Regonen mit
grosser räumlicher Variabiltät und zeitlich stabilen räumlichen Mustern sinnvoll. In Regio-
nen mit geringer Variabilität bieten sich eher Flächendeckende Massnahmen zur Reduktion
der Herbizidbelastung an.

Die Schätzungen der Bodensättigungsdauern aus der Bodenkarte stimmen gut mit den Pie-

zometermessungen überein. Diese Schätzungen wurden - als zusätzliche räumliche Daten zum Bodenwasserhaushalt - zur Modellvalidierung verwendet.

Die Modellresultate dieser Studie waren allerdings nicht exakt genug für die Vorhersage von beitragenden Flächen, die durch Sättigungs - Oberflächenabfluss verursacht werden. Die Dynamik der Grundwasserstände und deren räumliche Verteilung wurden vom Modell nicht korrekt wiedergegeben. Die Resultate deuten darauf hin, dass eine detailiertere Abbildung der Prozesse am Übergang zwischen der gesättigten und der ungesättigten Zone notwendig ist. Auch eine feine räumliche Auflösung sowie die Art der Implementierung der Draingen scheinen wichtig zu sein für eine exakte Prognose der Grundwasserstände. Mit solch einem komplexeren Modell könnte es möglich sein beitragende Flächen verlässlich vorherzusagen. Allerdings sind komplexe Modelle - die für die Forschung zweifellos wichtig sind - nicht unbedingt nützlich für praktische Anwendungen. Dies liegt am Aufwand solche Modelle aufzusetzten, am grossen Datenbedarf und an der benötigten Rechenleistung. Aussedem können kleinskalige Details wie die Pflugrichtung oder die Beschaffenheit von Feldrändern, die nicht vernünftig modelliert werden können, das Herbizidtransportverhalten dominieren.

Insgesamt zeigt diese Studie eine Reihe von Gründen auf weshalb es schwierig ist das Konzept der beitragenden Flächen für Herbizidtransport in Oberflächengewässer in der Praxis anzuwenden. Einerseits kann die räumliche Variabilität so klein sein, dass eher flächendeckende Massnahmen sinnvoll erscheinen. Andererseits kann sich die Lage der beitragenden Flächen von Regenereignis zu Regenereignis verschieben. Eine sichere und exakte Modellvorhersage für beitragende Flächen, die nur auf vorhandenen Daten basiert, scheint ausserdem nicht realistisch. Dies liegt am hohen Datenbedarf und den Unsicherheiten die mit der Modellvorhersage verbunden sind.

Aus den Resultaten dieser Studie können trotzdem Empfehlungen zur Reduktion der Gewässerbelastung mit Herbiziden abgleitet werden. Die wichtigsten Empfehlungen sind:

1. Das Aufteten von Infiltrationsüberschuss-Oberflächenabfluss sollte durch Erosionsschutzmassnahmen vermindert werden.

2. Die Bewirtschaftung sollte darauf abzielen, dass Oberflächenabfluss nicht direkt ins Gewässer oder einen Kurzschluss zum Gewässer (Unterhaltsschächte, Strassenentwässerung) gelangt sonderen eine Bodenpassage durchmacht bevor er ins Gewässer gelangt.

3. In Situationen wo standortspezifische Bewirtschaftung sinnvoll ist, sollten beitragende Flächen weniger intensiv bewirtschaftet werden. Für eine verlässliche Identifizierung der beitragenden Flächen sind Feldbegehungen durch Experten sowie Gespräche

mit den Landwirten der Region notwendig. Karten können helfen potentielle beitragende Flächen zu identifizieren. Die wichtigsten Karten in diesem Zusammenhang sind i) eine Erosionsrisikokarte, ii) eine Drainagenkarte (mit Unterhaltschächten und Strassenentwässerung), iii) eine Karte der Oberflächekonnektivität, iv) eine Bodenkarte (falls möglich mit Schätzungen der Bodensättigungsdauern), und v) eine Karte des topographischen Bodenfeuchte-Index.

Chapter 1

Introduction

Surface waters in basins with strong anthropogenic controls are exposed to a wide variety of anthropogenic compounds with effects on the aquatic ecosystems that are only partially known and understood. In areas of predominant agricultural land use, the pollution of streams with pesticides is one of the major threats for the aquatic ecosystem. Pesticides are widely used in modern agriculture to increase crop productivity by controlling unwanted species and pests. Herbicides belong to the pesticide class with the highest consumption rates and they are found in concentrations that might harm aquatic organisms (Chèvre et al., 2006). The concentrations of herbicides in surface waters mainly follow the application pattern with concentration peaks in spring and autumn, which are the main application periods (Larson et al., 1995; Leu et al., 2005; Thurman et al., 1991; Wittmer, 2010). Because of the potential damage to aquatic ecosystems, the Swiss law on water protection prescribes a maximum concentration of 0.1 $\mu g\,L^{-1}$ per single compound in surface waters (GschV , 2005). During the application periods for herbicides, this limit can often not be achieved (Munz et al., 2012). This leads to a threat for the aquatic ecosystems. Measures to efficiently reduce the input of herbicides into surface waters are therefore needed.

1.1   Why to focus on critical source areas

1.1.1   Sources and input pathways of herbicides

The sources of herbicides from agricultural use can be divided into point and diffuse sources. Point sources can be spills from filling and cleaning the spraying equipment, which enter the stream via the storm sewer system or are deliberately disposed left-overs entering the streams via waste water treatment plants (Müller et al., 2002; Wittmer et al., 2010).

Diffuse sources include inputs via spray drift during application and those originating from the treated fields. Point sources can be controlled rather well with good management practice and new equipment (Gerecke et al., 2002). A comprehensive study in a Swiss watershed revealed in the 1990s that about 15% of the total agricultural herbicide load could be attributed to point sources (Gerecke et al., 2002) while the main part stems from diffuse sources which are much less controllable. There is no indication that the relevance of diffuse herbicide pollution has diminished since that study (Munz et al., 2012).

1.1.2 Critical source areas

The contributions of different parts of a catchment to the overall diffuse pollution in the stream can vary significantly. Several case studies have shown that diffuse herbicide losses from different fields or subcatchments within a catchment can differ by more than an order of magnitude (Gomides Freitas et al., 2008; Leu et al., 2004b; Louchart et al., 2001). This implies that a relatively small proportion of a catchment can cause the major part of surface water pollution with herbicides. If such especially critical areas can be reliably identified this offers the possibility for efficient mitigation measures to reduce diffuse pollution because actions on a small proportion of the area can significantly reduce the herbicide input to the stream. The same has been observed for diffuse pollution of surface waters with phosphorus (Pionke et al., 1996, 2000). A useful concept to identify these especially critical areas comes from the research on phosphorus pollution. The areas that contribute a large fraction of the pollution load are called critical source areas (CSAs) or contributing areas (Pionke et al., 1996). An area has to fulfil three conditions to be a critical source area:

1. It needs to be a substance source, i.e. the areas where herbicides are applied.

2. It has to be hydrologically active, i.e. the relevant mobilization and transport processes occur in the area.

3. It has to be connected to the stream thus implying that the water with the mobilized herbicides has to reach the stream without relevant retention processes.

1.1.3 Aim of the study

Based on the above argumentation it would be beneficial to have a tool to identify critical source areas for diffuse surface water pollution with herbicides. Once identified they could be managed differently (e.g. planted with less herbicide intensive crops or even take out

of crop rotation). This would reduce the herbicide input to the stream without the need to take actions in the whole catchment. Should a prediction of CSAs serve as basis for pollution mitigation measures, it has to fulfill several criteria. It has to be reliable and its uncertainties have to be assessable. It should only be based on available information and it has to be applicable to larger areas while the scale of the prediction should be in the order of 10 × 10 m (the scale at which land management can be adapted under typical Swiss conditions). The need for efficient pollution mitigation measures and the requirements that come with a potential practical application lead to the following research question which is addressed in this thesis:

How can critical source areas for herbicides in the Swiss Plateau be predicted solely based on available information and how reliable are such predictions?

In the following, the state of the art in the related research fields is presented, research gaps are identified and finally the chosen approach is introduced.

1.2   Background

1.2.1   Herbicide mobilization and transport

Diffuse herbicide losses from the treated fields mainly occur during rain events when herbicides are washed off and transported to the stream (Larson et al., 1995; Leu et al., 2005; Thurman et al., 1991). The major transport pathways are overland flow that directly enters the stream and preferential flow to the drainage system (Brown and van Beinum, 2009; Leu et al., 2004a, 2010). The pathway through groundwater feeding baseflow is of little importance for most pesticides because of sorption and degradation (Thurman et al., 1991). Saturation excess overland flow usually dominates in humid climate and in well vegetated catchments (Anderson and Burt, 1978; Dunne and Black, 1970; Moore et al., 1976). Infiltration excess overland flow is rather the dominant process in arid and semiarid climate (e.g. Goodrich et al., 1997). Previous studies have demonstrated the relevance of saturation excess overland flow for herbicide transport under conditions prevailing in the Swiss Plateau (Leu et al., 2004a). Preferential flow carrying significant amounts of pesticides to tile drains is closely linked to the occurrence of surface runoff, because preferential flow requires the lateral flow of water to the preferential flow paths (Flühler et al., 1996; Weiler and Naef, 2003). Furthermore, preferential flow paths may intercept surface runoff and direct it towards tile drains (Stamm et al., 2002). Usually concentrations in tile drains are lower than concentrations in overland flow (Brown and van Beinum, 2009).

Herbicide fate and transport are well understood in laboratory and plot scale systems (Müller et al., 2002). However, the transport to real streams always occurs in a catchment where different processes can be relevant than in plot scale studies. The spatial arrangement of fields can play an important role and features like field roads and field edges can strongly influence the flow paths. Only few comprehensive field studies exist at catchment scale that allow a quantification of the spatial variability of pesticide loss behaviour (Gomides Freitas et al., 2008; Leu et al., 2004b). Also the transport of herbicides through subsurface drainage systems is not well understood at catchment scale. This is in contrast to the significance of drained soils for agriculture in Switzerland. About 30% of the crop production area in Switzerland is artificially drained (Béguin and Smola, 2010). Often these areas are flat and have productive soils after drainage. Therefore, they are subject to intensive agriculture.

1.2.2   Prediction of critical source areas

Basically there are two strategies to identify CSAs. They can be identified in the field or predicted with a model that captures the dominant features of the underlying mechanisms. The identification in the field is rather time consuming; it requires extensive field visits by experts and interviews with the local farmers. Such an approach is e.g. implemented in France with the CORPEN system (Groupe diagnostic du CORPEN, 1996). The basic steps of the CSA identification in this system (as described in Reichenberger et al. (2008)) are:

1. Identification of the basic soiltypes and geology.

2. Hydrological characterisation at plot scale in autumn or winter (no soil moisture deficit).

3. Categorisation of likely transfers of pesticides to surface water at the landscape level.

A model prediction can have advantages over the field identification with respect to the consistency of the CSA identification in a larger area and time demand. If CSAs should be predicted in different environments where different processes are relevant (e.g. with / without drainage, varying topography and soil characteristics) then a reliable spatial prediction requires a thorough process understanding at the desired scale. Several studies have been carried out to predict CSAs for different substances (nutrients, pesticides and sediment) on field and catchment scale (e.g. Agnew et al., 2006; Heathwaite et al., 2005; Lyon et al., 2006; Srinivasan and McDowell, 2009) with a variety of different modeling approaches (see Borah and Bera, 2003, for a review on model concepts).

If one assumes the herbicide application patterns to be known then the main part of the prediction models are spatially distributed hydrological models. The models need to predict i) where the relevant mobilization processes occur and ii) if and how the substances are transported to the stream. Process oriented models have the advantage that they are better transferable to other regions (where different mechanisms can be important) than models that rely on empirical relationships. Process based models were found to be more suitable for CSA prediction by Srinivasan and McDowell (2009).

A major problem with the prediction of CSAs is the lack of spatial calibration and validation data. Spatially distributed measurements of hydrological state variables or even herbicide input to the stream are costly and can not be carried out everywhere. Therefore, spatially distributed hydrological models are often calibrated on discharge time series at specific locations. The lack of spatial data renders the application of distributed models difficult. It has been known to hydrologists since a while that without spatial data the model parameters and even the model structure are only poorly identifiable (Grayson et al., 1992a,b). Since that time a lot of progress has been made with respect to the use of spatial data in distributed hydrological models (Grayson et al., 2002). Indeed it was shown that some model parameters can be constrained much better if spatial data was used in addition to stream discharge (e.g. Blazkova et al., 2002; Freer et al., 2004). However, the general lack of available spatial data sets to calibrate and / or validate models that predict CSAs has remained (Easton et al., 2008; Frey et al., 2011; Srinivasan and McDowell, 2009). For the prediction of CSAs this is critical since the prediciton goal is the location where certain hydrological processes occur. Especially if management decisions should be based on predicted CSAs a meaningful model calibraion and validation is warranted.

1.2.3 Soil maps as spatial data sets on soil hydrology

Conventional soil maps contain spatial information on soil hydrology. If this spatial hydrological information can be made usable for hydrological modeling, this would add an important spatial data set for model calibration and testing. The rationale behind this approach is that the presence of groundwater influences soil morphological features that are related to changing oxygen availability due to permanent water logging or fluctuating groundwater levels. These hydromorphic features are usually related to redox reactions and transport of iron and manganese (see e.g. Terribile et al., 2011). Accordingly, soil morphology as described in soil maps contains information on the soil water regime. Several studies have shown a relationship between soil morphology (especially soil matrix color and the presence and type of iron mottles) and the frequency of soil saturation (Franzmeier et al., 1983; Jacobs et al., 2002; Morgan and Stolt, 2006; Simonson and Boersma, 1972).

However, a translation of soil morphology into soil saturation frequencies is not straight-forward. Soil morphology does not necessarily reflect the current water regime, especially when the water regime has recently changed because of artificial drainage. According to Hayes and Vepraskas (2000), soil drainage can alter morphology within decades. In addition, it is possible that the morphological signs of wetness do not evolve in a certain soil, even though the same water regime persists since a longer time. A possibility for this is soil saturation without oxygen depletion (e.g. frequent but short periods of saturation), which does not lead to morphological changes (Evans and Franzmeier, 1986; Pickering and Veneman, 1984). Therefore, a spatial data set on the frequency of soil saturation estimated from soil maps remains uncertain to some degree. However, usually there are no spatial data on the soil water regime at all, so an uncertain data set can be considered as an improvement, especially if the uncertainty can be quantified. To our knowledge these morphological features have not yet been used as quantitative spatial proxies of state variables in order to calibrate and / or validate spatially distributed models.

1.3   Scope of this work

The main research gaps identified in the section above are:

1. The lack of process understanding with respect to herbicide mobilization from field soil to overland flow and transport pathways at catchment scale, especially in catchments with artificial drainage where the water with dissolved herbicides can either enter the stram as overland flow or as preferential flow to tile drains.

2. The lack of field data sets on the spatial variability of diffuse herbicide losses to surface waters at the scale of individual fields.

3. The possibilitiy to use soil morphology information as spatial proxy for the soil water regime which could then be used as validation data for spatially distributed hydrological models has not been explored so far.

The following goals were defined to approach the research gaps mentioned above:

1. To increase the understanding of how herbicides are mobilized and transported to the stream at catchment scale with a special focus on transport through subsurface drainage systems. Such a process understanding is crucial for predictions of CSAs because it shows which are the contolling processes that determine the spatial pattern of herbicide losses to the stream. These processes have to be understood to be implemented in a prediction model.

2. To provide a data set on the spatial variability of herbicide losses at field scale to assess the usefulnes of the critical source area concept for diffuse herbicide pollution in surface waters. Such data sets are rare and they are needed to validate model predictions.

3. To test the predictability of CSAs with a spatially distributed model. The prediction test should show if, at the current state of research and data availability, models can be used to support management decisions. In this context, it should be explored how soil morphology data can be used to estimate soil saturation durations and how such a data set can be used for model validation.

1.4 Approach

The approach we chose to address these goals was a combination of field experiment and modeling.

1.4.1 Field experiment

For the field experiment we chose a small catchment with, for Swiss conditions, intensive agricultural use. About 40% of the agricultural land in the catchment are artificially drained and the soils in the catchment have differing water regimes. This allowed us to investigate herbicide transport through subsurface drainage systems and to assess the influence of different soil water regimes. The quantification of spatial differences of herbicide input to the stream is not possible with conventional monitoring data because the different fields are usually not sprayed at the same day with the same substances. Therefore different weather conditions after application and different substance properties would strongly influence the results and prevent a meaningful spatial interpretation. To quantify spatial differences, we performed controlled applications (same substances applied on the same day to different fields) and sampled the stream and the drainage system at several locations. We monitored different hydrological variables in the experimental catchment to relate soil water regimes to the observed herbicide loads.

The results of the field experiment are described in chapters 2 and 3. Chapter 2 focuses on the insights gained with regard to herbicide mobilization and transport processes and pathways. Chapter 3 is about the spatial patterns of herbicide losses that were observed in the field experiment and how these spatial patterns relate to field characteristics.

1.4.2   Modeling

For the prediction of critical source areas we focused on the prediction of areas that are often saturated to the surface because of high groundwater levels and are therefore prone to saturation excess overland flow. In areas with only crop production, saturation excess areas do not strongly depend on the land management (in contrast to infiltration excess areas) since they are more influenced by their topographic position and hydrological subsoil properties (Frey et al., 2009; Gerits et al., 1990; Lyon et al., 2006). For a prediction of saturated areas caused by high groundwater levels, the shape and postition of the groundwater table has to be accurately represented in the model. Lateral flow in the saturated zone is therefore an important process to be modeled. Instead of using surface topography as proxy for the groundwater level gradients, the gradients should be calculated explicitly in the prediction model, especially for situations with artificial drainage. This should result in more realistic predictions of the location of saturated areas (Grabs et al., 2009).

If pollution mitigation measures should be based on model predictions an uncertainty analysis of the predction, which requires tenthousends of model runs, is needed. With this background, coputational speed was an important factor in model development. The model which was developed in this study was optimized for computational speed and mainly relies on generally available data. A compromise had to be found between model complexity and spatial resolution on the one hand and computational speed on the other hand. The prediction model that was used has a lumped and conceptual representation of the unsaturated zone and a spatially distributed, process based representation of the saturated zone. For the saturated zone we chose an approach similar to HillVI (Weiler and McDonnell, 2004) where the groundwater level gradients are calculated in each time step and do not rely on surface topography. We additionally implemented the lateral and preferential flow to tile drains. The model was then simultaneously calibrated to discharge at the outlet of the catchment and groundwater levels in eleven groundwater wells.

In addition, this thesis presents an approach to enlarge the spatial data for model calibration and testing by making use of soil morphology information contained in conventional soil maps that exist for many locations. It shows how soil morphology information can be used to derive estimates of the average duration of soil saturation at a given depth. This data set was used to validate the spatial prediciton of the model. This approach allows a judgment of the predictive capabilities of such a model.

The results of the model based CSA prediction and how they relate to the soil map estimate of saturation duration are reported in chapter 4.

Chapter 2

Spatial variability of herbicide mobilisation and transport at catchment scale: insights from a field experiment

Tobias Doppler, Louise Camenzuli, Guido Hirzel, Martin Krauss,
Alfred Lück, and Christian Stamm

T. Dopplers contribution to this chapter: Planing, setup and maintenance of the field experiment including the hydrological measurements, the planing of the herbicide application and the soil and water sampling; GIS analysis; data processing and interpretation; writing.

2.1   Introduction

In modern agriculture, a wide variety of pesticides[1] is used to increase crop productivity. Pesticides encompass a broad range of chemicals. They are used to control weeds, to fight plant diseases, insects, arachnids and other pests. Pesticides can enter the water system, where they can harm aquatic organisms even in low concentrations. Small streams in catchments with intensive crop production are especially at risk (Liess and Schulz, 1999), as diffuse pollution from agricultural fields causes major inputs to the stream in these areas (Leu et al., 2010). Pesticides mainly enter surface waters during rain events, when they are mobilised and transported with fast runoff (Thurman et al., 1991). Under Swiss conditions, the two most important input pathways in this context are overland flow and, when subsurface drains are present, preferential flow to the drainage system. The pathway to groundwater and exfiltration into streams as baseflow is of little importance for most pesticides due to sorption and degradation (e.g. Thurman et al., 1991).

In several cases it has been shown that herbicide loss rates (relative to the applied amount) from different fields within a given catchment can differ by over an order of magnitude (Gomides Freitas et al., 2008; Leu et al., 2004b, 2005; Louchart et al., 2001). This implies that a relatively small proportion of a catchment can cause the major part of surface water pollution with herbicides. The same has been observed for diffuse pollution of surface waters with phosphorus (Pionke et al., 1996, 2000). These observations did not surprise hydrologists. It was recognized in the 1960s and 1970s that not all areas contribute to storm runoff (Betson, 1964; Dunne and Black, 1970) and that diffuse pollution should be expected from only a limited fraction of a catchment (Freeze, 1974). The areas that contribute a large fraction of the pollution load are called critical source areas (CSAs) or contributing areas (Pionke et al., 1996).

The insight that not all parts of a catchment have the same relevance for diffuse pollution offers efficient mitigation options, because actions on a small proportion of the area can strongly reduce the substance input to the stream. An area has to fulfil three conditions to become a critical source area: (1) The area needs to be a substance source, e.g. the areas where pesticides are applied. (2) The area has to be hydrologically active, i.e. the relevant mobilisation and transport processes occur in the area. For pesticides, these are overland flow and/or macropore flow. (3) The area has to be connected to the stream; for pesticides this implies that the overland flow or macropore flow with the mobilised pesticides has to reach the stream either directly or via the drainage system.

---

[1]We use the term pesticides when we refer to the full range of chemicals encompassing all plant protection agents (herbicides, fungicides, insecticides, etc.). The term herbicides is used when we specifically refer to herbicides.

The spatial extent of the CSAs (A_{CSA}) can be interpreted as the spatial intersection of the areas of a catchment where each condition is fulfilled:

$$A_{\mathrm{CSA}} = A_{\mathrm{source}} \cap A_{\mathrm{active}} \cap A_{\mathrm{connect}} \tag{2.1}$$

with A_{source} representing the source area of a given compound, A_{active} the hydrologically active area, and A_{connect} the part of the catchment in direct connection to the stream network. For pesticides, A_{source} depends on the pesticide applications and is not a property of the field per se. Every crop production field is a potential source area even though the pesticide applications change with crop rotation. However, the compound properties can modify A_{source} in space and time. Degradation and sorption both determine the amount of substance that is available for transport at the time of rainfall (Louchart et al., 2001). If there was substantial spatial variability in degradation rates and/or sorption of pesticides to soil, these properties may affect the spatial CSA distribution. Earlier studies in the Swiss Plateau (Leu et al., 2004b; Stamm et al., 2004) indicate, however, that degradation rates and sorption coefficients do not vary strongly between fields in a catchment and could not account for observed spatial differences in herbicide loss rates. Under these conditions, and under the assumption that the areas of pesticide application are known, the CSA delineation is reduced to a hydrological problem involving the prediction of A_{active} and A_{connect}.

For pesticide transport, the relevant flow components are fast flow like surface runoff and preferential flow to tile drains. Hence, A_{active} is determined by the spatial extent of areas where these processes are generated in relevant amounts. Two different processes can lead to overland flow. Horton (1933) described the occurrence of infiltration excess overland flow, where rain intensity exceeds the infiltration capacity of the soil. In contrast, saturation excess overland flow occurs when the soil is saturated from below until the water table reaches the surface (Dunne and Black, 1970). Saturation excess overland flow usually dominates in humid climate and in well vegetated catchments (Anderson and Burt, 1978; Dunne and Black, 1970; Moore et al., 1976). Consequently, saturation excess overland flow appears to dominate phosphorus transport to surface waters in agricultural areas in humid climates (Easton et al., 2008; Lyon et al., 2006). Infiltration excess overland flow is rather the dominant process in arid and semiarid climate (e.g. Goodrich et al., 1997). However, not all studies show a clear spatial separation of these two processes. Descroix et al. (2007) for example found that saturation excess overland flow can also be important in semiarid climate, while infiltration excess overland flow also occurs in more humid climates. The simultaneous occurrence of infiltration excess and saturation excess overland flow was also observed in field experiments e.g. by Srinivasan et al. (2002). Preferential flow carrying significant amounts of pesticides to tile drains is closely linked to the occurrence of

surface runoff, because preferential flow requires the lateral flow of water to the preferential flow paths (Flühler et al., 1996; Weiler and Naef, 2003). Furthermore, preferential flow paths may intercept surface runoff and direct it towards tile drains (Stamm et al., 2002). Preferential flow can also be fed by subsurface lateral flow and therefore occur without overland flow (e.g. Jarvis, 2007). However, the lateral flow towards the preferential flow paths requires high pesticide concentrations to result in significant pesticide transport. Therefore it needs to be initiated close to the surface where soil concentrations are high. We focus here on macropore flow that is fed by surface runoff. Therefore, the two runoff-generating mechanisms (infiltration excess and saturation excess) are also relevant for the input of pesticides into surface waters via preferential flow to tile drains.

Even though the chemical properties of the pesticides may not affect the spatial pattern of losses, they are important in determining the pesticide mobilisation and transport behaviour. While the pesticide half life in soil determines the amount of pesticide that is present in soil at the time of rainfall (e.g. Louchart et al., 2001), the sorption behaviour can affect both mobilisation and transport. For many pesticides it has been shown that sorption equilibrium is only reached after weeks or months and therefore kinetic sorption has to be considered (see e.g. Vereecken et al., 2011, for a recent review of pesticide sorption studies). Several field studies have shown that sorption strength influences pesticide losses to streams and tile drains, leading to lower loss rates and lower peak concentrations for substances with stronger sorption (Brown and van Beinum, 2009; Gomides Freitas et al., 2008; Leu et al., 2004a; Louchart et al., 2001). Simulation models for catchment-scale pesticide transport usually assume equilibrium between sorbed and dissolved pesticide in soil. For example SWAT describes the mobilisation of pesticides into mobile water as follows:

$$m_{\mathrm{rel}} = \exp\left(\frac{-1}{\theta_{\mathrm{sat}} + K_{\mathrm{d}} \times \rho} \times \frac{q_{\mathrm{mobile}}}{z}\right) \tag{2.2}$$

where m_{rel} [–] is the amount of mobilised pesticide relative to the initial amount, q_{mobile} [mm] is the flux of mobile water per time-step, θ_{sat} [–] is the volumetric water content at saturation, K_{d} [l kg^{-1}] is the distribution coefficient, ρ [g cm^{-3}] is soil bulk density and z [mm] is the depth of the soil layer (Neitsch et al., 2005).

For A_{connect}, the focus is on the connectivity of fast flow processes that are relevant for pesticide transport. In the analysis of overland flow connectivity, natural and anthropogenic depressions within a catchment are of major importance since they can retain large amounts of overland flow, which are prevented from reaching the stream (Barron et al., 2011; Frey et al., 2009; Kiesel et al., 2010). In addition to the depressions, man-made networks have a large influence on connectivity. Subsurface pipe networks (tile drains, road drainage etc.) can increase connectivity immensely. Areas outside the topographic catchment can also contribute as a result (Noll and Magee, 2009). Roads can act as

barriers for overland flow or alternatively concentrate flow (Carluer and De Marsily, 2004; Payraudeau et al., 2009) and direct it to the stream via road drainage (e.g. Ledermann et al., 2010). Other small linear features such as tramlines and field edges may influence flow directions and therefore also connectivity substantially (e.g. Aurousseau et al., 2009; Heathwaite et al., 2005). Many of these spatial processes are subject to regional differences. They depend on climate and agricultural land management practices but also on general structural properties of agricultural catchments (field sizes, proportion of drained area, length and type of road network etc.).

A reliable spatial prediction of CSAs is necessary if site specific mitigation measures should be implemented in practice. However, a sound prediction requires a detailed understanding of the governing processes and their interactions. Such an understanding can be gained in field studies and field experiments at catchment scale, where the interplay of processes can be observed. There are only few comprehensive field data sets available for validating spatial predictions of herbicide losses within agricultural catchments (Gomides Freitas et al., 2008; Leu et al., 2004a,b). In these studies, the herbicide input into the catchments and the output through the stream were controlled and monitored. This setup does not allow investigation of individual processes occurring along the transport pathway from the field to the stream. Furthermore, only limited data on the catchment hydrology were collected, and all studies were carried out in the same region southeast of Zürich (Greifensee) in a small number of test catchments. The goal of this study was to improve the understanding of the process chain causing herbicide transport from the fields of application to streams, including:

1. Understanding the link between hydrological processes and herbicide mobilisation at catchment scale. Based on the knowledge from earlier studies (Gomides Freitas et al., 2008; Leu et al., 2004a,b), we expected that saturation excess overland flow would be the main mobilisation and transport process under the climatic conditions of the Swiss plateau. Accordingly, soil hydrology and connectivity were expected to be the drivers for herbicide transport.

2. Understanding the influence of the herbicide's chemical properties on mobilisation and transport. The expectations were that sorption plays an important role during the mobilisation of herbicides from soil to overland flow, while it should not affect transport once the substance is mobilised.

3. Understanding connectivity in a situation where a large part of the stream system is subsurface. We expected that only areas that are directly connected to the stream and drained areas can contribute to the herbicide load in the stream.

The understanding of the concentration dynamics in the stream requires the understanding of all three abovementioned topics and their interactions. The paper is structured as follows: In the results and discussion sections we first present the hydrologic results, then we show how chemical properties influenced mobilisation and transport of the herbicides and finally we report on the concentration dynamics in the stream.

2.2   Materials and methods

2.2.1   Site description

The study catchment is located in the northeast of Switzerland (see Fig. 2.1). The catchment area is $1.2 \, \text{km}^2$, topography is moderate with altitudes ranging from 423 to $477 \, \text{m}$ a.s.l. and an average slope of $4.3°$ ($\text{min} = 0°$, $\text{max} = 42°$, based on $2 \times 2 \, \text{m}$ digital elevation model (DEM), absolute accuracy: $\sigma = 0.5 \, \text{m}$, resolution $= 1 \, \text{cm}$, Swisstopo, 2003). The twenty-year mean annual precipitation at the closest permanent measurement station (Schaffhausen, $11 \, \text{km}$ north of the catchment) is $883 \, \text{mm}$ (Meteoschweiz, 2009). The soils developed on moraine material with a thickness of around ten metres, which is underlain with Süßwassermolasse (freshwater molasse) (Swisstopo, 2007). Soils in the centre of the catchment are poorly drained gleysoils. Well drained cambisols and eroded regosols are located in the higher parts of the catchment (FAL, 1997, see Fig. 2.1). Soil thickness (surface to C horizon) varies between $30 \, \text{cm}$ at the eroded locations and more than $2 \, \text{m}$ in the depressions and near the stream. The catchment is heavily modified by human activities; it encompasses a road network with a total length of $11.5 \, \text{km}$ (approximately $3 \, \text{km}$ are paved and drained, the rest is unpaved and not drained). The dominant land use is crop production ($75 \, \%$ of the area), mainly corn, sugar beet, winter wheat and rape seed. Around $13 \, \%$ of the catchment is covered by forest, and a small settlement area is located in the southeast of the catchment. Three farms lie at least partly within the catchment (see Fig. 2.1). $47 \, \%$ of the agricultural land is drained by tile drains with a total length of over $21 \, \text{km}$ (Gemeinde Ossingen, 1995, the open stream has a length of $550 \, \text{m}$). The stream system consists of two branches, an open ditch that was partly built as recipient for the drainage water and the main branch of the stream that runs in a culvert (see Fig. 2.1). The stream also receives the runoff from two main roads and from two farmyards (Gemeinde Ossingen, 2008). The paved area that drains into the catchment is approximately $15\,000 \, \text{m}^2$ ($1.2 \, \%$ of the area).
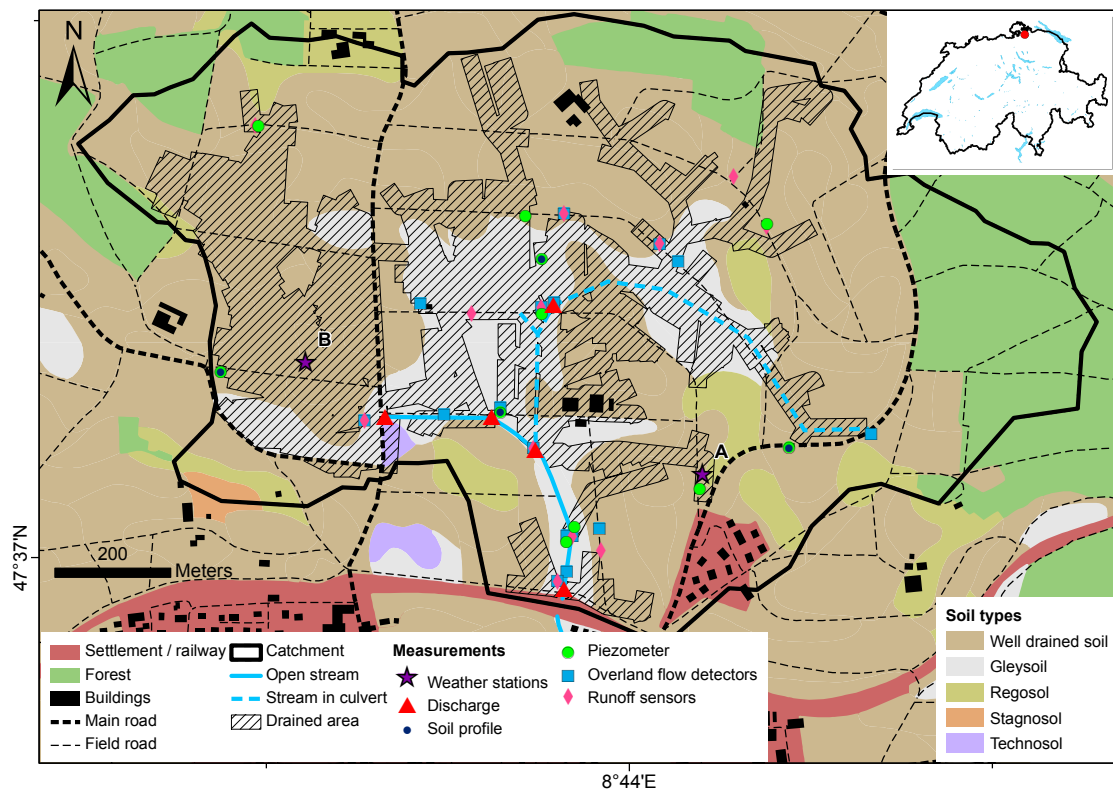
Figure 2.1: The experimental catchment with soil types, land use and the hydrological measurement locations. Cambisols and luvisols were combined to the category of well drained soils. The small map in the top right corner depicts the location of the study site within Switzerland. Sources: FAL (1997); Gemeinde Ossingen (1995); Swisstopo (2008).

2.2.2 Hydrological measurements

Several hydrological variables were monitored in the catchment from summer 2008 to autumn 2009. Not all measurements cover the whole time period. However, during the experimental period from February 2009 to October 2009 all measurements depicted in Fig. 2.1 were running.

Discharge and electrical conductivity of stream and drainage water

We measured discharge at five locations in the catchment. At four sites (O_d, O_u, S_d, S_u, see Fig. 2.2), water level and flow velocity were measured using a Doppler probe and a pressure transducer (ISCO 750 area velocity flow module, Teledyne Inc., Los Angeles, CA, USA). Discharge was calculated using the exact cross section of these sites. At the fifth site (O_m, Fig. 2.2), discharge was determined by measuring the water level at a V-notch weir with a pressure transducer (Keller PR-46X, KELLER AG für Druckmesstechnik, Winterthur,

CH) and using a rating curve of the form $Q = \alpha \times (h - \beta)^\gamma$, where h is the water level and α, β and γ are parameters (Herschy, 1995). The curve was fitted to 15 data points obtained by dilution experiments with NaCl (6 data points, CS547 Conductivity and Temperature Probe, Campbell Scientific, Inc., Loughborough, UK) and bucket measurements (9 data points). Discharge data from all stations were stored at 5 min intervals, either by the data logger of the sampler (ISCO 6700, ISCO 6712, Teledyne Inc., Los Angeles, CA, USA), or by an external data logger (CR10X, Campbell Scientific, Inc., Loughborough, UK). Runoff ratios were calculated for individual events by dividing the event discharge sum by the rain depth of the event. Figure 2.3 shows the time intervals used for the discharge sums.
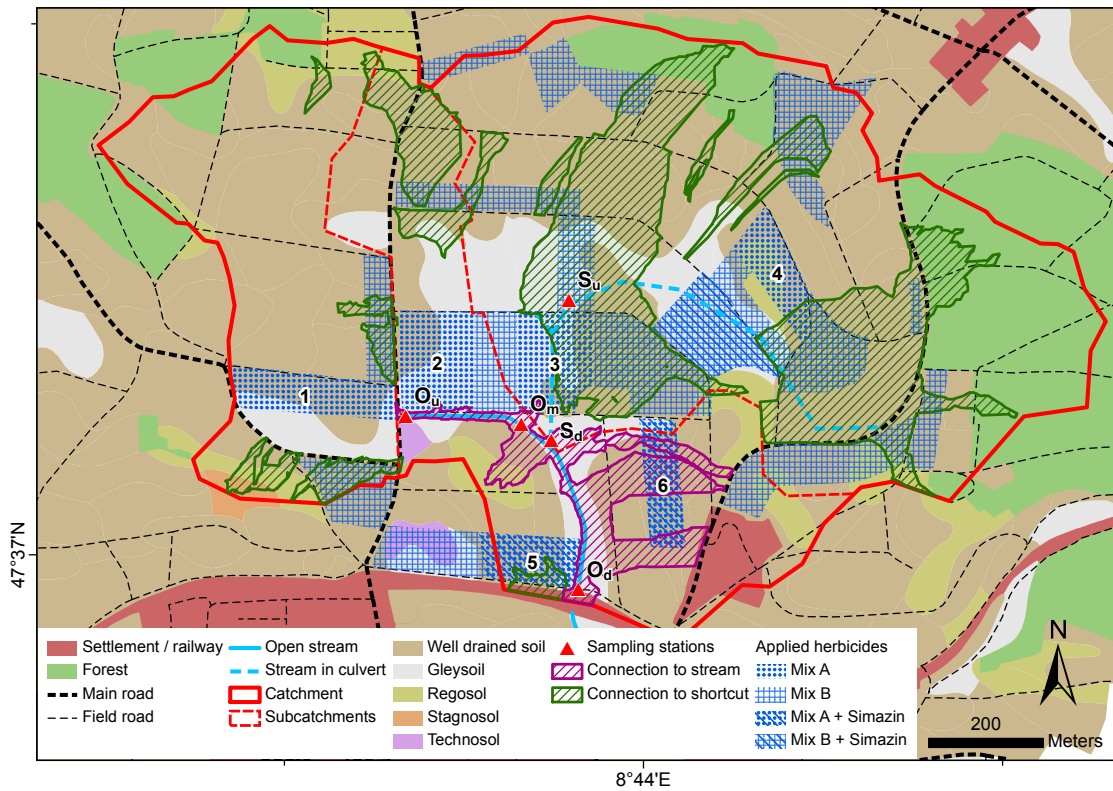
Figure 2.2: Experimental setup with the six experimental fields (1 to 6, Mix A = atrazine, S-metolachlor and sulcotrione), the alternative fields (Mix B = terbuthylazine and mesotrione) and the five sampling locations: S_u and S_d (subsurface upstream and downstream) and O_u, O_m and O_d (open upstream, middle and downstream). The subcatchments of the sampling stations O_u and S_d are displayed. The area with a direct surface connection to the stream is shown together with the areas connected to manholes and storm drains (only connected areas $>1000\,\mathrm{m}^2$ are shown, see Sect. 2.3.1). Sources: FAL (1997); Swisstopo (2008).

At four discharge measurement stations (O_d, O_m, O_u, S_d, Fig. 2.2), we also obtained electrical conductivity data at 5 min intervals (STS DL/N, STS Sensor Technik Sirnach

AG, Sirnach, CH, and CS547 Conductivity and Temperature Probe, Campbell Scientific, Inc., Loughborough, UK).

Weather stations

At weather station A (see Fig. 2.1) precipitation was measured at 15 min resolution with a tipping bucket rain gauge (R102, Campbell Scientific, Inc., Loughborough, UK). This rain gauge was out of order for 22 days (4 June 2009 to 25 June 2009). During this time, rain data from weather station B (see Fig. 2.1) were used (a mobile HP 100 Station run by Agroscope ART with a tipping bucket rain gauge: HP 100, Lufft GmbH, Fellbach, Germany). For two of the major rain events in the experimental period (events E2 and E9 in Table 2.1), rain data from both rain gauges are available.

Piezometers

We installed 11 piezometers to monitor groundwater levels at 15 min intervals (STS DL/N, STS Sensor Technik Sirnach AG, Sirnach, CH, and Keller DCX-22, KELLER AG für Druckmesstechnik, Winterthur, CH). The installation depth varied between 1.5 and 2.7 m below the surface.
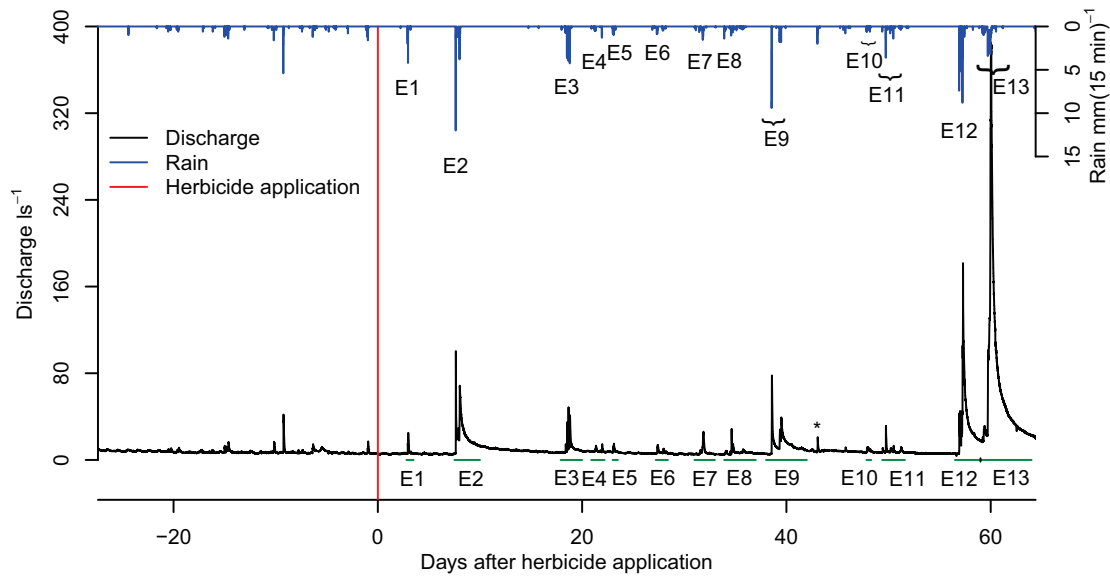
Figure 2.3: Rainfall and discharge at the outlet of the catchment (station O_d) prior to and after the controlled herbicide application (19 May 2009). The event numbers refer to the events described in Table 2.1. The green lines indicate the duration of discharge used for runoff ratio calculation. *: event with <5 mm rain.

Soil moisture

TDR probes and tensiometers were installed in four soil profiles to measure soil water content and suction pressure at four depths between 0.1 and 1.1 m below the surface. The exact depths at the different locations were selected according to the soil horizons. Two TDR probes (TDR100, Campbell Scientific, Inc., Loughborough, UK, and two rod probes) and three tensiometers (ceramic cups: High Flow Porous Ceramic Cup $653 \times 1B1M3$ 1 bar, Soil Moisture Equipment, Goleta, CA, USA; pressure transducers: 26 PCCFA3D, Honeywell, Minneapolis, MN, USA) were installed at each depth. All soil profile data were stored at hourly intervals in a data logger (CR10X, Campbell Scientific, Inc., Loughborough, UK).

Overland flow and erosion

Two different devices were used to detect overland flow:

1. The runoff sensor is an electronic device based on the idea by Srinivasan et al. (2000). It detects overland flow by electric contacts on a small V-notch weir and stores the data in a data logger. This system delivers time-resolved occurrence of overland flow.

2. The overland flow detector is a simple collection bottle similar to the device described by Kirkby et al. (1976). If it collects water during a rain event, this indicates that overland flow occurred.

A total of twelve runoff sensors and 16 overland flow detectors were installed at 21 locations (seven locations were equipped with both instruments, see Fig. 2.1). During and after some of the events, signs of overland flow (E2, E9, E13), ponding (E2, E9, E12, E13) and erosion (E2, E9, E12, E13) were mapped (see Fig. 2.4). The mapping was carried out on an ad-hoc basis by different people and without systematic coverage of the entire catchment. Nevertheless, it complements the information on the spatial extent of overland flow and erosion from the point measurements of the runoff sensors and overland flow detectors, and therefore adds important spatial information.

In addition to registering the locations of overland flow, we also analysed the chemical composition of overland flow samples. We used the samples taken by the overland flow detectors and additionally collected grab samples of overland flow at several locations during events E2 and E9. We measured herbicide concentrations in these samples (see Sect. 2.2.5). In the samples from the overland flow detectors, we also determined electrical conductivity (STS DL/N, STS Sensor Technik Sirnach AG, Sirnach, CH).

Table 2.1: Characteristics of the 13 rain events with the number of locations where overland flow (OF) was observed (results from runoff sensors and overland flow detectors), the number of overland flow samples, the average electrical conductivity (EC) in the overland flow samples and the number of piezometers that had maximum water levels (WL) less than 30 cm below the surface during the event.

Event	Rain depth mm	Max rain intensity mm $(15\,\mathrm{min})^{-1}$	Runoff ratio %	Locations with OF (out of 21)	Samples OF	Mean EC $\mu\,\mathrm{S\,cm}^{-1}$	Piezometers with WL $< 0.3\,\mathrm{m}$
E1	9.8	4.2	6	1	0	–	0/10
E2	45.6	12.0	11	8	7	565*	2/10
E3	22.2	4.2	10	9	6	187	1/10
E4	7.8	1.3	13	1	0	–	0/10
E5	5.6	1.0	8	2	0	–	0/10
E6	9.6	0.8	9	4	0	–	0/10
E7	18.2	1.6	9	7	3	183	0/10
E8	14.6	1.4	12	7	4	206	0/10
E9	36.8	9.4	12	11	8	209	3/10
E10	6.4	0.6	4	5	0	–	0/9
E11	15.2	3.6	7	8	3	192	0/9
E12	51.6	8.8	12	15	12	167	4/9
E13	57	3.4	41	17	14	409	7/9

* Fertilizer applied at the day of the event.

2.2.3   Herbicide application

On 19 May 2009 we performed a controlled herbicide application on corn fields in the catchment. The fields were divided into two groups. Six of the corn fields were selected as experimental fields (labelled 1 to 6 in Fig. 2.2), where we had full control over the application. All experimental fields were sprayed on the same day with the same spraying device. The rest of the corn fields in the catchment (alternative fields) received a different herbicide mixture. Not all of the alternative fields could be sprayed on the same day with the same spraying device. The herbicides atrazine (CAS no.: 1912-24-9), S-metolachlor (87392-12-9), sulcotrione (99105-77-8) and simazine (122-34-9) (see Table 2.2) were applied on the six experimental fields in two different mixtures. The experimental fields 1 to 4 received Mix A (atrazine $800\,\mathrm{g\,ha}^{-1}$, S-metolachlor $960\,\mathrm{g\,ha}^{-1}$ and sulcotrione $450\,\mathrm{g\,ha}^{-1}$) while fields 5 and 6 were sprayed with Mix A and simazine ($200\,\mathrm{g\,ha}^{-1}$, see Fig. 2.2). The alternative fields were sprayed with a mixture of terbuthylazine (5915-41-3, $495\,\mathrm{g\,ha}^{-1}$)
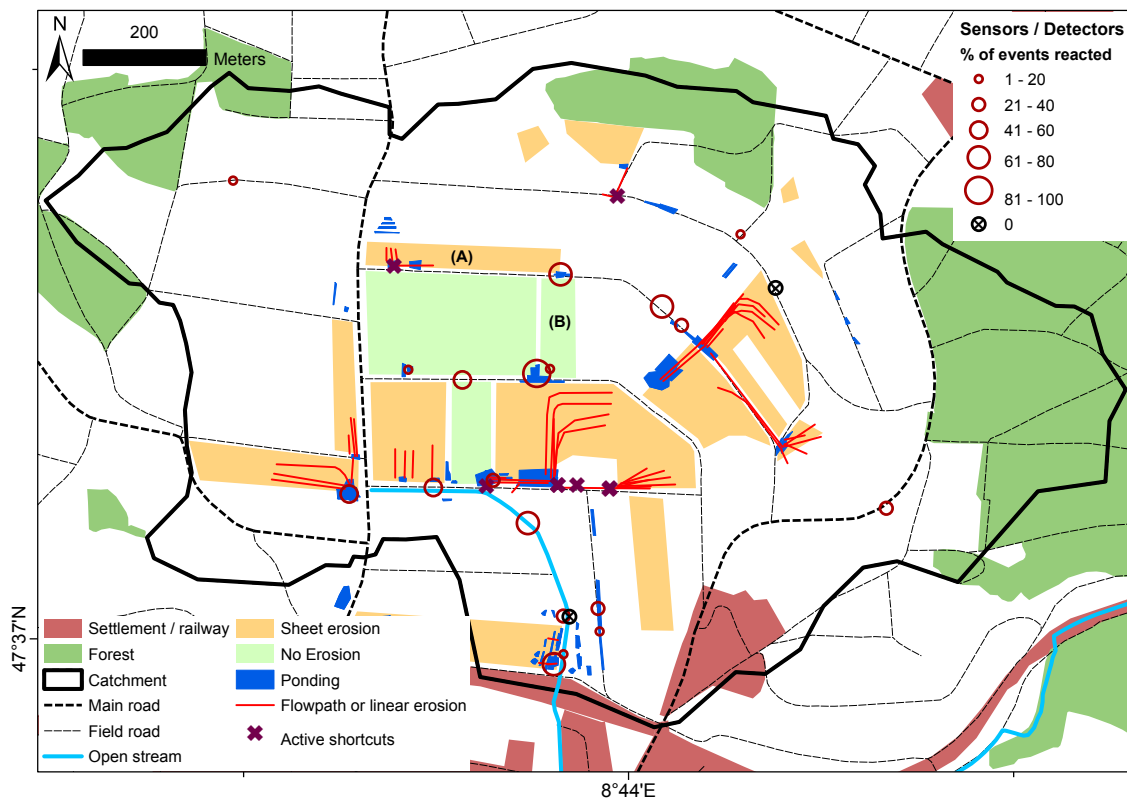
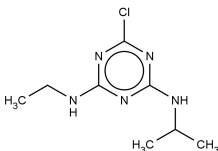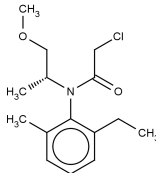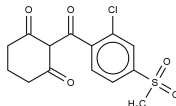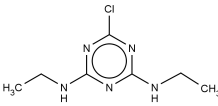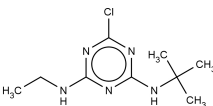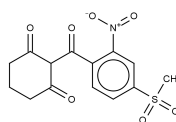**Figure 2.4:** Erosion mapping (sheet and linear erosion) for four events (E2, E9, E12, E13), direct observation of overland flow paths (E2, E9, E13) and ponding (E2, E9, E12, E13) and results from runoff sensors and overland flow detectors showing the percentage of events in which overland flow occurred. (A) and (B) are two corn fields discussed in Sect. 2.3.1. White areas were either unobserved, or no erosion or overland flow were observed (see text). Fields marked "No Erosion" were surveyed but did not show signs of erosion. Source: Swisstopo (2008).

and mesotrione (104206-82-8, $105 \, \mathrm{g \, ha^{-1}}$) (Mix B in Fig. 2.2). None of these substances was used elsewhere in the catchment. Moreover, we recorded the substance amounts and application dates of all the alternative fields.

To ensure the correct dose and concentration in the spray solution, the experimental herbicides were weighed exactly before being mixed in the spraying tank. Samples from each tank filling were taken and analysed. The exact amount of spray solution applied on each field was determined by a flow meter mounted on the spraying equipment. A calibrated scale bar on the spraying tank was also used to estimate the applied volume per field in addition to the flow meter. The extent of the sprayed area was marked with wooden sticks; their exact location was determined by a differential GPS (Leica GPS1200, Leica Geosystems AG, Heerbrugg, Switzerland). Owing to these control measures, the exact areas and applied rates are known for each field and each substance.

Table 2.2: The molecular structures of the applied substances with their sorption coefficient to organic carbon (K_{oc}) and their half life in field soil (DT$_{50}$). All data taken from PPDB (2010).

	Atrazine	S-Metolachlor	Sulcotrione
K_{oc} ($l\,kg^{-1}$)	89 to 513	110 to 339	17 to 58
DT$_{50}$ (d)	6 to 108	11 to 31	1 to 11
	Simazine	Terbuthylazine	Mesotrione
K_{oc} ($l\,kg^{-1}$)	128 to 138	151 to 333	19 to 141
DT$_{50}$ (d)	27 to 102	10 to 36	3 to 7

2.2.4 Water sampling

Water samples from stream and tile drains were taken at the five discharge measurement stations prior to the herbicide application and during two months after application. These five locations were sampled at high temporal resolution during the 13 rain events that occurred during the experimental period. The sampling strategy was as in Wittmer et al. (2010). Time-proportional samples were taken by automatic water samplers equipped with 24 polypropylene bottles (ISCO 2900, 6700, 6712, Teledyne Inc., Los Angeles, CA, USA). The samplers were triggered when a predefined water level was exceeded. During the first six hours of an event, time-proportional 15-min composite samples (three aliquots every 5 min) were taken. Afterwards, the sampling frequency was reduced to one composite sample per hour (four aliquots every 15 min). This sampling strategy yielded enough samples for short events, and lasted long enough (max. 30 h) to restart the samplers during large events. Grab samples were taken during base flow periods.

To keep the number of samples in a feasible range for subsequent analysis in the lab, the samples were selected in a two-step procedure. First, they were pre-selected in the field to cover the entire hydrograph of the event. A total of 1500 samples was brought to the lab in 250 ml glass bottles and stored at 4 °C. Every other sample was additionally stored at −20 °C (150 ml in a 250 ml glass bottle). Out of the total of 1500 samples, six hundred were selected for analysis in a step-by-step procedure. First, the seven events with the

highest rain amounts were selected for analysis (events E1, E2, E3, E7, E9, E12, E13 in Table 2.1, see also Fig. 2.3) and a few samples per event were analysed (beginning, peak, recession). Finally, we selected further samples to adequately represent the dynamics of the chemograph.

2.2.5   Analysis of water samples

Sorption of the analytes to the bottles in the automatic water samplers was investigated previously and sorption was found to be negligible. Stability of the analytes was investigated over a period of four months at $4\,°C$. No degradation was observed during the first two months of storage. However, sulcotrione and mesotrione showed slight degradation after two months in unfiltered samples; therefore, data for these two analytes are only reported from samples stored at $-20\,°C$ after this time (two months).

Analysis of the herbicides was performed according to Singer et al. (2010). The samples were filtered through glass-fibre filters (GF/F, $0.7\,\mu m$, Whatman) and isotope-labelled internal standards for all compounds were spiked to $50\,ml$ of filtered sample. The samples were analysed by online solid-phase extraction (SPE) coupled to liquid chromatography followed by a triple quadrupole mass spectrometer (LC-MS/MS). Sample enrichment was achieved on a Strata-X extraction cartridge ($20 \times 2.1\,mm$ I.D. $33\,\mu m$ particle size, Phenomenex, Brechbühler AG, Schlieren, Switzerland). LC separation was performed on a XBridge C18 column ($50\,mm \times 2$, Waters, Baden-Dättwil, Switzerland), and detection by a TSQ Quantum triple quadrupole MS (Thermo, San Jose, CA, USA). The limit of detection (LOD) was in the range of 2 to $10\,ng\,l^{-1}$ for all compounds. Quality control consisted of aliquots of spiked and un-spiked environmental samples analysed with each analytical run. The resulting inter-day precision of the method was 5 to $12\,\%$ for the six compounds. The average accuracy for each analyte was between 101 and $105\,\%$.

2.2.6   Soil sampling and sample preparation

From each of the six experimental fields (see Fig. 2.2), we took topsoil samples at seven dates: before herbicide application, directly after application and on days 3, 7, 15, 30 and 60 after application. Every one of these soil samples consisted of 20 subsamples taken randomly across the field. The 20 subsamples were mixed and combined to one topsoil sample to represent the whole field. A stainless steel probe with $5.4\,cm$ diameter was used for soil sampling, the samples were taken from 0 to $5\,cm$ depth. The samples were stored in a polypropylene box tightly sealed with a lid.

After sampling, all soil samples were stored at $-20\,°C$. Prior to analysis, all soil samples were crushed with a hammer mill and kept frozen by adding dry ice. After milling, the soils were left outside for twelve hours with open lids to eliminate the CO_2 added during milling. The soil samples were then stored at $-20\,°C$ until further analysis.

2.2.7 Soil extraction and analytics

Herbicide concentrations were measured in all soil samples using two different extraction methods. For the total soil concentration we used pressurized liquid extraction (PLE). The concentration in the centrifugation solution (see below) was used as a proxy for the porewater concentration.

Total soil concentration

The herbicides were extracted by PLE using an ASE 350 Accelerated Solvent Extractor (Dionex, Sunnyvale, CA, USA). Extraction took place with a solvent mixture of acetone: $1\,\%$ phosphoric acid, 70:30 (volume ratio) at $100\,°C$. The PLE extract was stored at $-20\,°C$. The clean-up of the PLE extract was done in four main steps after addition of an internal standard solution. (1) The acetone was removed by rotary evaporation at $35\,°C$. (2) HPLC grade water, $3.9\,g$ of acetonitrile, $1.6\,g$ of anhydrous magnesium sulfate and $0.3\,g$ of ammonium chloride were added to the remaining extract for the liquid-liquid extraction. The tube was shaken for about $2\,min$ and centrifuged for $4\,min$ at $500 \times g$ (Ultrafuge Filtron, Heraeus) to separate the acetonitrile phase. (3) The acetonitrile phase was reduced to a volume of $500\,\mu l$ under a nitrogen stream; $500\,\mu l$ of methanol were then added. (4) The solution was filtered with a syringe through a $0.2\,\mu m$ PTFE filter and stored at $4\,°C$ until quantification.

Pore water

In order to extract pore water from dry soil samples ($<80\,\%$ of the water holding capacity, WHC), the water content of these samples was adjusted to $80\,\%$ of the WHC by adding the appropriate volume of water. The WHC is the amount of water a soil can retain against gravity. The WHC was determined for two soil samples per field as follows. Approximately $2\,cm$ of glass wool were packed into the bottom of a glass tube containing a porous glass frit at the bottom, followed by a weighed amount of wet soil. The soil was then saturated from the bottom by placing the glass tube in a beaker filled with water for $24\,h$. The glass tubes were then taken out of the beaker and placed on a dry surface to drain for $4\,h$;

they were covered with a beaker to prevent evaporation. The water content at the end of the 4 h was used as WHC, and the average value of the two soils from each field was used for all samples from the respective field. To obtain the pore water sample, a weighed amount of approximately 3 g of thawed soil sample (with the added water if necessary, see above) was placed into a centrifuge filter tube with a $0.45\,\mu$m PTFE membrane (Ultrafree-CL, Millipore). The centrifuge tubes were then stored at 4 °C for roughly 24 h to obtain an apparent equilibrium between the pore water and the solid phase. The samples were centrifuged for 20 min at $2000 \times$ g. After centrifugation, the internal standard mixture was added to the collected pore water and the solution was stored at 4 °C until quantification.

Quantification

Analysis of the extracts was done with liquid chromatography coupled to a triple quadrupole mass spectrometer (LC-MS/MS). Compounds were separated by reversed-phase LC using a Synergi C18 polar RP column (100×3 mm ID, $2.5\,\mu$m particle size, equipped with an inline-filter, Phenomenex, Torrance, CA, USA) and detected by a TSQ Quantum triple quadrupole MS (Thermo, San Jose, CA, USA).

Half life calculation

We calculated the herbicides' half lives in soil based on the total soil concentrations (corresponding to the concentration measured with PLE) with first-order kinetics. Dissipation of sulcotrione on all fields and of atrazine and S-metolachlor on some fields slowed down after day 30. For these cases only concentration data until day 30 were used for the calculation of the half lives, while for the other cases all data points (until day 60) were used.

Distribution coefficients

The distribution of the herbicides between the dissolved and the sorbed phase was expressed by the apparent distribution coefficient K_d [l kg^{-1}] in all soil samples:

$$K_\mathrm{d} = \frac{C_\mathrm{sorbed}}{C_\mathrm{porewater}} = \frac{C_\mathrm{PLE} - C_\mathrm{PWfraction}}{C_\mathrm{porewater}} \tag{2.3}$$

C_PLE [ng kg^{-1}] is the concentration obtained by PLE expressed per mass of dry soil, $C_\mathrm{PWfraction}$ [ng kg^{-1}] is the pore water concentration expressed per mass of dry soil, and $C_\mathrm{porewater}$ [ng l^{-1}] is the measured pore water concentration in the water phase. A more detailed description of soil extraction and analysis is given in Camenzuli (2010).

2.2.8   Mobilisation coefficient

A mobilisation coefficient M was used to compare the mobilisation of different herbicides from soil to overland flow. The coefficient M is defined as the ratio of overland flow concentration to total soil concentration (PLE concentration). We only used overland flow samples where the origin of the water could be attributed to one single experimental field.

2.2.9   Retention coefficient

We define a retention coefficient R to describe the effect of sorption on herbicide transport from ponding overland flow to tile drains. R is the ratio of overland flow concentration on a given field to the concentration in the tile drain of that field at the corresponding time. For event E2 (Fig. 2.3), we calculated retention coefficients for all the experimental substances on experimental field 1 (Fig. 2.2). Two samples of ponding overland flow on field 1 were available, one at the beginning of the event and one at the end. These samples were used for calculating R together with the two samples from station O_u that were taken briefly after sampling the overland flow.

2.2.10   GIS analysis

Catchment delineation

The catchment boundary was calculated in ArcGIS (ESRI, ArcGIS Desktop, 9.3.1) based on the $2 \times 2\,\mathrm{m}$ DEM (Swisstopo, 2003) and manually adapted after field observations. The topographical catchment does not coincide completely with the subsurface catchment. In some areas that belong to the topographical catchment, the tile drains divert the water outside of the catchment. These areas were excluded. In contrast, the settlement area in the southeast was kept in the catchment, even though the water from sealed areas in the settlement leaves the catchment. The subcatchments of the discharge and sampling stations were delineated based on topography and the detailed tile drain map (Gemeinde Ossingen, 1995; Swisstopo, 2003). Subcatchments calculated from surface topography were not always congruent with the tile drain subcatchments. Priority was given to the tile drain catchments.

Drained area

The drained area shown in Fig. 2.1 was calculated as a buffer of 15 m around the drainage pipes. This area does not correspond to the actual catchment of the drainage pipes, but was used to calculate the drained area percentage of the whole catchment and to visualize the drained area.

Connectivity analysis

The original 2×2 m DEM (Swisstopo, 2003) was used for the analysis of surface connectivity. Firstly, very small or shallow depressions were removed, as these can either be artifacts in the DEM or too shallow to trap significant amounts of overland flow. Depressions consisting of one or two cells and those with a maximum depth of less than 5 cm were filled. Secondly, the cells in the open stream were incised to the depth of the average water level. Depression analysis and filling as well as stream incision were performed in TAS (TAS geographical information system version 2.0.9, John Lindsey 2005). Based on this corrected DEM, flow directions and flow accumulation were calculated in ArcGIS (ESRI, ArcGIS Desktop, 9.3.1). The lowest stream channel cell was used as pour point for the catchment calculation to determine the area connected directly to the stream on the surface. For the determination of areas connected to manholes of the drainage system or to storm drains for road and farmyard runoff, the locations of these features were used as pour points for the catchment calculation (Gemeinde Ossingen, 1995, 2008). One farmyard storm drain was manually shifted to a cell with higher flow accumulation, because the flow accumulation raster was affected by the farm buildings in this area.

2.3   Results

2.3.1   Rainfall and hydrological processes

The period before the herbicide application was rather dry, with 66 mm of rain in the 50 days before application. There was no significant discharge event in this period (Fig. 2.3). Afterwards, the weather conditions changed: From 19 May 2009 to 21 July 2009, thirteen rain events of more than 5 mm were recorded. Five of them had more than 20 mm of rain, and a total of 333 mm rainfall was measured in this period (see Fig. 2.3 and Table 2.1). Four of the five largest events (E2, E3, E9, E12, E13) were thunderstorms with rather high rain intensities and short duration; only event E13 was a longer lasting, low intensity rain event (see Fig. 2.3 and Table 2.1). Runoff ratios were between 4 and 13 % for events E1

to E12. Event E13 had a runoff ratio of more than 40 %, indicating that this event had a different runoff regime than the other events in the experimental period.

Human modification has a strong influence on the catchment hydrology. The largest part of the stream network is subsurface and tile drains provided most of the discharge. Even though the catchment has a large storage capacity due to the artificial drainage and therefore reacts slowly (low runoff ratios in most of the events, see Table 2.1), the hydrograph at some of the measurement stations showed very pronounced discharge peaks, because road and farmyard runoff is directly connected to the drainage system and the stream (see Figs. 2.5 and 2.6).
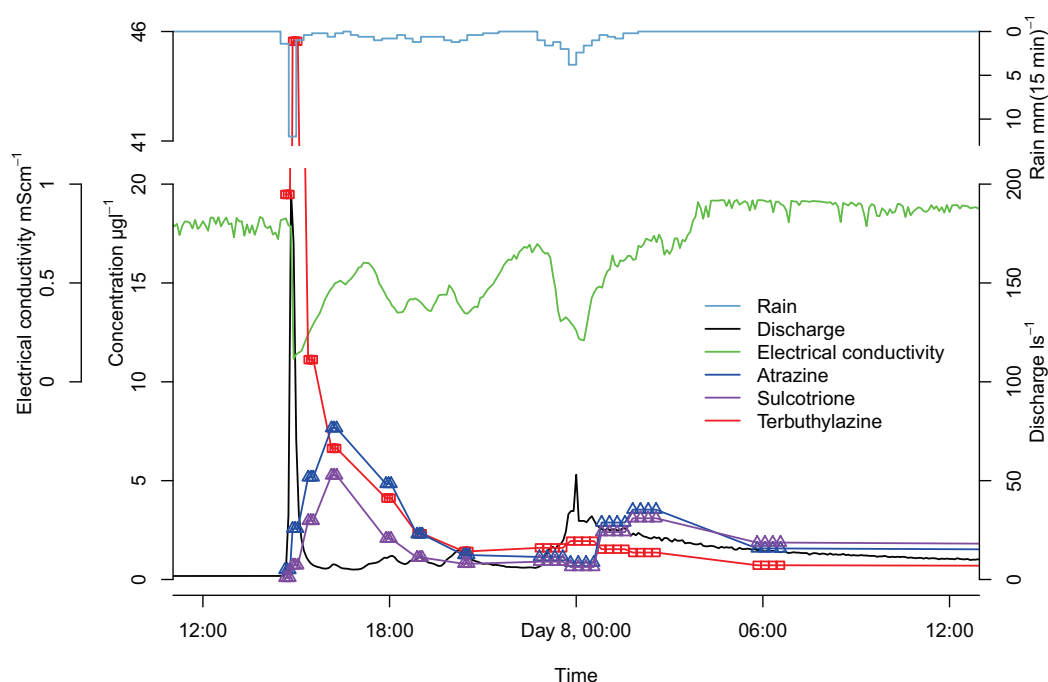
Figure 2.5: Concentration dynamics of three substances at station S_d together with rain intensity, discharge, and electrical conductivity in the stream during event E2 (26 June 2009, seven days after application). The symbols represent the sampling time of the individual sample aliquots (see Sect. 2.2.4).

Overland flow and erosion

During the experimental period, we frequently observed overland flow and erosion on different fields distributed over the whole catchment (see Fig. 2.4 and Table 2.1). Overland flow was observed at least at one location in all of the rain events (Table 2.1).

Piezometer data showed that the groundwater level was often low before and during rain
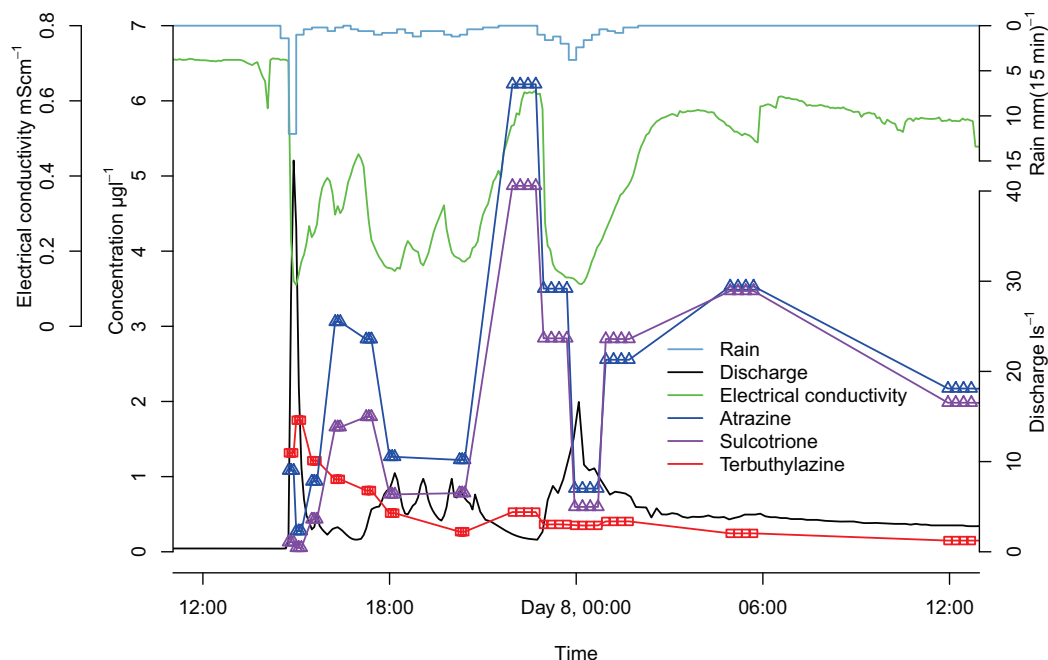
Figure 2.6: Concentration dynamics of three substances at station O_u together with rain intensity, discharge, and electrical conductivity in the stream during event E2 (26 June 2009, seven days after application). The symbols represent the sampling time of the individual sample aliquots (see Sect. 2.2.4).

events. During events E2, E3 and E9 it rose to a level of less than 30 cm below the surface in two, one and three piezometers, respectively. Four piezometers reached this level during event E12. However, during event E13, the groundwater level rose close to the surface in seven out of nine piezometers (Table 2.1). We did not observe perched water tables in any of the four soil profiles. Rising groundwater levels were therefore not limited to locations with low conductivity layers in the soil profile.

Table 2.1 shows the mean electrical conductivities (EC) in the overland flow samples from eight events. Except for events E2 and E13 (EC > 400 μS cm^{-1}), all the values were around 200 μS cm^{-1}.

Figure 2.4 gives a spatial overview of the field observations of overland flow and erosion. Neither of these processes was limited to locations with high groundwater levels, but they were distributed across the whole catchment area. However, erosion was only observed on corn fields during the study period, not on wheat fields with high soil coverage. In addition, the land management on the corn fields played an important role for the risk of overland flow. The type of ploughing and harrowing as well as the addition of organic material in the past years seemed to be important factors affecting the infiltration capacity of a field.

This can be illustrated with fields (A) and (B) in Fig. 2.4. Both were corn fields with comparable soil coverage and similar soil texture and topography. Erosion and overland flow were frequently observed on field (A), but rarely on field (B). The differences can be explained with the land management: field (A) was harrowed very finely, leading to very small and crushed soil aggregates at the surface, low surface roughness and small detention storage. On the contrary, field (B) was harrowed only roughly, leading to a more irregular soil surface with intact soil aggregates, a high surface roughness and larger detention storage. Additionally solid manure was applied on field (B) before ploughing.

Connectivity

Based on the connectivity analysis (Sect. 2.2.10), only 4.4 % of the catchment area is directly connected to the stream on the surface (see Fig. 2.2), due to depressions within the catchment or topographic barriers (e.g. field roads) preventing the overland flow from flowing to the stream directly (see Fig. 2.4, which shows that ponding was often observed beside roads). However, the extended pipe network in the underground (tile drains as well as road and farmyard drainage), which is directly connected to the stream, offered two additional fast transport pathways for herbicides in overland flow: (i) direct shortcuts via maintenance manholes of the drainage system or storm drains for road and farmyard runoff (this pathway will be called shortcut in the following) and (ii) ponding of overland flow in depressions and macropore flow to the drainage system. Figure 2.7 shows examples of these two pathways observed during event E2. The connectivity analysis revealed that the area connected to shortcuts is much larger (23 % of the catchment area) than the area connected to the stream directly (Fig. 2.2). Several shortcuts were observed to be active during the experiment. Figure 2.4 shows all shortcuts that were observed (in the field) to be active at least once, Fig. 2.7 shows a picture of an active shortcut.

2.3.2   Influence of compound properties

Herbicide dissipation and sorption

Average half lives on the six experimental fields were 9.5, 13.8 and 5.5 days for atrazine, S-metolachlor and sulcotrione, respectively (Camenzuli, 2010). These values are well within the range reported in literature (see Table 2.2).

Sorption of the herbicides to soil was assessed by the apparent distribution coefficient K_d between the sorbed and the dissolved fraction (Eq. 2.3). Sorption was strongest for S-metolachlor, followed by atrazine and sulcotrione on all the experimental fields. On
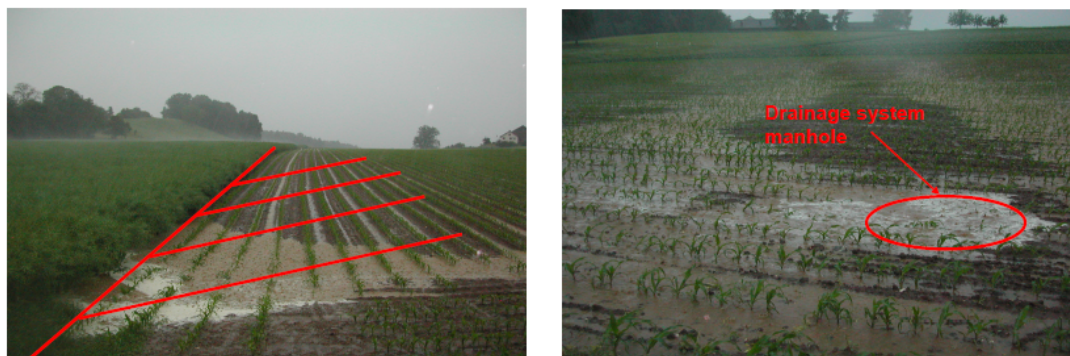
Figure 2.7: Example pictures from event E2. Ponding overland flow in a drained depression on experimental field 1 (left) and overland flow entering a shortcut (right).

the application day, the K_d values on the experimental fields were in the range of 0.7 to $1.5\,l\,kg^{-1}$, 1.4 to $2.6\,l\,kg^{-1}$, and 0.1 to $0.2\,l\,kg^{-1}$ for atrazine, S-metolachlor and sulcotrione, respectively. The apparent distribution coefficient K_d of all substances increased with time. The magnitude of this kinetic sorption effect was largest for sulcotrione (3.2- to 14-fold increase from day 0 to day 30), followed by atrazine (1.3- to 10-fold increase) and S-metolachlor (1.3- to 2.5-fold increase). As it can be seen from the large ranges of K_d increase, the variance between the different fields was large (Camenzuli, 2010). The magnitude of the kinetic sorption effect and its variability are comparable to the observations reported by Gomides Freitas et al. (2008).

Overland flow concentration and herbicide mobilisation

Herbicide concentrations in the overland flow samples varied heavily in space and time. The concentrations at each overland flow sampling site decreased with time. The concentrations in overland flow samples measured during event E2 differed by three orders of magnitude depending on the sampling location (atrazine: 0.58 to $426.3\,\mu g\,l^{-1}$, S-metolachlor: 0.42 to $466.8\,\mu g\,l^{-1}$, sulcotrione: <0.125 to $97.9\,\mu g\,l^{-1}$).

The mobilisation coefficient M was used to investigate the influence of sorption on the mobilisation of the herbicides. We calculated M ratios for all substance pairs ($M_{\text{substance1}}/M_{\text{substance2}}$) and compared them with the respective ratios of K_d values ($K_{d,\text{substance1}}/K_{d,\text{substance2}}$). We used the distribution coefficients that had been determined in the last soil sample taken before the respective rain event. Figure 2.8 shows the field data for all experimental substances, all the events with overland flow samples and different experimental fields. In Fig. 2.8 we also show two lines based on Eq. 2.2 with the following assumptions: $z = 50\,\text{mm}$, $\theta_{\text{sat}} = 0.5$, $\rho = 1.2\,\text{g\,cm}^{-3}$ and $q_{\text{mobile}} = 10\,\text{mm}$ (dashed

line) and $q_{mobile} = 100\,mm$ (solid line). No dependence can be detected between M ratios and K_d ratios of the field data, and they do not correspond to the expected behaviour expressed in Eq. 2.2. All M ratios scatter around one. Obviously, the different substances were mobilised into overland flow to a similar degree, independent of their distribution coefficients K_d. This implies that the influence of substance properties affected mobilisation in a different manner than expected and/or that other factors were more influential than the apparent equilibrium distribution.
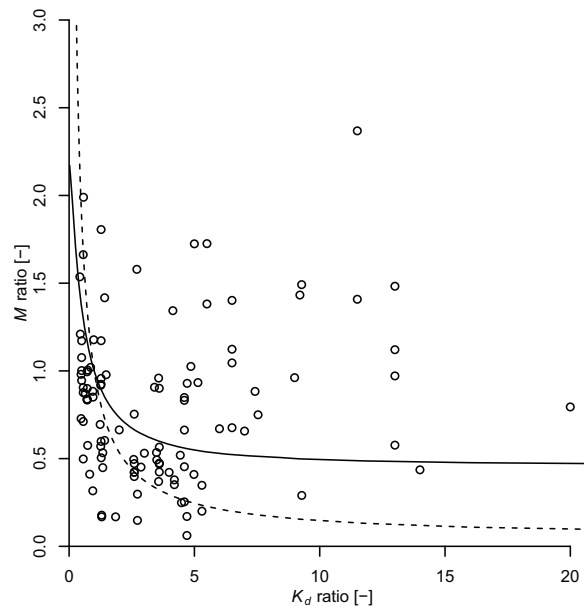
Figure 2.8: The ratio of the mobilisation coefficients M of two substances in the same sample, plotted against the respective ratio of distribution coefficients K_d from the corresponding field. Dashed line: SWAT prediction with a flux of 10 mm of mobile water (see text), solid line: SWAT prediction with a flux of 100 mm of mobile water.

Retention during infiltration

While the field data do not show an influence of substance properties on the mobilisation process, the data suggest that the transport through macropores was affected by sorption. We compared retention coefficients R (Sect. 2.2.9) of different substances (all applied together on field 1) within the same samples at two time points during event E2. Figure 2.9 shows the ratios of R of substance pairs plotted against the K_d ratios of the respective substance pairs. The figure reveals that the retention coefficients were larger for substances with higher K_d values. This means that sorption played a role during the fast transport from ponding overland flow through macropores to tile drains. From the compounds dis-

solved in ponding water, a larger fraction of the stronger sorbing compounds was retained in the soil. This implies that the herbicide load was reduced during the soil passage, even though the flow was fast and the travel time short.
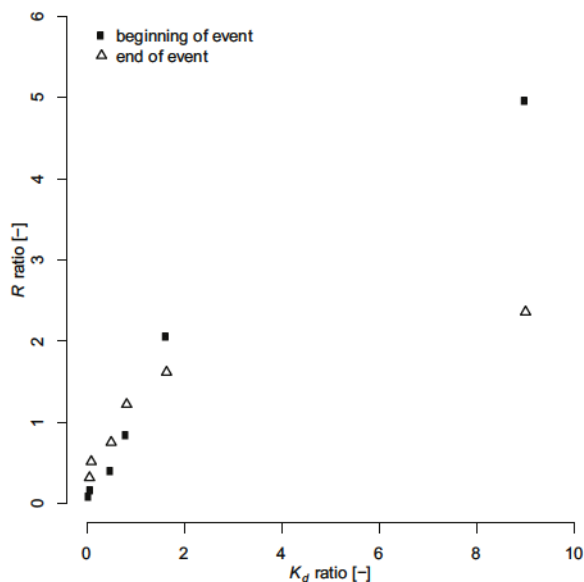
Figure 2.9: Ratio of retention coefficients R of two substances plotted against the respective K_d ratio.

2.3.3   Concentration dynamics

We observed elevated concentrations of all the applied substances in the stream and in tile drains during all of the sampled events. Additionally, we observed that the substances applied to the same fields showed very similar dynamics. Atrazine, S-metolachlor and sulcotrione (the substances on the experimental fields) always peaked at the same time. The same holds for terbuthylazine and mesotrione, which were spayed on the alternative fields. However, the dynamics of these two mixtures differed during most events. Figures 2.5 and 2.6 show examples for this behaviour. Correlation coefficients were calculated for the concentrations during event E2 at the stations S_d and O_u (shown in Figs. 2.5 and 2.6). The correlation between atrazine and sulcotrione was 0.90 and 0.95 at the stations S_d and O_u, respectively; between atrazine and terbuthylazine it was 0.02 and -0.38.

The terbuthylazine concentration followed the hydrograph dynamics at station S_d closely (correlation coefficient of 0.71 during event E2). At station O_u, some correlation between discharge and terbuthylazine concentration can also be observed (correlation coefficient of

0.47 during event E2, see Figs. 2.5 and 2.6). For atrazine and sulcotrione, no correspondence between discharge dynamics and concentration can be observed in Figs. 2.5 and 2.6; the correlation between atrazine and discharge during event E2 was -0.20 and -0.45 at the stations S_d and O_u, respectively. These data suggest a decoupling of discharge and concentration peaks for atrazine, S-metolachlor and sulcotrione in several events.

Upstream of the two stations S_d and O_u, there is no open stream; they have purely subsurface catchments. Nevertheless, we observed rather high herbicide concentrations (Figs. 2.5 and 2.6).

2.4 Discussion

2.4.1 Transport processes and CSAs

The differentiation between saturation excess and infiltration excess overland flow at catchment scale is not an easy task. However, the observed groundwater levels and the electrical conductivity of overland flow samples indicate that both infiltration excess and saturation excess overland flow occurred during the study period. The widespread occurrence of overland flow during the events E1 to E12 (Table 2.1 and Fig. 2.4), when most groundwater levels were low (Table 2.1), can only be explained with infiltration excess. During the event E13 groundwater levels were high, indicating that saturation excess may have occurred at several locations. Electrical conductivity of the overland flow samples supports this interpretation as follows. Rain typically has a very low electrical conductivity ($<50\,\mu\mathrm{S\,cm^{-1}}$), while groundwater and soil porewater have significantly higher electrical conductivities (baseflow in this catchment has an electrical conductivity around $800\,\mu\mathrm{S\,cm^{-1}}$). Infiltration excess overland flow does not contain any groundwater, and we argue that mixing with soil pore water is limited (Hahn et al., 2012). We therefore expected infiltration excess overland flow to have low conductivity. Areas that produce saturation excess overland flow (groundwater level at the surface) often also produce return flow (exfiltrating groundwater). We therefore expected saturation excess overland flow to consist of a mixture of return flow, pre-event pore water and rain, thus having higher electrical conductivity. The electrical conductivity of overland flow is additionally influenced by easily dissolved substances at the surface, which makes the interpretation more difficult. The electrical conductivities in the overland flow samples show a clear separation between events. Except for events E2 and E13, the average electrical conductivities in the overland flow samples were around $200\,\mu\mathrm{S\,cm^{-1}}$, while it was above $400\,\mu\mathrm{S\,cm^{-1}}$ in events E2 and E13. Event E2 was a special case because fertilizer was applied on several fields directly before the event.

The high electrical conductivity in the overland flow was probably caused by dissolved fertilizer in this case. Therefore, we concluded that the herbicides were mainly mobilised by infiltration excess overland flow. Only during event E13 was saturation excess overland flow the more important process (Hirzel, 2009). This interpretation is supported by the runoff ratios being low for all events except E13 ($>40\%$). This shows that a different runoff regime was active during event E13. Our observation that infiltration excess overland flow is the main transport process for herbicides is in contrast to previous studies in the Swiss Plateau (Gomides Freitas et al., 2008; Leu et al., 2004a, 2010), which indicated that saturation excess overland flow was the dominant process controlling diffuse herbicide pollution.

The differences between these studies are most probably caused by different rainfall characteristics of the events that led to the main herbicide losses. In the studies by Leu et al. (2004a) and Gomides Freitas (2005), the maximum rainfall intensity of the events that led to the main herbicide losses were 3.2 and $2.4\,\text{mm}\,(15\,\text{min})^{-1}$, respectively. In contrast, the main loss event in this study had a maximum intensity of $12\,\text{mm}\,(15\,\text{min})^{-1}$ (see Fig. 2.10 and Table 2.1). Figure 2.10 shows the histograms of rain intensities of the months May to July in these three field studies (Gomides Freitas, 2005; Leu et al., 2004a, and this study) together with the 30-yr average intensities during these months at Schaffhausen (closest permanent weather station to this study site, Meteoschweiz, 2012). The figure shows that the timing of the rain events determined the process that lead to the main herbicide losses. If the first event with a substantial hydrological response after application was a high intensity event, infiltration excess overland flow was dominant, but if it was a low intensity event, saturation excess overland flow dominated the herbicide losses. The histograms also show that none of the field experiment years was an extreme year compared to the 30-yr average. However, high intensities were much more common in 2003 and 2009 than in 2000.

Saturation excess and infiltration excess overland flow are influenced by different site characteristics. While the position in the relief and the subsoil properties play a major role in triggering saturation excess runoff, infiltration excess overland flow is strongly affected by topsoil properties (Easton et al., 2008; Gerits et al., 1990; Lyon et al., 2006). Accordingly, one may expect the two runoff processes to occur in different parts in the landscape. Equation (2.1) can be re-formulated to take this into consideration:

$$A_{\text{CSA}} = \left(A_{\text{source}} \cap A_{\text{inf\_ex}} \cap A_{\text{connect}}\right) \cup \left(A_{\text{source}} \cap A_{\text{sat\_ex}} \cap A_{\text{connect}}\right) \qquad (2.4)$$

This equation states that the CSA extent is an overlay of CSAs with active areas for infiltration excess with those causing saturation excess runoff. As discussed above, the occurrence of the two processes may differ substantially in time, depending on the mete-
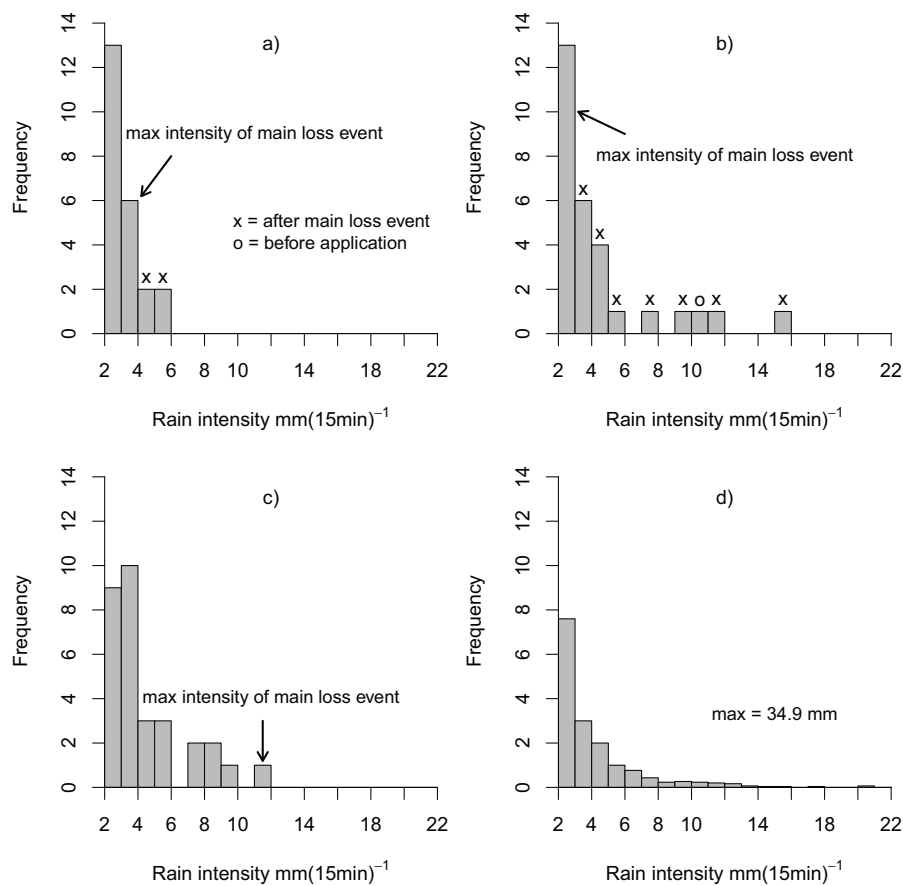
Figure 2.10: Comparison of frequencies of rain intensities $>2\,\mathrm{mm}\,(15\,\mathrm{min})^{-1}$ for the period May to July from **(a)** the field experiment in 2000 (Leu et al., 2004a), **(b)** the field experiment in 2003 (Gomides Freitas et al., 2008), **(c)** this field experiment and **(d)** the 30-yr average at the permanent weather station in Schaffhausen (Meteoschweiz, 2012).

orological conditions.

The distinction between the two processes has further implications for CSA management. The risk for pesticide transport by infiltration excess overland flow depends on the crop and stage of crop growth at the time of pesticide application. Additionally land management practices play a role for soil surface properties. This makes $A_{\mathrm{inf\_ex}}$ very variable in time and hard to predict without very local information on the actual land management. Furthermore, the spatial pattern of infiltration excess overland flow can be dominated by the spatial variability of rain intensity. These disadvantages for the prediction of infiltration excess runoff areas are combined with the advantage that prevention of infiltration excess overland flow is much easier as compared to saturation excess overland flow. Because infiltration excess depends strongly on topsoil properties, it can be influenced by

land management and cropping practices. This is much less of an option for saturation excess overland flow, which is strongly controlled by constant site characteristics like the position in the landscape.

The finding that infiltration excess overland flow can be an important process on agricultural land in humid climate is not surprising per se. Other studies have shown this process before (Church and Woo, 1990; Deasy et al., 2011; Moore et al., 1976; Srinivasan et al., 2002). However, most of the work on critical source areas focuses on saturation excess overland flow (e.g. Easton et al., 2008; Frey et al., 2009; Gburek and Sharpley, 1998; Lyon et al., 2006; Pionke et al., 2000). The particularity of this study is that it could show the importance of infiltration excess overland flow for the transport of herbicides to the stream at catchment scale under climate conditions that were characterised by considerable amounts of rain during the application period.

2.4.2   Substance properties and transport

Previous observations have shown that the loss rates of herbicides depended on the K_d values of the substances (lower losses for substances with higher K_d, Brown and van Beinum, 2009; Gomides Freitas et al., 2008; Leu et al., 2004a; Louchart et al., 2001) and that the sorption strengths did not affect the timing of concentration peaks (Gomides Freitas et al., 2008; Leu et al., 2004a). Based on these observations, it was concluded that the substance properties of the herbicides have an influence on how much of a compound is mobilised into fast flow, but that these properties do not affect the transport of the compound once it gets into the fast flow component (Gomides Freitas et al., 2008; Leu et al., 2004a). The results observed in this study were the opposite of what we expected: Sorption did not yield any measurable influence on the mobilisation of the compounds into surface runoff (no dependence of M on K_d, see Fig. 2.8), but it did so during the transport by preferential flow towards tile drains (R depends on K_d, see Fig. 2.9).

These (apparent) contradictions can probably be explained by the different levels of detail during the investigation of transport along the flow paths. In previous work, the interpretation was based on the knowledge of input into and output from the catchments. In this study, we also obtained information along the flow path by sampling ponding water. This more detailed information allows for differentiation between sorption effects during mobilisation and sorption effects during transport.

We expected that substances that sorb more strongly would be mobilised less compared with less sorbing substances. Hence, one can expect that the ratio of the M values of two compounds decreases as a function of the respective K_d ratio. The lack of sorption

effect with regard to the mobilisation of the compounds (see Fig. 2.8) may be caused by the fact that the equilibrium concept behind the K_d values is not adequate to describe the mobilisation of the herbicides from soil to overland flow. Under field conditions following application, pore water and solid phase concentration are barely in equilibrium due to several reasons. Firstly, the equilibrium takes weeks to months to establish for many compounds due to slow kinetic sorption. This is likely for the herbicides studied (e.g. Altfelder et al., 2000; Mamy and Barriuso, 2007; Streck et al., 1995; Zhu and Selim, 2000) and our results showing increasing K_d with time (Sect. 2.3.2 and Fig. A.1 in the Appendix) also indicate that slow kinetic sorption takes place. Secondly, a continuous, rather rapid degradation of the compounds and changing soil moisture due to precipitation and evapotranspiration permanently change porewater concentrations in the topsoil. Furthermore, the addition of water for the pore water extraction (see Sect. 2.2.7) can also influence the measured apparent K_d resulting in artifacts of the extraction method. However, the natural porewater in a soil sample taken one day after a rain event is also not in equilibrium with the solid phase. The measured apparent K_d values in the soil samples show a steady increase with time for most of our study fields and substances. They do not seem to be influenced by changing soil moisture or the amount of added water (see Fig. A.1 in the Appendix for examples). We are therefore confident that our results are not strongly influenced by methodological artifacts.

Conceptually, a mobilisation of compounds from soil into overland flow can be considered in terms of at least two processes: a displacement of pore water with a certain herbicide concentration at near-equilibrium with the solid phase, and a kinetic desorption of herbicides into infiltrating water at lower concentrations following a chemical potential gradient. It is therefore possible that faster desorption kinetics compensate for lower equilibrium concentrations in water. It was shown that the kinetic sorption of many compounds can be explained with diffusion into organic matter (Brusseau and Rao, 1989). In addition, Villaverde et al. (2009) postulated that sorption kinetics in undisturbed soil aggregates are negatively correlated with sorption strength. With both of these mechanisms (diffusion into organic matter and diffusion into soil aggregates), at a given time, stronger sorbing compounds rather sorb at the surface of organic matter or soil aggregates, while compounds with weaker sorption can diffuse farther into these particles. If diffusion out of organic matter or soil aggregates was the rate limiting step, stronger sorbing compounds could have faster desorption kinetics. This could explain our results. Furthermore, it is possible that our soil sampling depth of 5 cm is not representative for the layer at the surface where mobilisation takes place. Stronger sorbing compounds could be overrepresented in the top layer, compared with our sampling depth. In addition, our substance selection does not cover the full range of sorption strengths. Possibly, the sorption effects during

mobilisation were masked by other factors for our substances, but they would become visible for substances that differ more in their sorption properties.

We do not have time-resolved samples of overland flow to directly prove the statement that different desorption kinetics compensate for different equilibrium concentrations as we postulate in the paragraph above. However, different desorption kinetics should still be visible in the concentration dynamics at the stream sampling sites where we do have time-resolved samples. The concentration ratio of a less sorbing substance relative to a stronger sorbing one should increase during the event, because the substance with weaker sorption is mobilised more slowly. This behaviour was indeed observed for sulcotrione and atrazine, where sulcotrione concentration increased relative to atrazine concentration in several events at the sampling sites (see Fig. A.2 in the Appendix for an example). Even though the interpretation of our results on herbicide mobilisation remain speculative to some degree, they indicate that equilibrium sorption is not the only relevant process during herbicide mobilisation. The shift in concentraion ratios in the stream demonstrates that pore scale mobilisation processes can result in effects that are visible at catchment scale.

Our results on retention indicate that sorption affected the transport through preferential flow paths to tile drains (Sect. 2.3.2, Fig. 2.9). This should lead to a retardation of stronger sorbing compounds. However, no retardation was visible in the timing of the peak concentrations. This can have two reasons. Firstly, the water at sampling station O_u was a mixture of several flow components (see Sect. 2.4.4), whereas the retardation would only appear in the macropore flow originating from the ponding overland flow. The timing of the concentration peak of all substances, however, was determined by the mixing ratio of the flow components; this can mask the retardation occurring in one flow component. Secondly, the travel times were so short that any retardation effects were too subtle to be detected with our temporal sampling scheme.

2.4.3 Connectivity

This study confirmed previous work (Barron et al., 2011; Frey et al., 2009; Kiesel et al., 2010) in demonstrating that only a very small part of the catchment has a direct surface connectivity to the open stream; the largest part of the catchment is connected to topographic depressions within the catchment. One main reason for the low surface connectivity is the moderate topography in the catchments, which is typical for major crop production areas. In areas with more pronounced topography, it is expected that larger areas are directly connected to the stream. Field roads, which are common in crop pro-

duction regions, also often act as small topographic barriers to overland flow. Figure 2.4 shows that ponding was often mapped directly alongside field roads as shown earlier by Frey et al. (2009).

However, the road network can also have the opposite effect and can increase connectivity by offering new routes for fast transport (Ledermann et al., 2010; Payraudeau et al., 2009). This holds especially true for Switzerland, where a large percentage of roads have a drainage system conveying runoff water directly to the stream network. For natural catchments it may be sufficient to analyse the topography in order to assess the connectivity to the stream network. For agricultural areas like the Swiss Plateau, such an analysis has to be complemented by information on all anthropogenic interventions affecting the flow paths of water through the catchment. Such interventions may be quite region-specific and difficult to generalize. Our connectivity analysis showed that the area connected to shortcuts is much larger than the area directly connected to the stream (see Sect. 2.3.1). The analysis of the connectivity to shortcuts (see Sect. 2.2.10) is based on the assumption that all the overland flow in the catchment of a shortcut also enters the shortcut, which is a worst-case assumption. Several reasons can prevent overland flow from entering shortcuts: (1) Manholes with closed lids (not intended to collect overland flow) do not collect all the water that reaches them. (2) Small-scale topography around the potential shortcut can divert overland flow in another direction. (3) The rim of manholes can be slightly higher than ground surface and prevent overland flow from entering. Furthermore, overland flow can re-infiltrate on its way to the shortcut. Despite these possible restrictions, several shortcuts (storm drains and maintenance manholes) were observed to be active during the study period (Fig. 2.4).

Spatial sequences of different processes at different locations also caused transport to the stream, even from fields that did not seem to be connected to the stream in any way. This was observed for experimental field 4, which is not directly connected to the stream and only small parts of the field are potentially connected to shortcuts (see Fig. 2.2). Furthermore, only one drainage tube crosses a corner of the field, which lies entirely on well drained soils and regosols (Fig. 2.1). Therefore, we did not expect any herbicides from field 4 to be found in the stream. However, we observed the experimental substances in sampling station S_u, where field 4 was the only possible source area. Field observations during and after rain events revealed that overland flow and erosion occurred on field 4, such that the flow including the herbicides was routed off-field to a depression on the neighbouring field, where ponding was observed (see Fig. 2.4 for observed flow paths and ponding and Fig. 2.11 for the catchment of the depression). The depression is drained and herbicides reached the stream via macropore flow to the drainage system (concentration data not shown). This observation implies that the risk for herbicide transport to streams

can not be assessed by investigating single fields; fields always have to be seen in their context within the catchment. Fields that are not connected to a stream or shortcut and are not drained can still be contributing areas as shown for experimental field 4. Furthermore, fields that do not produce overland flow can be affected by run-on from an upslope field as it was shown by Ledermann et al. (2010).
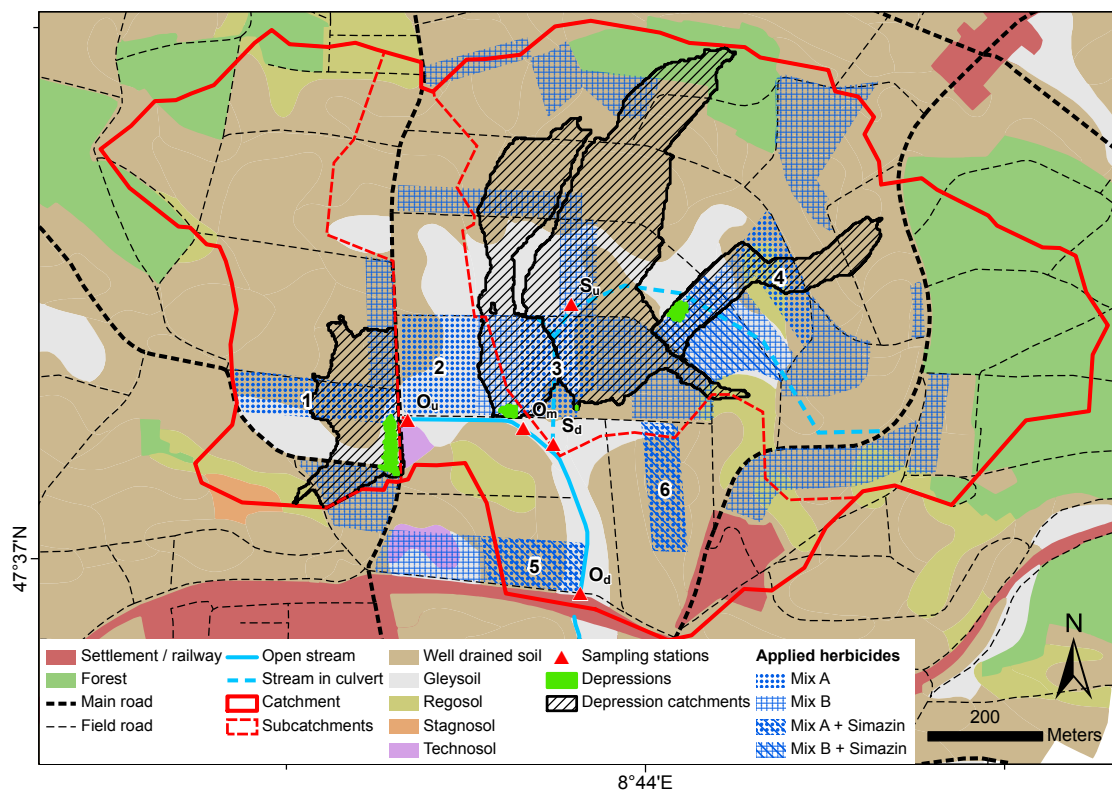
Figure 2.11: Map of four major depressions and their corresponding topographic catchments together with the subcatchments of the sampling stations O_u and S_d. Sources: FAL (1997); Swisstopo (2008).

Although most of the fields showed no surface connectivity, herbicides were lost from the fields to the stream network. Obviously, herbicides were transported to the stream even if they were accumulating first in depressions in the landscape. To understand the risk for herbicide losses from different fields, it is important that areas connected to the stream via different pathways do not pose the same risk for losses to the stream. Areas connected via shortcuts are less risky than those directly connected to the stream, because not all of the overland flow might enter the shortcut (see above). Furthermore, areas connected to drained depressions pose an even lower risk because of sorption during the transport to the drainage system (see Sect. 2.3.2). In addition to sorption, the ponding of overland flow in depressions also lowers peak concentrations by retarding the contaminated water.

If the contaminated water reaches the stream directly (no ponding), this leads to a sharp concentration peak (see e.g. terbuthylazine in Fig. 2.5). With ponding, the contaminated water enters the stream more slowly. This leads to elevated concentrations for a longer time but lower peak concentration (see e.g. atrazine in Fig. 2.5). It has already been shown that drainage water typically has lower concentrations than surface runoff (Brown and van Beinum, 2009; Kladivko et al., 2001). Our findings concerning connectivity suggest that the question whether an area is connected to the stream cannot be answered with yes or no. The question should rather be how well an area is connected to the stream.

2.4.4   Concentration dynamics

The strong correlation of concentration dynamics between compounds applied on the same fields and the missing correlation of concentration dynamics between compounds on different fields (Sect. 2.3.3) imply that the concentration dynamics were influenced substantially by the spatial origin of the compounds and the flow paths but not by substance properties. Based on previous studies (Gomides Freitas et al., 2008; Leu et al., 2004a,b, 2005) we expected the concentrations to follow the hydrograph dynamics very closely, which was not the case for all substances in this study. In order to understand these chemographs and the apparent contradiction to the observations by Gomides Freitas et al. (2008) and Leu et al. (2004a,b, 2005), one has to consider the relevant flow paths that have been observed in this catchment. Based on our results and field observations, we distinguish three major flow components:

1. Surface runoff that entered the stream via shortcuts. This included runoff from roads and farmyards but also overland flow from fields that entered one of the abovementioned shortcuts. This was the fastest flow component; it dominated discharge during times with high rain intensities and its proportion in discharge mainly followed the rain intensity pattern.

2. Macropore flow to tile drains. This water partly consisted of overland flow that ponded in small depressions that are drained; but it also contained water from other sources. This was also a fast flow component that was only active during rain events, but slower and longer lasting than component one.

3. Groundwater flow to tile drains. This was the slowest flow component that made up the base flow and increased with rising ground water tables during rain events. It was characterized by low herbicide concentrations.

The chemograph observed for a given compound was the result of the mixture of these three flow components and their respective herbicide concentrations. The connectivity analysis revealed that not all measuring sites were affected by the first two flow components to the same degree. Only small parts of the experimental fields – receiving atrazine, S-metolachlor and sulcotrione – in the catchment of S_d (fields 3 and 4) for example, were connected to a direct shortcut (see Fig. 2.2). The largest part of the fields drained into three important depressions (Fig. 2.11), from where overland flow reached the tile drains via macropore flow (flow component 2). Large areas of alternative corn fields – receiving terbuthylazine – were, however, connected to shortcuts (Fig. 2.2; flow component 1). This led to faster transport and therefore a sharper concentration peak (Fig. 2.5). Due to the different travel times along the two different fast flow paths, the chemographs of the two herbicide mixtures differed. This interpretation is supported by the electrical conductivity data. Measurements at S_d showed that the terbuthylazine peak occurred simultaneously with lowest electrical conductivity, indicating transport with water that did not travel through soil (Fig. 2.5). In contrast, atrazine and sulcotrione concentrations peaked at higher electrical conductivity within the event. This was the time of less intense rainfall, where discharge was dominated by the macropore flow from ponding overland flow to the tile drains.

A similar behaviour with less complexity was observed at station O_u (Fig. 2.6). Only one experimental field (field 1) and two alternative corn fields lie in O_u's catchment. Experimental field 1 was only connected to the stream via infiltration to the drainage system, direct shortcuts were not present (Fig. 2.2). Overland flow from the field was collected in a depression on field 1, where it infiltrated to the drainage system (see Fig. 2.11 for the catchment of the depression; Fig. 2.7 shows a picture of this depression). Overland flow originating from the alternative fields in O_u's catchment (terbuthylazine) could take two flow paths. It either flowed to the depression on field 1 and infiltrated to the drainage system or it could enter the stream via storm drains for road runoff (Figs. 2.2 and 2.11). Figure 2.6 shows that the concentration of the experimental substances (atrazine and sulcotrione) again correlated well with the electrical conductivity in the stream during the event. Directly upstream of this sampling station, the road runoff from the main road in the west of the catchment enters the stream. Discharge peaks were therefore dominated by road runoff, which led to strong dilution of herbicide concentration and to low electrical conductivities during times with intense rainfall. Again, the concentration dynamics clearly supported the connectivity analysis; both indicated transport via infiltration to the drainage system for the experimental substances atrazine and sulcotrione. The terbuthylazine concentration dynamics reflected the two possible flow paths: the very fast pathway via storm drains for road runoff (concentration peak simultaneous with first dis-

charge peak and no significant dilution in second discharge peak at day 8, 00:00 LT) and the pathway via infiltration to the drainage system (elevated concentration at times of low discharge during the event). The resulting concentration dynamics of terbuthylazine was an overlay of the two processes. However, as soon as groundwater flow into the drains dominated discharge (at the end of the event and in base flow periods), the concentrations of all substances were low and no longer correlated with the electrical conductivity.

2.5 Conclusions

This catchment-scale experiment aimed at improving the process understanding of herbicide transport from the fields of application to first-order streams. This was achieved by controlling the herbicide input in an experimental way, simultaneously analysing samples along the entire pathway of herbicide transport from the field to the stream (soil samples, overland flow samples, samples from drainage tubes and the open stream) and monitoring a variety of hydrological state variables. This combination of observations was crucial for improving the process understanding. We could show that most of the catchment is not connected to the stream at the surface, but herbicides were transported to the stream via man-made structures which considerably increased connectivity. Our findings on the role of compound properties for mobilisation and transport of herbicides contradict common concepts to some degree. The study also showed that infiltration excess overland flow can be relevant for the transfer of herbicides under humid climate.

Our findings also have implications for mitigation measures against diffuse herbicide pollution. One of these measures is based on the concept of contributing areas (CSA) and aims at targeting measures to those parts of a catchment that contribute the main part of the pollution. This concept relies on the temporal stability of the spatial extent of CSAs, which is a reasonable assumption for saturation excess runoff. The spatial occurrence of infiltration excess overland flow may, however, vary substantially through time due to e.g. crop growth and land management. Although the CSA concept may still be a useful heuristic for analysing transport in such situations, it will be more difficult to apply in practice. However, the risk for infiltration excess runoff can be relatively easily mitigated by adapting land management or crop rotations.

The observations in this study suggest that the mobilisation process may be less affected by sorption than expected, whereas herbicides were partially retained during the fast transport through preferential flow paths underneath a depression with ponding water. This improved process understanding is not only of scientific interest but also indicates that hydraulic shortcuts should be avoided in practice. Land management should aim at

a soil passage for all water before it enters the stream.

Acknowledgements

Chapter 3

Critical source areas for herbicides can change location depending on rain events

Tobias Doppler, Alfred Lück, Louise Camenzuli, Martin Krauss and
Christian Stamm

T. Dopplers contribution to this chapter: Planing, setup and maintenance of the whole field experiment including the hydrological measurements, the planing of the herbicide application and the soil and water sampling; load calculations; GIS analysis; data processing and interpretation; writing.

3.1   Introduction

In modern agriculture, a wide variety of pesticides is used to increase crop productivity. They encompass a broad range of chemicals and are used to control weeds, to fight plant diseases, insects, arachnids and other pests. Pesticides can enter the water system, where they can harm aquatic organisms even in low concentrations. Small streams in catchments with intensive crop production are especially at risk (Liess and Schulz, 1999), as diffuse pollution from agricultural fields causes major inputs to the stream in these areas (Leu et al., 2010; Stehle et al., 2011). Pesticides mainly enter surface waters during rain events, when they are mobilized and transported with fast runoff (surface runoff and preferential flow to subsurface drainage systems), with the pathway through groundwater and baseflow being of little importance for most pesticides (Thurman et al., 1991). Several cases showed that herbicide loss rates (relative to the applied amount) from different fields within a given catchment can differ by over an order of magnitude (Gomides Freitas et al., 2008; Leu et al., 2004b; Louchart et al., 2001). This implies that a relatively small proportion of a catchment can cause the major part of surface water pollution with herbicides. The same has been observed for diffuse pollution of surface waters with phosphorus (Pionke et al., 1996, 2000). The areas that contribute a large fraction of the pollution load are called critical source areas (CSAs) or contributing areas (Pionke et al., 1996). The insight that not all parts of a catchment have the same relevance for diffuse pollution offers efficient mitigation options, because actions on a small proportion of the area can strongly reduce the substance input to the stream. An area has to fulfill three conditions to become a critical source area for pesticides: (1) Pesticides have to be applied on the area (or reach the area by drift in relevant amounts). (2) The area has to be hydrologically active, i.e. the relevant mobilization and fast transport processes do occur. (3) The area has to be directly connected to the stream such that fast flow reaches the stream without relevant retention processes (Frey et al., 2009). The spatial extent of the CSAs (ACSA) can be interpreted as the spatial intersection of the areas of a catchment where each condition is fulfilled:

$$A_{\mathrm{CSA}} = A_{\mathrm{source}} \cap A_{\mathrm{active}} \cap A_{\mathrm{connect}} \qquad (3.1)$$

with A_{source} representing the source area of a given compound, A_{active} the hydrologically active area, and A_{connect} the part of the catchment in direct connection to the stream network. For pesticides, the source areas A_{source} correspond primarily to the areas of pesticide applications but may encompass also additional surfaces where pesticide are deposited in relevant amounts due to drift deposition. The compound's chemical properties can modify A_{source} in space and time. Degradation and sorption both determine the amount of substance that is available for transport at the time of rainfall (Louchart et al., 2001).

There may be substantial spatial variability in sorption and degradation rates of pesticides in soils (Ghafoor et al., 2011a,b) within fields and small catchments possibly affecting the spatial CSA distribution. Earlier studies in the Swiss Plateau (Leu et al., 2004b; Stamm et al., 2004), however, indicate that degradation rates and sorption coefficients did not vary strongly between fields in the corresponding study catchment and could not account for observed spatial differences in herbicide loss rates (Gomides Freitas et al., 2008; Leu et al., 2004b, 2005). In those studies the spatial variability of herbicide loss rates was attributed to the susceptibility of the fields to generate fast flow and the connectivity of the fields with the stream.

Even though the chemical properties of the pesticides may not necessarily determine the spatial pattern of losses, they are important in determining the pesticide mobilization and transport behavior. While the pesticide half life in soil determines the amount of pesticide that is present in soil at the time of rainfall (e.g., Louchart et al., 2001), the sorption behavior can affect both mobilization and transport. For many pesticides it has been shown that sorption equilibrium is only reached after weeks or months and therefore kinetic sorption has to be considered (see Vereecken et al., 2011, for a recent review of pesticide sorption studies). Several field studies have shown that sorption strength influences pesticide losses to streams and tile drains, leading to lower loss rates and lower peak concentrations for substances with stronger sorption (Brown and van Beinum, 2009; Gomides Freitas et al., 2008; Leu et al., 2004b; Louchart et al., 2001).

A reliable spatial prediction of CSAs is necessary if site-specific mitigation measures like reduced application rates or changes in crop rotations should be implemented in practice. The relevant scale for a site-specific management of CSA is the sub-field to small subcatchment scale (i.e. fractions of a hectare to few hectares under typical Swiss conditions). However, there are only few comprehensive field data sets available that allow a quantification of spatial differences in herbicide losses at this scale (Gomides Freitas et al., 2008; Leu et al., 2004b). The quantification of spatial differences is not possible with conventional monitoring data because the different fields are usually not sprayed at the same day with the same substances. Therefore different weather conditions after application and different substance properties would strongly influence the results and prevent a meaningful spatial interpretation. To quantify spatial differences, a controlled application (same substances applied at the same day on different fields) and spatially distributed sampling are required.

In this paper we present the results of a controlled herbicide application in the catchment of a first order stream where we quantified the spatial differences of herbicide loss rates at the scale of fields and small subcatchments. We selected a catchment with a high

variability of soil types ranging from well-drained Cambisols to poorly drained Gleysols (high tendency for topsoil saturation) to test the hypothesis that the soil moisture regime determines the generation of fast flow (surface runoff and preferential flow to tile drains) and therefore the spatial variability of herbicide losses. Although soil texture and organic matter content did not vary to large degree across the catchment, the treated fields vary strongly in the percentage of areas with a high tendency for topsoil saturation and hence also in their drainage density. We therefore expected a high spatial variability of herbicide loss rates because previous studies in the region had demonstrated saturation-excess runoff is a major process for herbicide transport under the prevailing soil and climatic conditions.

In a previous paper (Doppler et al., 2012), we have demonstrated that the main process of herbicide mobilization and the initial transport mechanism is surface runoff on the fields. However, overland flow hardly reaches the stream directly but it is redirected into the wide–spread subsurface drainage systems. Surface connectivity to the open stream, which means a topographic situation such that surface runoff generated within the catchment can flow on the soil surface into the stream without being retained in a topographic depression, is very low in our catchment (4.4% of the area). However, hydraulic shortcuts like manholes in topographic depressions or storm drains on roads and farmyards establish the connectivity for surface runoff by routing it to subsurface drains or storm sewers connected to the stream. This direct connectivity is complemented by indirect connectivity which means that runoff may be transmitted through macropores to underlying drains (Doppler et al., 2012) from local depressions. Such conditions of direct and indirect connectivity are widespread in the Swiss Plateau.

This paper focuses on quantifying the spatial heterogeneity of herbicide losses within the catchment and investigates whether the spatial patterns observed can be explained by the site-specific factors and herbicide properties like dissipation rates.

3.2   Materials and Methods

3.2.1   Site description

The Eschibach catchment is located in the northeast of Switzerland (Fig. 3.1). The catchment area is $1.2\,\text{km}^2$, topography is moderate with altitudes ranging from 423 to 477 m above sea level. The twenty-year mean annual precipitation at the closest permanent measurement station (Schaffhausen, 11 km north of the catchment, 1989 − 2008) is 900 ± 165 mm (Meteoschweiz, 2009). The soils developed on moraine material with a thickness of around 10 m which is underlain by Freshwater molasse (Süsswassermolasse; (Einsele, 2000;

Swisstopo, 2007). Soils in the centre of the catchment are poorly drained Gleysols. Well drained Cambisols, and eroded Regosols are located in the higher parts of the catchment. Topsoil texture is rather homogeneous in the catchment with clay contents between 20 and 30% and silt contents of around 30% (FAL, 1997). The dominant land use is crop production (75% of the area), around 13% of the catchment is covered by forest, and a small settlement area is located in the southeast of the catchment. Forty seven percent of the agricultural land is drained by tile drains. The stream system consists of two branches, an open ditch that was partly built as recipient for the drainage water, and the main branch of the stream that runs in a culvert (Fig. 3.1). Further details on the catchment can be found in Doppler et al. (2012). Table 3.1 shows some soil characteristics of the experimental corn fields.
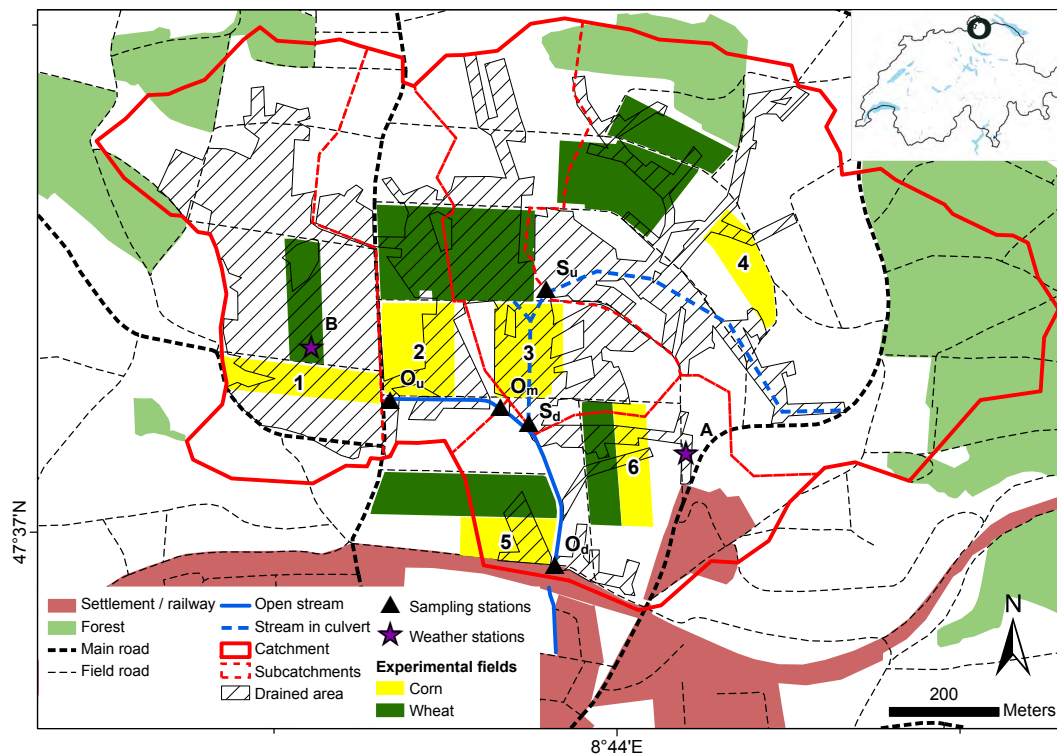
Figure 3.1: The Eschibach catchment with the experimental setup showing the stream system, the five sampling stations with their corresponding subcatchments (S_u and S_d: subsurface upstream and downstream, O_u, O_m and O_d: open upstream, middle and downstream), the weather stations A and B, land use, drained area and the experimental wheat and corn fields (experimental corn fields numbered 1 to 6). The small map depicts the location within Switzerland. Source: Gemeinde Ossingen (1995); Swisstopo (2008).

Table 3.1: Characteristics of the experimental corn fields.

	Size ha	% Gleysol	% Organic carbon
Field 1	1.6	20	2.2
Field 2	2.2	51	3.4
Field 3	2.1	54	3.1
Field 4	1.2	0	2.8
Field 5	1.3	19	3.0
Field 6	1.3	9	2.5
Total	9.7	30	2.9

3.2.2   Catchment delineation

The catchment boundary was calculated in ArcGIS (ESRI, 2009) based on the $2 \times 2\,\text{m}$ DEM (Swisstopo, 2003) and manually adapted after field observations. The topographical catchment does not coincide completely with the subsurface catchment. In some areas that belong to the topographical catchment, the tile drains divert the water out of the catchment. These areas were considered not to be part of the catchment in this study. The settlement area in the southeast was kept in the catchment, even though the water from impervious areas in the settlement leaves the catchment. The subcatchments of the discharge and sampling stations were delineated based on topography and the detailed tile drain map (Gemeinde Ossingen, 1995; Swisstopo, 2003). Subcatchments calculated from surface topography were not always congruent with the tile drain subcatchments. Priority was given to the tile drain catchments. This is a reasonable approach because of the low importance of direct transfer of surface runoff into the stream (Doppler et al., 2012).

3.2.3   Discharge measurement

We measured discharge at five locations in the catchment, where we continuously recorded water levels (ISCO 750 area velocity flow module, Teledyne Inc., Los Angeles, CA, USA and Keller PR-46X, KELLER AG für Druckmesstechnik, Winterthur, CH). To determine rating curves, we performed dilution experiments with NaCl. Additionally, we directly measured flow rates with a bucket and a stop watch where this method was applicable. The rating curves

$$Q = \alpha \times (h - \beta)^{\gamma} \tag{3.2}$$

have been based on 9 to 27 experiments per site where Q is discharge, h is the water level and α, β and γ are parameters (Herschy, 1995). At four sites (O_d, O_u, S_d, S_u,

see Fig. 3.1), we additionally measured discharge with a Doppler probe (flow velocity) and a pressure transducer (ISCO 750 area velocity flow module). Discharge was then calculated using the exact cross section of these sites. Discharge data from all stations were stored at five-minute intervals, either by the data logger of the sampler (ISCO 6700, ISCO 6712), or by an external data logger (CR10X; Campbell Scientific Inc., Loughborough UK). The two discharge measuring methods differed systematically, with the dilution experiment discharge being lower than Doppler probe discharge. In addition, the flow velocity measurement did not always produce usable signals during low flow, while data points from dilution experiments where scarce at high discharge. At the stations O_u and S_u, the final discharge series is composed of dilution experiment discharge for low flow and velocity measurement discharge for high flows because both methods alone did not yield satisfying results. At the two stations O_d and S_d both discharge series are credible over the entire flow range, we therefore have an estimate for the uncertainty in the discharge measurement (relative mean standard error being 29% and 30% at O_d and S_d, respectively).

Runoff ratios were calculated for seven individual events (E1 - E7; Fig. 3.2) after the controlled application of herbicides on corn (Sect. 3.2.5) by dividing the event discharge sum by the rain depth of the event. These events accounted for 78% of total rainfall and 59% of total discharge in the sampling campaign (the first two months after the corn application).
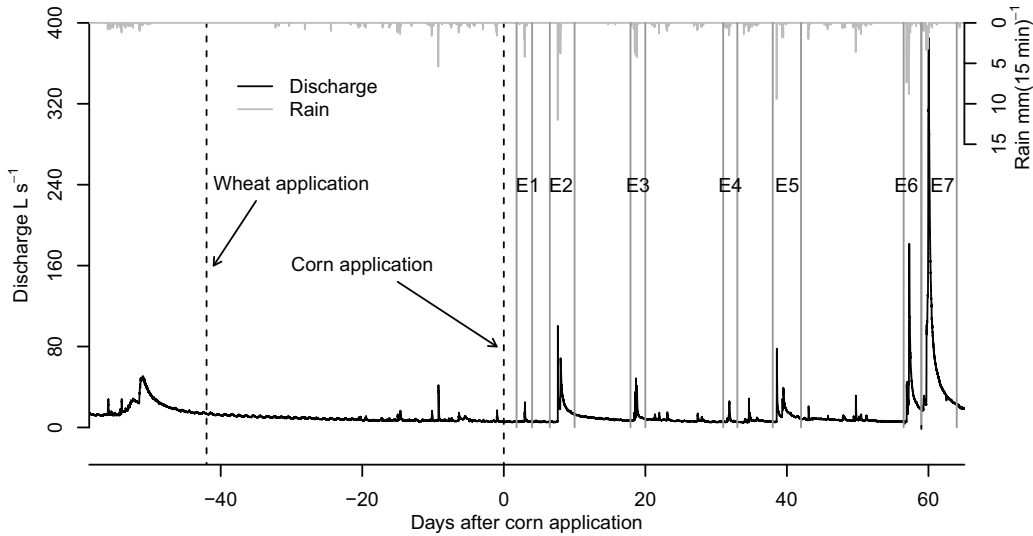
Figure 3.2: Discharge at the outlet of the catchment (station O_d) and precipitation during the experimental period. The sampled events are marked E1 to E7.

3.2.4 Weather stations

At weather station A (Fig. 3.1) precipitation was measured at 15 min resolution with a tipping bucket rain gauge (R102, Campbell Scientific Inc.). This rain gauge was out of order for 22 days (4 June 2009 to 25 June 2009). During this time, rain data from weather station B (Fig. 3.1) were used (a mobile HP 100 Station run by Agroscope Reckenholz-Tänikon with a tipping bucket rain gauge: HP 100, Lufft GmbH, Fellbach Germany). In two of the rain events (E2 and E5) we have rain data from both stations.

3.2.5 Herbicide applications

We performed two controlled herbicide applications in spring 2009, one on winter wheat (*Triticum aestivum* L., 7 April 2009), and one on corn (*Zea mays* L., 19 May 2009). For both crops, some fields within the catchment were selected as experimental fields (Fig. 3.1); all experimental fields of one crop were sprayed on the same day with the same spraying device and the same herbicide mixture. We applied isoproturon (3-(4-Isopropylphenyl)-1,1-dimethylurea, 500 g ha^{-1}) on the experimental wheat fields (14.2 ha or 11.8% of the catchment area), the other wheat fields (11.2 ha) received different herbicides. On the experimental corn fields (9.7 ha, Table 3.1), we applied the herbicides atrazine (1-Chloro-3-(ethylamino)-5-(isopropylamino)-2,4,6-triazine, 800 g ha^{-1}), S-metolachlor (2-Chloro-N-(2-ethyl-6-methylphenyl)-N-[(1S)-2-methoxy-1-methylethyl]acetamide, 960 g ha^{-1}) and sulcotrione (2-(2-Chloro-4-(methylsulfonyl)benzoyl)-1,3-cyclohexanedione, 450 g ha^{-1}). These substances were not used elsewhere in the catchment, except for S-metolachlor, which was accidentally applied on a sugar beet field (1.03 ha) close to corn field 4. On all other corn fields (18 ha), a mixture of terbuthylazine (N2-tert-butyl-6-chloro-N4-ethyl-1,3,5-triazine-2,4-diamine) and mesotrione (2-(4-mesyl-2-nitrobenzoyl)cyclohexane-1,3-dione) was applied.

To ensure the correct dose and concentration in the spray solution of the experimental fields, the experimental herbicides were weighed exactly before being mixed in the spraying tank. Samples from each tank filling were taken and analyzed to double check the correct application. The exact amount of spray solution applied on each field was determined by a flow meter mounted on the spraying equipment. A calibrated scale bar at the spraying tank was also used to estimate the applied volume per field in addition to the flow meter. The extent of the sprayed area was marked with wooden sticks; their exact locations were determined by a differential GPS (Leica GPS1200, Leica Geosystems AG, Heerbrugg Switzerland). With these control measures, the exact areas and applied rates are known for each field and each substance.

3.2.6 Water sampling and analysis

Water samples from stream and tile drains were taken at the five discharge measurement stations from 17 March 2009 to 22 July 2009. These five locations were sampled at high temporal resolution during rain events in the experimental period. The sampling strategy was similar to the one described in Wittmer et al. (2010). Time-proportional (15 min to hourly) samples were taken by automatic water samplers equipped with 24 polypropylene bottles (ISCO 2900, 6700, 6712 Teledyne Inc., Los Angeles USA). The samplers were triggered when a predefined water level was exceeded. Grab samples were taken during base flow periods. The seven events with the highest rain amounts (Events E1 to E7 in Fig. 3.2) were selected for analysis and a sufficiently high number of samples were analyzed in each event to adequately represent the dynamics of the chemograph. At the stations O_u, O_d, S_u, and S_d we have samples from all seven events. Sampling station O_m was out of order during events E4 and E5. In addition to the event sampling, we also took samples at the day of the two controlled herbicide applications, where the main input pathway was spray drift.

The samples were analyzed by online solid-phase extraction (SPE) coupled to liquid chromatography followed by a triple quadrupole mass spectrometer (LC-MS/MS) according to Singer et al. (2010). The samples were filtered through glass-fiber filters (GF/F, $0.7\,\mu$m, Whatman) and isotope-labeled internal standards for all compounds were spiked to 50 mL of filtered sample. Sample enrichment was achieved on a Strata-X extraction cartridge ($20 \times 2.1\,$mm I.D. $33\,\mu$m particle size, Phenomenex, Brechbühler AG, Schlieren, Switzerland). LC separation was performed on an XBridge C18 column ($50\,$mm $\times 2$, Waters, Baden-Dättwil, Switzerland), and detection by a TSQ Quantum triple quadrupole MS (Thermo, San Jose, CA, USA). The limit of detection (LOD) was in the range of 1 to $5\,$ng$\,$L^{-1} for all compounds; LOQ were between 2, 6 and $15\,$ng$\,$L^{-1} for isoproturon, atrazine and metolachlor, and for sulcotrione, respectively. Quality control consisted of aliquots of spiked and un-spiked environmental samples analyzed with each analytical run. The resulting inter-day precision of the method (relative standard deviation of these repeated measurements) was 5 to 12% for our compounds. The average recovery for each analyte was between 101 and 105%. Further details to the water sampling and analysis can be found in Doppler et al. (2012).

3.2.7 Soil sampling and analysis

From each of the six experimental corn fields (Fig. 3.1), we took topsoil samples consisting of 20 subsamples each (top 5 cm) on seven dates: before herbicide application, directly

after application and on days 3, 7, 15, 30 and 60 after application. The samples were stored at $-20\,°C$, crushed with a hammer mill and kept at $-20\,°C$ until further analysis. Further details can be found in Doppler et al. (2012). We did not take soil samples from the wheat fields.

Herbicide concentrations were measured in all soil samples using two different extraction methods. The total soil concentration was measured by pressurized liquid extraction (PLE) using an ASE 350 Accelerated Solvent Extractor (Dionex, Sunnyvale, CA). Extraction took place with a solvent mixture of acetone : 1% phosphoric acid, 70:30 (volume ratio) at $100\,°C$. To receive a proxy for the pore water concentration, we analyzed the solution obtained by centrifugation of the soil sample after re-adjusting the water content (Doppler et al., 2012).

Analysis of both extracts (PLE and pore water) was done with liquid chromatography coupled to a triple quadrupole mass spectrometer (LC-MS/MS). Compounds were separated by reversed-phase LC using a Synergi C18 polar RP column ($100 \times 3\,mm$ ID, $2.5\,\mu m$ particle size, equipped with an inline-filter, Phenomenex, Torrance, CA, USA) and detected by a TSQ Quantum triple quadrupole MS (Thermo, San Jose, CA, USA). The LOQ was set to $2\,ng\,mL^{-1}$ (corresponding to about $1\,ng\,g^{-1}$ of dry soil) for all compounds (the concentration of the lowest calibration standard). Recoveries were above 70% for PLE and above 75% for the pore water extracts. The full details to the soil sampling and analysis can be found in Camenzuli (2010).

Half life calculation

We calculated the herbicide's half-life in soil based on the total soil concentrations (corresponding to the concentration measured with PLE) assuming first-order kinetics. Dissipation of sulcotrione on all fields and of atrazine and S-metolachlor on some fields slowed down after day 30. For these cases only concentration data until day 30 were used for the calculation of the half-lives while for the other cases all data points (until day 60) were used.

Distribution coefficients

The distribution of the herbicides between the dissolved and the sorbed phase was expressed by the apparent distribution coefficient K_d [L kg^{-1}] in all soil samples:

$$K_d = \frac{C_{\mathrm{sorbed}}}{C_{\mathrm{porewater}}} = \frac{C_{\mathrm{PLE}} - \left(\frac{V_{\mathrm{water}}}{M_{\mathrm{solid}}} C_{\mathrm{porewater}} \right)}{C_{\mathrm{porewater}}} \qquad (3.3)$$

C_{PLE} [ng kg^{-1}] is the concentration obtained by PLE expressed per mass of dry soil, $C_{\mathrm{porewater}}$ [ng L^{-1}] is the measured pore water concentration in the water phase, V_{water} [L] is the pore-water volume and M_{solid} [kg] is the mass of dry soil.

3.2.8 Load and loss rate calculation

Herbicide loads were calculated by linearly interpolating the concentration time series at the sampling stations. Where necessary, additional data points with baseflow concentrations were added to the concentration time series at the beginning and end of events to avoid interpolation artifacts. By multiplying the interpolated concentration time series with discharge, we obtained the herbicide loads at the five sampling sites. The uncertainty in the discharge measurement (Sect. 3.2.3) does also affect the load calculation. To assess the uncertainty in the calculated loads, we calculated the loads with the two different discharge time series that were available at the stations O_{d} and S_{d} (Sect. 3.2.3) and used the relative deviation to assess the uncertainty at the other sampling sites. When concentrations were below the limit of quantification (LOQ) we calculated minimum and maximum possible loads. For the minimum estimate, we set concentrations below LOD to 0 and concentrations below LOQ were set to LOD. For the maximum load estimate we set values below LOD to LOD and values below LOQ to LOQ. The load uncertainties originating from discharge uncertainty were about ten times higher than the uncertainties from treatment of values below LOQ. The loads shown in this paper are the average of the minimum and maximum load calculations, the error bars show the highest and the lowest load obtained by these calculations. The relative errors of the loads are in the range of $\pm$ 20% which is in line with the findings by Gomides Freitas et al. (2008). However, the calculated loads contain additional uncertainty that originates from the concentration time series interpolation and from the concentration measurement itself. We did not include loads of individual events into the analysis, when most samples within the event had concentrations below LOQ, because these values are too uncertain for a meaningful interpretation. This was especially the case for sulcotrione (the substance with the fastest dissipation) at the end of the sampling period.

For events with samples from all the sampling sites and sufficiently high loads at all the sampling sites (events E2, E3, E6 and E7) we calculated loads for individual corn fields by subtracting subcatchment loads from each other. Details of this calculation can be found in the supporting information.

From the total loads we calculated two different types of loss rates for the herbicides. The loss rate relative to the applied amount was calculated by dividing the load by the

applied herbicide amount. From the total soil concentrations (PLE), we estimated the total available herbicide amount on the experimental fields right before the events by linearly interpolating the time series of soil concentrations. We could therefore also calculate loss rates of single events relative to the substance amount that was available on the field.

3.3   Results

3.3.1   Herbicide Dissipation and Sorption

Half lives and distribution coefficients of the herbicides strongly influence their transport behavior. The mean half life of the six fields was longest for S-metolachlor, followed by atrazine and sulcotrione; sorption was strongest for S-metolachlor followed by atrazine and sulcotrione(Table 3.2 and Tables A.1 to A.4 in the Appendix). Table 3.2 also shows the increase of the apparent distribution coefficient during the experiment showing that sorption became stronger with time for all substances (similar as reported by Gomides Freitas et al. (2008); Mamy and Barriuso (2007)). This effect was most pronounced for sulcotrione, followed by atrazine and S-metolachlor. The sorption increase differed strongly between the different fields.

Table 3.2: Average half lives and average apparent distribution coefficients (and standard deviation) of the three corn herbicides, on the six experimental fields.

		K_d [L kg^{-1}]					
	Half life [d]	Day 0	Day 3	Day 7	Day 15	Day 30	Day 60
Atrazine	9.5 ($\pm$ 2.0)	1.1 ($\pm$ 0.3)	0.8 ($\pm$ 0.2)	1.0 ($\pm$ 0.3)	2.0 ($\pm$ 0.6)	4.3 ($\pm$ 1.8)	16.5 ($\pm$ 9.1)
S-metolachlor	13.8 ($\pm$ 3.3)	2.0 ($\pm$ 0.4)	2.0 ($\pm$ 0.3)	2.1 ($\pm$ 0.5)	2.5 ($\pm$ 0.6)	3.6 ($\pm$ 0.8)	6.9 ($\pm$ 1.2)
Sulcotrione	5.5 ($\pm$ 0.7)	0.1 ($\pm$ 0.1)	0.1 ($\pm$ 0.1)	0.2 ($\pm$ 0.1)	0.5 ($\pm$ 0.1)	0.8 ($\pm$ 0.2)	2.9 ($\pm$ 1.6)

3.3.2   Concentrations, loads and loss rates at the catchment outlet

After the herbicide application on wheat, the weather was rather dry. In total 66 mm of rain, distributed in many small events, were recorded during the 42 days between wheat and corn application. These events did not cause a hydrological reaction beyond road runoff (Fig. 3.2). In contrast, after the corn application, several rain events caused considerable discharge. These events encompass a broad range of intensities, magnitudes and antecedent conditions (Table 3.3).

The different precipitation conditions after the wheat and corn herbicide application, respectively, were clearly reflected in the observed concentrations and loads of the respective

Table 3.3: Hydrological characteristics of the sampled events after the application of corn herbicides with precipitation characteristics, average antecedent soil moisture in 10 cm depth, the average groundwater (GW) level before the event and runoff ratio. For details to the piezometers and soil moisture measurements see Doppler et al. (2012).

Event	Rain depth	Max intensity	Antecedent soil moisture	Average GW level before event below surface	Runoff ratio
	(mm)	$mm\,(15\,min)^{-1}$	(v/v)	(m)	(%)
E1	9.8	4.2	0.22	1.17	6
E2	45.6	12.0	0.2	1.2	8
E3	22.2	4.2	0.2	1.13	10
E4	18.2	1.6	0.21	1.25	9
E5	36.8	9.4	0.3	1.2	12
E6	51.6	8.8	0.24	1.28	12
E7	57	3.4	0.31	0.82	37

herbicides. The dry weather conditions after the application of isoproturon on wheat resulted in low isoproturon concentrations and loads. The first rain event with a significant discharge reaction (E2, see Fig. 3.2) occurred 50 days after application. Most of the applied isoproturon had dissipated by then (the typical time needed to degrade 90% of isoproturon (DT90) in field soil is 51 d (PPDB, 2010)) and the concentrations in the stream were mostly below the quantification limit. The maximum isoproturon concentration was measured during the application day and amounted to $110\,ng\,L^{-1}$ at station O_d. This input was most probably caused by drift from the two fields closest to the open stream (Fig. 3.1). The maximum estimate for the isoproturon loss rate from the whole catchment relative to the applied amount is 0.005%.

In contrast, much larger concentrations of the corn herbicides were observed during the corn herbicide application day (up to $1820\,ng\,L^{-1}$) and during the seven discharge events (up to $13'000\,ng\,L^{-1}$, see Table 3.4). Accordingly, the loads of the corn herbicides of the whole catchment summed up over the experimental period were much higher than the isoproturon load in absolute and in relative terms. They amounted to 20.9 ± 2.6 g for atrazine, 15.3 ± 1.9 g for S-metolachlor and 11.6 ± 1.3 g for sulcotrione. This corresponds to loss rates (relative to the applied amount) of $0.26 \pm 0.03\%$ for atrazine, $0.16 \pm 0.02\%$ for S-metolachlor and $0.26 \pm 0.03\%$ for sulcotrione.

Figure 3.3 shows the cumulative loads of the three corn herbicides at the outlet of the catchment together with cumulative rain and discharge for the period after corn appli-

Table 3.4: Maximum concentrations of the three corn herbicides during application day and the seven events at the catchment outlet (station O_d).

	Maximum concentration [μg L^{-1}]		
	Atrazine	S-metolachlor	Sulcotrione
Application day	1.82	0.67	0.24
E1	1.56	0.84	0.20
E2	13.0	9.96	7.4
E3	3.29	2.57	0.47
E4	0.067	0.1	0.008
E5	0.59	0.93	0.061
E6	0.08	0.075	0.006
E7	0.075	0.12	0.007

cation. The figure clearly reveals that event E2 was the major loss event for all three substances. This event delivered 63% of the total atrazine load; for S-metolachlor and sulcotrione it contributed 62% and 91% respectively. This highlights the importance of the first rain event after application that causes a significant hydrological response (Fig. 3.2). Also the concentrations were by far the highest during this event (see Table 3.4).

Despite the concentrations observed, the application day was of minor relevance for the herbicide loads. Only 1.4% (atrazine), 0.8% (S-metolachlor) and 0.4% (sulcotrione) of the total loads were lost during the application day.

3.3.3   Loss rates relative to available amount

Figure 3.4 shows the loss rates of the corn herbicides for the whole catchment expressed as percentage of the substance amount that was available in the soil directly before the event. The PLE concentration (total concentration) was used as proxy for the available amount (Section 2.8). Because the dissipation rate of the substances does not influence the loss rate expressed as percent of available amount, differences between substances are only caused by their sorption properties. Figure 3.4 shows that the susceptibility of the substances to be transported changed with time. Sulcotrione had a higher initial mobility relative to atrazine and S-metolachlor. This pattern, however, changes through time. In the events E3 and E5, the sulcotrione loss rate relative to the available amount is similar to the atrazine loss rate. The ratio between atrazine and S-metolachlor however, remains stable throughout the sampling period.

Figure 3.4 also allows comparing the different rain events in their ability to transport
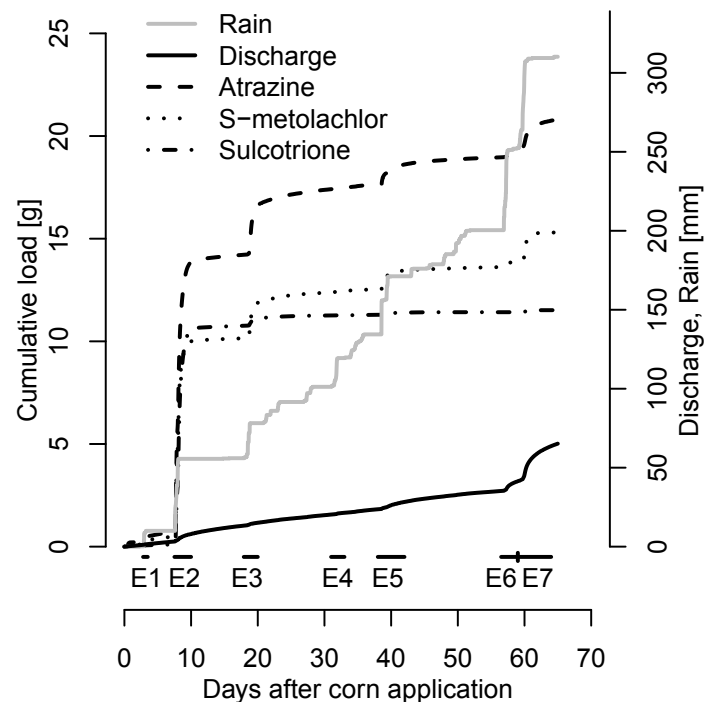
Figure 3.3: Cumulative rain, discharge and corn herbicide loads at the outlet of the catchment (Station O_d).

herbicides without the influence of herbicide dissipation. Events E2 and E7 clearly had the highest transport power and events E1 and E4 the lowest. It is interesting to note that E7, occurring 60 d after herbicide application, exhibited the largest loss rate relative to the amount extractable in the soil. It was the largest rainfall event after the herbicide application and resulted in the highest runoff ratio (37%, Table 3.3). Obviously, these hydrological conditions mobilized more of the available herbicides than more intensive rainfall events like E2 and E6, for which the antecedent soil moisture and the groundwater level were lower (Table 3.3).

3.3.4   Spatial variability of loss rates

Figure 3.5 shows the total loss rates relative to the applied amount at the different sampling sites representing different fields. The loss rates of atrazine and sulcotrione were very similar to each other at all the stations, while S-metolachlor showed lower loss rates at all sites. The figure also shows that the stations S_d (fields 3 and 4), O_m (fields 1 and 2) and the full catchment (station O_d) had similar loss rates for all the substances, while the loss rates at S_u (only field 4) and O_u (only field 1) were lower by about a factor of two.
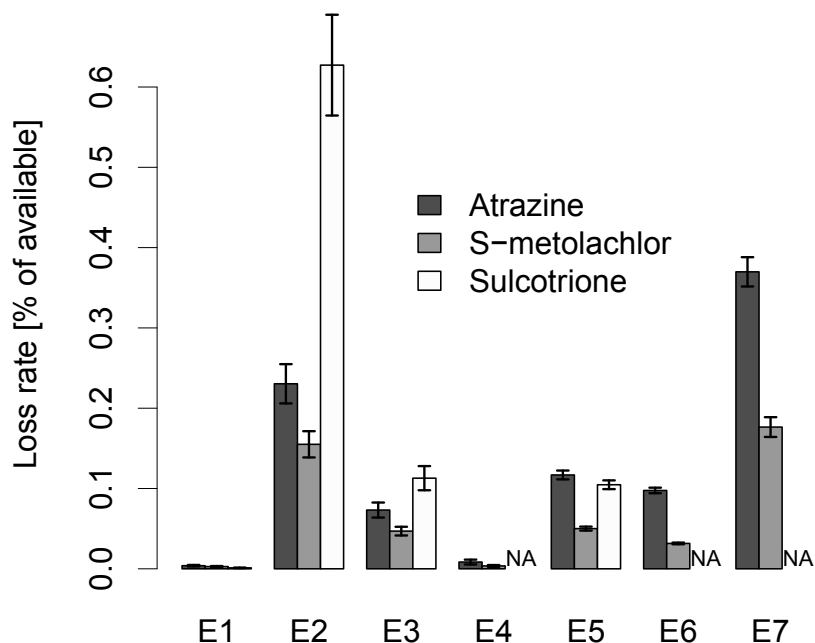
Figure 3.4: Loss rates (percent of available) of the whole catchment for the seven events (NA = too many sulcotrione concentrations < LOQ. Minimum and maximum estimations for sulcotrione loss rates are 0.0034 to 0.011% in E4, 0.015 to 0.063% in E6 and 0.11 to 0.38% in E7). The error bars represent the uncertainty in the loss rate calculation, see Section 3.2.8 for explanation.

In Fig. 3.6 the spatial variations of atrazine loss rates relative to the applied amount are shown for individual events (the same figure for S-metolachlor and sulcotrione can be found in the Appendix (Figs. A.3 and A.4)). Since event E2 was the most important loss event, the spatial pattern of the entire period (Fig. 3.5) strongly resembles the pattern of event E2 in Fig. 3.6. Moreover, Fig. 3.6 shows that the spatial pattern of loss rates can change from event to event. In some of the events the loss rates in the subcatchments are similar (e.g. E6, maximum difference of a factor 1.6 between O_m and O_d) while the spatial differences are more pronounced in other events (e.g. E3, maximum difference of a factor 5.5 between S_u and O_d). Furthermore the relative order of the subcatchments changes in different events (compare e.g. E1 and E7). However, the entire catchment (O_d) always shows comparatively high loss rates in all events. This is only explicable if the fields 5 and 6 always have above-average loss rates (Fig. 3.1). For a more detailed spatial
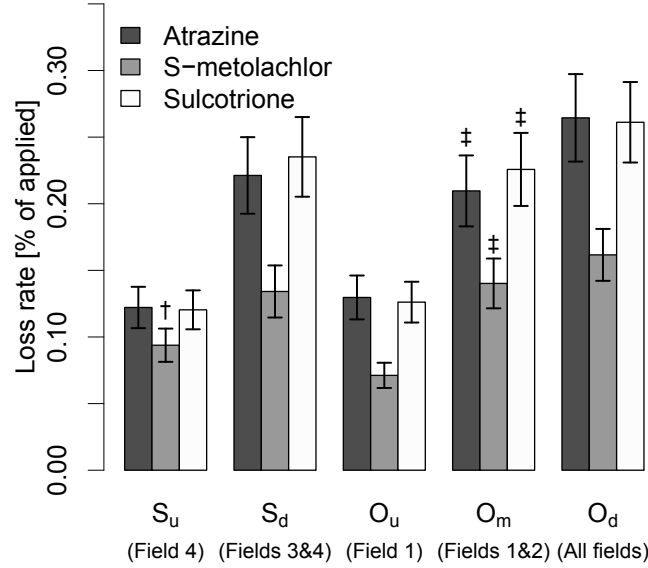
Figure 3.5: Loss rates (relative to the applied amounts) of the three corn herbicides from the experimental period at the five sampling sites. † Loss rate of S-metolachlor overestimated because of the accidental treatment of sugar beet field in the catchment of S_u (Sect. 3.2.5). ‡ Loss rates of the station O_m are underestimated because of the two missed events (Sect. 3.2.6). The error bars represent the uncertainty in the loss rate calculation, see Section 3.2.8 for explanation.

analysis, we therefore subtracted the subcatchment loads from each other to receive loss rates of individual fields (see Eq. A.2 in the Appendix for details of the subtraction). This was only possible for the four events (E2, E3, E6 and E7) where load data from all the stations were available (see Figure 3.7 for atrazine; the same figure for S-metolachlor and sulcotrione can be found in the Appendix (Figs. A.5 and A.6)).

This more detailed spatial analysis shows that the spatial variability is more pronounced at field scale than at the subcatchment scale (in E3 loss rates of Field 4 and Fields 5, 6 differ by a factor of 10.6). However, in the events E2, E6 and E7 the differences between the field with the highest and lowest loss rate was around a factor of three. Again the spatial pattern varies between the events. The spatial patterns of S-metolachlor and sulcotrione at subcatchment and field scale were similar to those of atrazine. They can be found in the Appendix (Figs. A.5 and A.6).

The observed spatial differences of the loss rates cannot be explained by the uncertainty of the loss rate estimates (about 20% for each site). Even if one keeps in mind that there
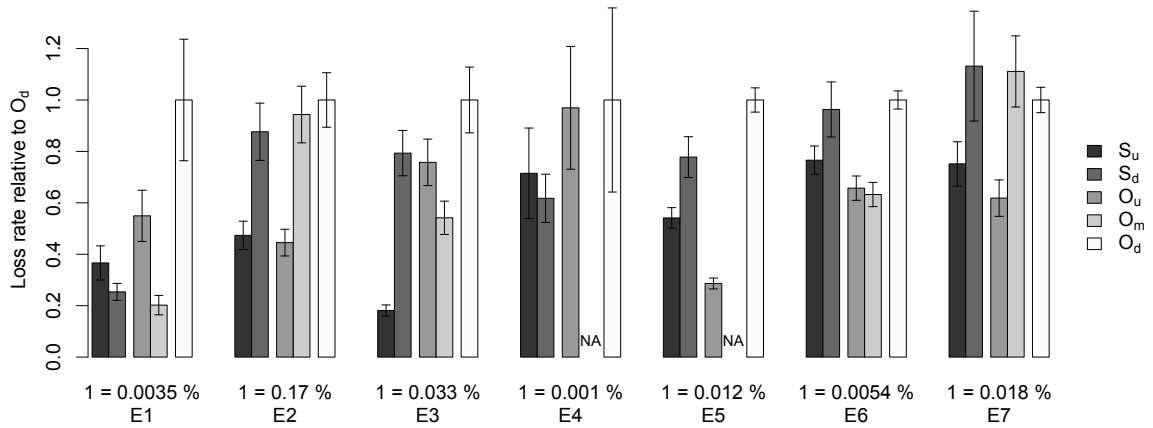
Figure 3.6: Spatial variability of atrazine loss rates in the seven sampled events. The loss rates of the subcatchments in each event are normalized to the loss rate of the full catchment (Station O_d) in the respective event (absolute values above event number). (NA = no samples from station O_m). The error bars represent the uncertainty in the loss rate calculation, see Section 3.2.8 for explanation.

are additional uncertainties in the load calculation, which are not included in the error bars (e.g. interpolation of the concentrations), the magnitude of spatial differences were most likely no artifacts of the measurement uncertainty. According, there is the question about the causes behind these spatial patterns.
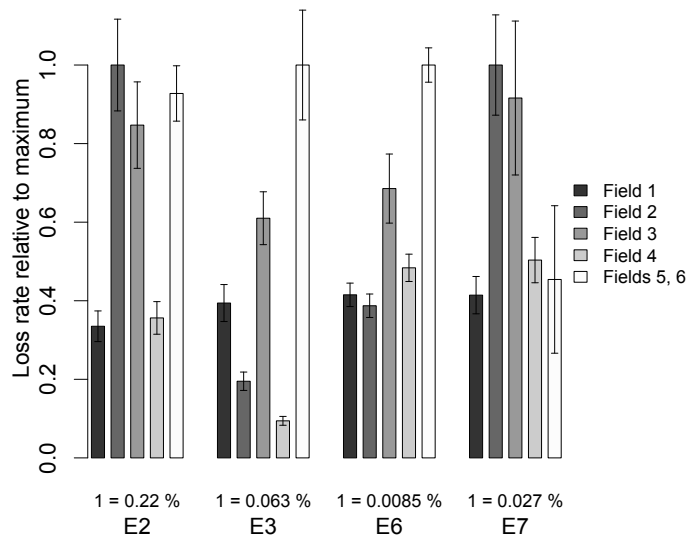
Figure 3.7: Spatial variability of atrazine loss rates in four events at field scale. The loss rates of the experimental fields are normalized to the loss rate of the field with the highest loss rate in the respective event (absolute values given above event number, in events E2 and E7 normalization to field 2, in E3 and E6, normalization to fields 5,6). The error bars represent the uncertainty in the loss rate calculation, see Section 3.2.8 for explanation.

3.4 Discussion

3.4.1 Overall loss behavior

The total loss rates of the corn herbicides were in the range of values reported in literature (Capel and Larson, 2001). However, they were rather low compared to loss rates measured in similar field studies in the Swiss Plateau (Gomides Freitas et al., 2008; Leu et al., 2004b, 2005) summarized in Table 3.5. Even though the weather conditions were not exceptionally dry during this study, and the event causing the main losses occurred only one week after the application, the total atrazine loss rate was clearly lower than in the other studies. The most probable reasons are the hydrological behavior of the treated corn fields and their connectivity to the stream. In the study by Leu et al. (2004b) the percentage of Gleysol (high tendency for runoff generation) on the treated fields was 72% while this soil type only covered 30% of the treated fields in our study (Table 3.1). Furthermore, some of the corn fields were fully connected to the stream in the study of Leu et al. (2004b) (Frey et al., 2009) while surface connectivity was very low in our catchment (only 4.4% of the entire area; (Doppler et al., 2012)). These differences between our study catchment and the region of the studies by Leu and Gomides Freitas are in line with the findings by Siber et al. (2009), who showed that the hydrological risk for herbicide losses is lower in the region of our study. Even though the loss rates were relatively low, we measured large herbicide concentrations in the stream (Table 3.4). A major reason for this is the high area percentage of treated corn fields in the catchment (8% of the catchment area).

Table 3.5: Comparison of atrazine loss rates and rain amounts in the two months after application in different field studies.

Location and year of study	Rain [mm]	Loss rate atrazine [% of applied]	Source
Isert 1999	512	0.6	Leu et al. (2005)
Tägernau 1999	512	0.7	Leu et al. (2005)
Ror 1999	512	3.5	Leu et al. (2005)
Ror 2000	260	0.82	Leu et al. (2004b)
Summerau 2003	377	1.3	Gomides Freitas et al. (2008)
Eschibach 2009	310	0.29	This study

3.4.2   Influence of sorption

The observation that the mobility of sulcotrione decreased relative to atrazine and S-metolachlor (Fig. 3.4) suggests that herbicide losses are affected by the increase in sorption strength over time (Table 3.2) where sulcotrione shows the strongest increase of the three substances. Sorption can influence herbicide losses either during mobilization from the fields or during transport. The increasing sorption on the fields with time can only influence the herbicide mobilization but not the transport of already dissolved herbicides. The shift in loss rates can therefore only be explained by the mobilization. This means that the mobilization of the substances from soil to overland flow - the main initial transport mechanism, even though it mostly reached the stream after being transferred into subsurface drains by macropores or shortcuts - is strongly affected by sorption. This result contradicts findings in an earlier paper (Doppler et al., 2012) suggesting that the mobilization was not affected by sorption. One tentative explanation for this apparent contradiction is the overland flow sampling performed and analyzed by Doppler et al. (2012). Most likely the sampled overland flow consisted of the first flush, and was not representative of the total flow of herbicide contaminated water entering the stream within an event, which is analyzed in this paper. Possibly the kinetics of the desorption process affected the overland flow samples and the stream flow samples over the entire event to different degrees.

3.4.3   Spatial differences

Earlier studies in the Swiss Plateau suggested that factors controlling the extent of the hydrologically active areas (A_{active}) and connectivity of fast flow to the stream (A_{connect}) determined the spatial heterogeneity of herbicide losses (Gomides Freitas et al., 2008; Leu et al., 2004b). However, these factors are static in time and cannot explain by themselves the observations reported here that the spatial patterns changed between events. Indeed, the loss rates of the individual fields in our study did neither correlate with the area percentage of Gleysols (high tendency for topsoil saturation; see Figs. A.7 to A.9 in the Appendix) nor with the drainage density or direct surface connectivity (see Figs. A.10 to A.15 in the Appendix).

Two factors that could explain changing patterns in time are herbicide dissipation rates and sorption affinities in the different soils. In the literature, it has been reported that spatial heterogeneity of herbicide dissipation rates and sorption affinities to soil can be relevant for spatial risk of herbicide losses (Ghafoor et al., 2011a,b). Indeed, the rate of herbicide dissipation varied between fields (see Table 3.2) as did the sorption strength of

all three compounds in this study. If these factors were the dominant causes of the spatial heterogeneity of loss rates in our study, one would expect that the loss rates would increase with decreasing dissipation rates and loss rates would decrease with increasing sorption. However, the data do not reveal any relationship pointing into this direction (see Figs. A.16 to A.21 in the Appendix).

Another factor that varies between events is rainfall. One the one hand, spatial heterogeneity of rainfall itself could cause spatially heterogeneous herbicide losses. For events E2 and E5 we have data from both weather stations showing that precipitation was rather homogeneous in event E2 (9% less in weather station B) while in event E5, weather station B had 35% less precipitation. This could explain the differences in the spatial pattern of loss rates between these events. The subcatchments O_u (close to weather station B) and S_u (close to weather station A) have similar loss rates in event E2, but in event E5, subcatchment O_u (with less rain) shows lower loss rates than S_u (see Fig 3.6 for the loss rates and Fig. 3.1 for the spatial setup).

On the other hand, rainfall could induce spatially variable herbicide losses despite being rather homogeneous in space during single events. This could happen if different rainfall events trigger different transport mechanisms, which occur on different fields within the catchment. Several field observations and measurements demonstrated that most events (E1 - E6) predominantly triggered infiltration-excess runoff, while the last event (E7) was dominated by saturation-excess overland flow. This interpretation is supported by the intensity of the rainfall events, the runoff ratios, data on electrical conductivity in overland flow samplers and visual inspection of the fields after the events (Doppler et al., 2012). These data reveal also that overland flow did not occur on all fields to the same degree during all events. Based on these observations, we conclude that the type of rain event influenced the spatial pattern of herbicide losses. This means that the CSAs are not a temporally stable property of the site. They change location with the type of rain event but also due to changes of surface properties of soils due to land management for example.

Compared to similar studies, the spatial differences of loss rates were rather small in this field study. Leu et al. (2004b) calculated herbicide loss rates in a $2.1 \, \text{km}^2$ catchment which they divided into three subcatchments. Two of the subcatchments differed by about a factor of 18 in atrazine loss rates during the main loss event (for dimethenamid it was a factor of 56). Gomides Freitas et al. (2008) found similar spatial differences in the same catchment in another year. In our study, the spatial difference of atrazine loss rates was only about a factor of three in the main loss event (E2) and one may wonder how these differences between different catchments (or years?) come about. The large differences could be explained with the topography of the fields, surface connectivity to the stream,

and the geology of the fields in the subcatchments (Frey et al., 2009; Leu et al., 2004a). On the one hand, the fields with the highest loss rates were prone to saturation-excess runoff and had a direct connection to stream with minimal retention in-between. On the other hand, the fields with the lowest loss rates, were too flat for overland flow to reach the stream and the soils had a well-drained subsoil preventing any topsoil saturation (Gomides Freitas et al., 2008).

In contrast, no such differences regarding controlling factors could be detected in our study catchment. Direct surface connectivity is low for all the experimental fields and the geology determining the lower boundary conditions of the soil profiles is very homogeneous (Swisstopo, 2007). Based on these comparative aspects we conclude that the large spatial differences found by Leu et al. (2004b) within a small catchment may be rather the exception than the rule and spatial differences in the order of a factor of three can be expected on the scale of fields or small subcatchments. However, small scale hotspots for herbicide losses (in the order of 10 x 10 m) as found by Gomides Freitas et al. (2008) could also have been present in our study. But the scale of our study was too coarse to detect these small scale differences.

3.5   Conclusions

It seems that the spatial variability of the risk for diffuse herbicide pollution can be reasonably well predicted on a regional scale (Siber et al., 2009). However, for management purposes, predictions need to be at field scale or smaller. Our results suggest that such predictions based only on existing data are difficult at the (sub-)field scale, because there is no simple correlation between site properties and herbicide losses. This is especially true if the spatial pattern of loss rates depends on the type of rain event and the CSAs are therefore not temporally stable. Given the complexity of the processes and the coarse resolution of the available data it may be more promising delineating CSAs in the field by experts from local extension services who are also familiar with the local pedology.

Such delineations however are quite difficult to achieve especially when considering the temporal changes in loss behavior reported in this paper. Instead of deriving complex decision systems for such CSA delineations we suggest focusing on interrupting connectivity for fast flow. In catchments as presented here, connectivity is rather stable in time because it is strongly influenced by artificial changes to the flow pathways like e.g. hydraulic shortcuts in depressions. This implies that irrespective of where exactly runoff is generated within the catchment preventing surface runoff from directly entering surface waters by interrupting such direct flow paths will always have an effect. Hence, it is a ro-

bust measure in areas where overland flow is routed to the streams via artificial pathways within the catchment.

Chapter 4

Validating a spatially distributed hydrological model with soil morphology data

Tobias Doppler, Mark Honti, Urs Zihlmann, Peter Weisskopf and
Christian Stamm

T. Dopplers contribution to this chapter: Field measurements; GIS analysis; selection of
model concept and setup; model calibration and model run; analysis and interpretation of
the results; writing.

4.1   Introduction

Spatially distributed hydrological models are popular tools in hydrology. They are claimed to be useful for supporting decisions in water resources management (e.g. Agnew et al., 2006; Frey et al., 2009; Heathwaite et al., 2005; Lyon et al., 2006). Despite the high spatial resolution of the computed variables, calibration and validation is often carried out only on discharge time–series at specific locations due to the lack of spatially distributed reference data (Srinivasan and McDowell, 2009). Furthermore, distributed models typically have a large computational demand because calculations are performed on several ten or hundred thousand cells. This huge resource requirement prevents meaningful uncertainty analysis that would require ten thousands of model runs. The predictive power of these models, with regard to predicted spatial patterns, can usually not be judged because of these restrictions.

An application of spatial predictions in hydrology is the prediction of critical source areas (CSAs) for diffuse pollution in agricultural areas. Herbicides are compounds for which diffuse pollution is important. Herbicides are widely used in agriculture and they can enter streams during rain events (e.g. Domagalski et al., 2008; Leu et al., 2004a; Rabiet et al., 2010; Thurman et al., 1991; Wittmer et al., 2010), where they can harm aquatic organisms even in low concentrations. Small streams in catchments with intensive crop production are especially at risk (Liess and Schulz, 1999), as diffuse pollution from agricultural fields causes major inputs to the stream in these areas (Leu et al., 2010). Several studies have shown that the contributions of different fields within a catchment to the total herbicide load in the stream can differ significantly (Gomides Freitas et al., 2008; Leu et al., 2004b; Louchart et al., 2001). This implies that a relatively small proportion of a catchment can cause the major part of surface water pollution with herbicides. These areas are called critical source areas or contributing areas (Pionke et al., 1996). An area has to fulfill three conditions to become a critical source area: (1) The area needs to be a substance source; for herbicides all treated arable fields are source areas. (2) The area has to be hydrologically active. For herbicides, this means areas where surface runoff and/or macropore flow occur. (3) The area has to be connected to the stream; for herbicides this implies that the overland flow or macropore flow with the mobilized herbicides has to reach the stream without re–infiltration within the catchment (Pionke et al., 1996).

If CSAs can be reliably predicted, this offers efficient mitigation options, because actions on a small proportion of the area can strongly reduce the substance input to the stream. Basically there are two strategies to identify CSAs. They can be identified in the field or predicted with a model that captures the dominant features of the underlying mechanisms. The identification in the field is rather time consuming; it requires extensive field visits by

experts and interviews with the local farmers. A model prediction can have advantages over the field identification with respect to the consistency of the CSA identification in a larger area and time demand.

Several studies have been carried out to predict CSAs for different substances (nutrients, pesticides and sediment) on field and catchment scale (e.g. Agnew et al., 2006; Heathwaite et al., 2005; Lyon et al., 2006; Srinivasan and McDowell, 2009) with a variety of different modeling approaches (see Borah and Bera, 2003, for review on model concepts for diffuse pollution). Process based models were found to be more suitable for CSA prediction by Srinivasan and McDowell (2009).

If the herbicide application patterns are known, the prediction of CSAs for herbicides reduces to a purely hydrological problem where the hydrologically active areas and their connectivity to the stream have to be predicted. In this paper we focus on the prediction of areas that can become saturated and produce saturation excess overland flow because of high groundwater levels. Previous studies have demonstrated the relevance of this process for herbicide transport under conditions prevailing in the Swiss Plateau (Leu et al., 2004a). In contrast to areas where infiltration excess overland flow occurs, the locations of saturation excess overland flow areas on agricultural fields are temporally more stable across rainfall events of similar magnitude. This is because saturation excess areas on agricultural fields do not strongly depend on the land management and soil coverage. They are more influenced by their topographic position and hydrological subsoil properties (Doppler et al., 2012; Gerits et al., 1990; Lyon et al., 2006).

A main problem with the prediction of CSAs is the lack of spatial data on hydrological state variables. Predicting hydrological conditions that generate CSAs would require a physically-based, fully distributed modeling of catchment hydrology. Such models - like SHE (Abbott et al., 1986) and its derivatives - could theoretically be applied without calibration given full catchment information. However, since it is not possible to get full spatial information on catchment structure and status and because there are still considerable knowledge gaps (Refsgaard et al., 2010), spatially distributed models are often calibrated on aggregate data (like discharge measurements at specific locations). However, the model parameters and even the model structure are only poorly identifiable when no spatial data are used for calibration (Grayson et al., 1992a,b). For several versions of the semi-distributed TOPMODEL it was shown that especially the transmissivity parameter can be better identified if spatial data on groundwater levels or saturated areas were included for calibration (Blazkova et al., 2002; Franks et al., 1998; Freer et al., 2004; Gallart et al., 2007; Lamb et al., 1998).

Soil maps are a spatial data base that exists for many locations. Besides soil texture infor-

mation, also the qualitative information on soil types contained in soil maps can be used in the context of hydrological models. Hrachowitz et al. (2013) state that hydrologically meaningful soil classification schemes are valuable for hydrological modeling. Boorman et al. (1995) developed the system of Hydrology Of Soil Types (HOST) where soils in the UK are classified according to a conceptual understanding of the water movement in these soils. It was shown that the HOST soil classes are related to the base flow index (the proportion of base flow on total stream flow). This system was successfully implemented in a hydrological model (Maréchal and Holman, 2005). The HOST system has also proven to be useful for a hydrological soil classification at European scale (Schneider et al., 2007). In addition to the development of conceptual hydrological understanding, as it was done in HOST, soil morphology information was also used to critically evaluate spatial model predictions. For example Güntner et al. (2004) used soil morphological and geobotanical criteria to delineate saturated areas in a mesoscale catchment to evaluate the predictions by different terrain indices.

Despite these efforts to make use of available spatial information, the general lack of available spatial data sets to calibrate and / or validate models that predict CSAs still remains (Easton et al., 2008; Frey et al., 2011; Srinivasan and McDowell, 2009). For the prediction of CSAs this is critical since the prediction goal is the location where certain hydrological processes occur. Especially if management decisions should be based on predicted CSAs a meaningful model calibration and validation is warranted.

We present an approach where we used soil morphology information from a traditional soil map to derive estimates of the average duration of soil saturation at a given depth. The resulting data set can then be used as model validation data. The rationale behind this approach is the fact that groundwater influences morphological features that are related to changing oxygen availability due to permanent water logging or fluctuating groundwater levels. These hydromorphic features are usually related to redox reactions and transport of iron and manganese (see e.g. Terribile et al., 2011). Accordingly, soil morphology as described in soil maps contains information on the soil water regime. Several studies have shown a relationship between soil morphology (especially soil matrix color and the presence and type of iron mottles) and the frequency of soil saturation (Franzmeier et al., 1983; Jacobs et al., 2002; Morgan and Stolt, 2006; Simonson and Boersma, 1972). To our knowledge these morphological features have only been interpreted as binary information (saturated area or not saturated area) (Güntner et al., 2004) but not as quantitative estimates (frequency of soil saturation). To do so, one has to be aware of possible pitfalls related to a quantitative interpretation of soil morphology. These features depend on various factors like the composition of the parent material (Evans and Franzmeier, 1986; Franzmeier et al., 1983), soil texture (Jacobs et al., 2002; Morgan and Stolt, 2006) and soil

chemistry (Terribile et al., 2011; Vepraskas and Wilding, 1983). Also, artificial drainage can influence soil morphology within decades (Hayes and Vepraskas, 2000; Montagne et al., 2009). We have tried to account for these uncertainties by the extensive field experience for soil mapping in this part of Switzerland by some of us (PW, UZ). The resulting map of soil saturation durations itself could serve as proxy map for the identification of areas where saturation excess runoff occurs. However, in combination with a model it could be used for a more detailed prediction with respect to the time of the year in which the saturation occurs or the amount of runoff produced on a certain area. Even if the resulting map of soil saturation frequencies remains uncertain to some degree, this additional information can reduce the uncertainty of model predictions (Franks et al., 1998).

If a model prediction of CSAs should serve as basis for site specific pollution mitigation measures, it has to fulfill several criteria. It has to be reliable and its uncertainties have to be assessable. It should only be based on information that is generally available and it has to be applicable to larger areas. At the same time the scale of the prediction should be in the order of 10×10 m (or smaller). The relevant transport processes for pesticides happen on the timescale of single events. A temporal resolution in the order of hours is therefore required for a dynamic prediction model. These requirements cause a high computational demand. Furthermore, the desired accuracy for the prediction of the groundwater level is high. It needs to distinguish between areas that are often saturated to the surface and therefore produce surface runoff, and areas where the maximum groundwater level remains little below the surface.

Hence, in this paper we describe a case study where we applied a spatially distributed hydrological model for delineating CSAs that are caused by the generation of saturation excess overland flow due to high groundwater levels. Similar to Frey et al. (2009) we chose to work with a process oriented model, which has the advantage that it is better transferable to other regions than models that rely on empirical relationships. The model was optimized for computational speed and mainly relies on generally available data so that it could be used for practical applications. As study site we selected a 1.2 km^2 catchment in the Swiss Plateau, with a high variability of soil types and soil moisture regimes ranging from very wet to rather dry soils. One question we try to answer in this paper is if the spatial variability of depth to groundwater in this catchment can be explained only by topography and the presence of tile drains or if other factors like hydraulic soil properties are important driving factors in determining the groudwater levels. The frequency of soil saturation resulting from the quantitative interpretation of the soil map was not used for the model setup but only to critically evaluate the model predictions.

This case study therefore investigates whether dynamic, spatially distributed hydrological

models can be used for the prediction of critical source areas so that land management decisions can be based on these predictions. Furthermore, we present an approach to increase the spatial information on soil water regimes. Soil morphological information was translated into spatially distributed data on water saturation as a function of soil depth in the study catchment. The result of this translation is a spatially distributed data set on the soil water regime which is based on generally available information. We used this data set to validate the spatial model predictions.

4.2   Materials and methods

4.2.1   Site description

The study catchment ($1.2\,\mathrm{km}^2$) is located in the northeast of Switzerland (see Fig. 4.1). Topography is moderate with altitudes ranging from 423 to 477 m a.s.l. and an average slope of $4.3°$ (min $= 0°$, max $= 42°$, based on $2 \times 2\,\mathrm{m}$ digital elevation model (DEM), absolute accuracy: $\sigma = 0.5\,\mathrm{m}$, resolution $= 1\,\mathrm{cm}$, Swisstopo, 2003). The twenty year mean annual precipitation at the closest permanent measurement station (Schaffhausen, 11 km north of the catchment) is 883 mm (Meteoschweiz, 2009). The soils have developed on moraine material with a thickness of around ten meters; underneath the moraine, we find fresh water molasse (Süsswassermolasse) (Einsele, 2000; Swisstopo, 2007). Soils in the center of the catchment are poorly drained gleysols. In the higher parts of the catchment well drained cambisols and eroded regosols are found (FAL, 1997, see Fig. 4.1). Soil thickness (surface to C horizon) varies between 30 cm at the eroded locations and more than 2 m in the depressions and near the stream. The catchment is heavily modified by human activities; it encompasses a road network with a total length of 11.5 km (approximately 3 km are paved and drained, the rest is unpaved and not drained). The dominant land use is crop production (75 % of the area), around 13 % of the catchment is covered by forest, and a small settlement area is located in the southeast of the catchment. Three farms lie at least partly within the catchment (Fig. 4.1). 47 % of the agricultural land is drained by tile drains with a total length of over 21 km (Gemeinde Ossingen, 1995), the open stream has a length of 550 m. The main part of the drainage system was built in the 1930s. The stream system consists of two branches, an open ditch that was partly built as recipient for the drainage water, and the main branch of the stream that runs in a culvert (Fig. 4.1). The stream also receives the runoff from two main roads and from two farm yards (Gemeinde Ossingen, 2008). The paved area that drains into the catchment is approximately 1.5 ha (1.2 % of the area).
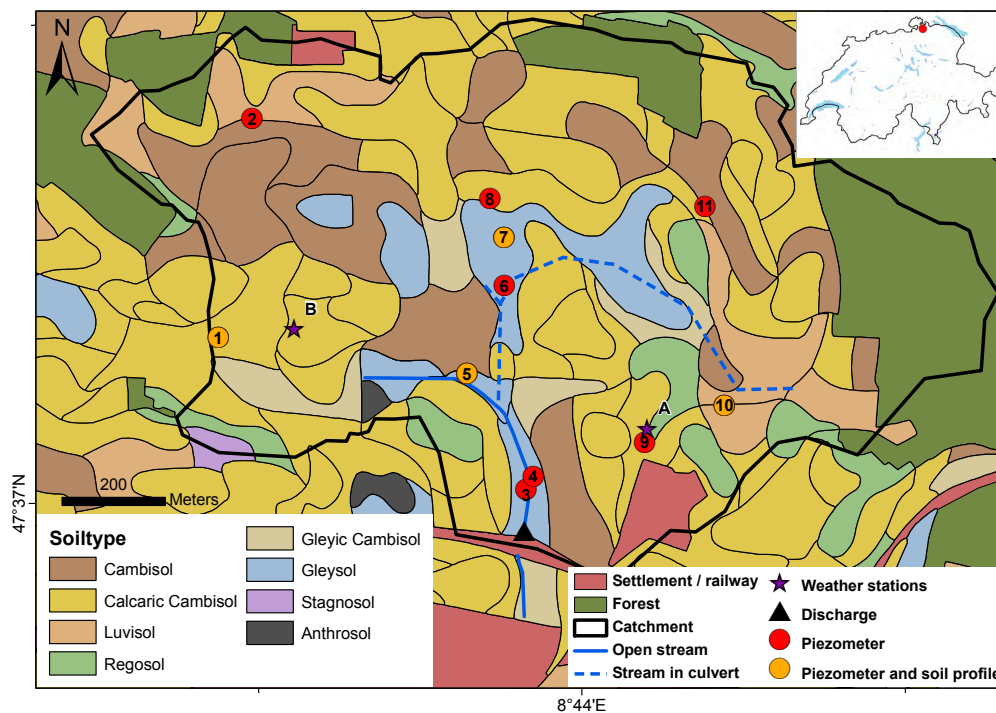
Figure 4.1: The experimental catchment with land use, soil types and the hydrological measurement locations. The small map in the top right corner depicts the location of the study site within Switzerland. Sources: FAL (1997); Swisstopo (2008).

4.2.2   Field measurements

From 25 August 2008 to 14 October 2009, we monitored several hydrological variables in the catchment. We measured discharge at the outlet of the catchment (Fig. 4.1). Water level and flow velocity were measured using a Doppler probe and a pressure transducer (ISCO 750 area velocity flow module, Teledyne Inc., Los Angeles). Discharge was calculated using the exact cross section of the site. Discharge data were stored at five-minute intervals by the data logger of an auto sampler (ISCO 6700, ISCO 6712, Teledyne Inc., Los Angeles USA).

At weather station A (Fig. 4.1), precipitation was measured at 15 min resolution with a tipping bucket rain gauge (R102, Campbell Scientific, Inc., Loughborough UK). This rain gauge was out of order for 22 days (4 June 2009 – 25 June 2009). During this time, rain data from weather station B (Fig. 4.1) were used (a mobile HP 100 Station run by Agroscope ART Reckenholz, CH with a tipping bucket rain gauge: HP 100, Lufft GmbH, Fellbach Germany). At weather station A we also recorded air temperature and relative humidity (Hygromer MP 100A, rotronic AG, Bassersdorf CH), wind speed (A100R switching anemometer, Campbell Scientific, Inc., Loughborough UK), net radiation (Q-

7 net radiometer, Campbell Scientific, Inc., Loughborough UK) and air pressure (Keller DCX-22, KELLER AG für Druckmesstechnik, Winterthur CH) in 15 min intervals. Daily reference evapotranspiration was calculated from the meteorological data after the FAO Penman-Monteith equation (Allen et al., 1998). This results in the evapotranspiration of a reference grass surface without water limitation.

We installed 11 piezometers (Fig. 4.1) to monitor groundwater levels in 15 min intervals (STS DL/N, STS Sensor Technik Sirnach AG, Sirnach CH and Keller DCX-22, KELLER AG für Druckmesstechnik, Winterthur CH). The installation depth varied between 1.5 and 2.7 m below the surface. At four of the piezometer locations, we additionally dug a 1.2 m deep soil pit (Fig. 4.1) to directly investigate hydromorphic features.

4.2.3   GIS analysis

The catchment boundary was calculated in ArcGIS (ESRI, ArcGIS Desktop, 9.3.1) based on the 2×2 m DEM (Swisstopo, 2003) and manually adapted according to field observations, the detailed tile drain map (Gemeinde Ossingen, 1995) and the rain sewer map (Gemeinde Ossingen, 2008). The topographical catchment does not coincide completely with the subsurface catchment. In some areas that belong to the topographical catchment, the tile drains divert the water outside of the catchment. These areas were excluded. In contrast, the settlement area in the southeast was kept in the catchment, even though the water from sealed areas in the settlement leaves the catchment.

The original 2×2 m DEM (Swisstopo, 2003) was used for the analysis of surface connectivity. Firstly, very small or shallow depressions were removed as these can either be artifacts in the DEM or are too shallow to trap significant amounts of overland flow. Depressions consisting of one or two cells and those with a maximum depth of less than 5 cm were filled. All other depressions were kept. Secondly, the cells in the open stream were incised to the depth of the average water level. Depression analysis and filling as well as stream incision were performed in TAS (TAS geographical information system version 2.0.9, John Lindsey 2005). Based on this corrected DEM, flow directions and flow accumulation were calculated in ArcGIS. The lowest stream channel cell was used as pour point for the catchment calculation to determine the area connected directly to the stream on the surface.

The corrected DEM was also used as surface topography in the model. The topographic wetness index was calculated with the D_{inf} algorithm implemented in TAS, based on the corrected DEM.

4.2.4   Soil map translation

We worked with the 1:5000 soil map of Canton Zurich (FAL, 1997). The soil map classifies agricultural soils after the Swiss soil classification system (FAL, 1997); forest soils are not classified. The soils are characterized according to their physical, chemical and morphological properties. For the estimation of the duration of soil saturation, the soil units (Fig. 4.1) were grouped into seven water regime classes, according to their expected water regime. For each of these classes we estimated how long it is saturated in six different depths (5, 30, 50, 75, 105, 135 cm). We used the following morphological redox features to estimate the duration of soil saturation within a soil horizon: i) the presence and abundance of manganese concretions in the horizon, ii) the presence and abundance of iron mottles, iii) the presence of iron mottles together with pale soil matrix, and iv) fully reduced horizons. These features of the horizons were interpreted within the context of the respective soil profile and the expected water regime of the soil water regime class. Since variations are expected within the classes and because the estimation itself is uncertain, we additionally estimated a range of soil saturation in which we expect two thirds of the soils that are classified in the respective class.

4.2.5   Model description

Model concept

The model we worked with has a conceptual representation of the unsaturated zone and a spatially distributed, more process based representation of the saturated zone. Under wet temperate climate lateral flow in the saturated zone is an important process to determine the shape of the groundwater table in shallow groundwaters and therefore the prediction of saturated areas. For the saturated zone we chose an approach similar to HillVI (Weiler and McDonnell, 2004) where the groundwater level gradients are calculated in each time step and do not rely on surface topography. This should result in more realistic predictions of the location of saturated areas (Grabs et al., 2009). We additionally implemented the lateral and preferential flow to tile drains. These are important processes because large parts of the crop production areas in Switzerland are artificiailly drained.

The model simulates water fluxes in a catchment. It is based on the following water balance equation:

$$\frac{dS}{dt} = P - ET - Q \tag{4.1}$$

with S [L] being the total water storage in the catchment, P [L T^{-1}] is precipitation, ET [L T^{-1}] is evapotranspiration and Q [L T^{-1}] is stream discharge. We do not consider

subsurface in– or outflow. The calculations were optimized for computational speed.

The model consists of three separate, linked modules (Fig.4.2):

1. The paved area module is a lumped and conceptual model that calculates runoff and evaporation from paved areas.

2. The unsaturated zone module calculates recharge from the unsaturated zone to the saturated zone, preferential flow that bypasses the unsaturated zone and directly enters the saturated zone, and evapotranspiration from the unsaturated zone.

3. The saturated zone module is spatially distributed (grid cells) and more process based. It simulates lateral groundwater flow, drain flow, evapotranspiration from the saturated zone, and saturation excess overland flow. The concept of the saturated zone module was inspired by HillVi (Weiler and McDonnell, 2004).

It is possible to have several unsaturated zone modules (e.g. one for each soil type), each of which recharges into different sections of the saturated zone module.

The modeled stream discharge consists of the following components:

$$Q = Q_{\text{paved}} + Q_{\text{surf}} + D_{\text{lat}} + D_{\text{pref}} \qquad (4.2)$$

where Q_{paved} [L T^{-1}] is runoff from the paved area, Q_{surf} [L T^{-1}] is saturation excess surface runoff (this term also comprises lateral groundwater flow to the stream, see below), D_{lat} [L T^{-1}] is lateral drainflow, and D_{pref} [L T^{-1}] is preferential drainflow.

The modeled evapotranspiration is calculated as follows:

$$ET = E_{\text{paved}} + ET_{\text{uns}} + ET_{\text{sat}} \qquad (4.3)$$

where E_{paved} [L T^{-1}] is the evaporation from paved areas, ET_{uns} [L T^{-1}] is the evapotranspiration from the unsaturated zone, and ET_{sat} [L T^{-1}] is the evapotranspiration from the saturated layer. In the following the three modules are described in detail.

Paved area module

The change in the paved storage is modeled as follows:

$$\frac{dS_{\text{paved}}}{dt} = P - E_{\text{paved}} - Q_{\text{paved}} \qquad (4.4)$$

with S_{paved} [L] being the paved storage.
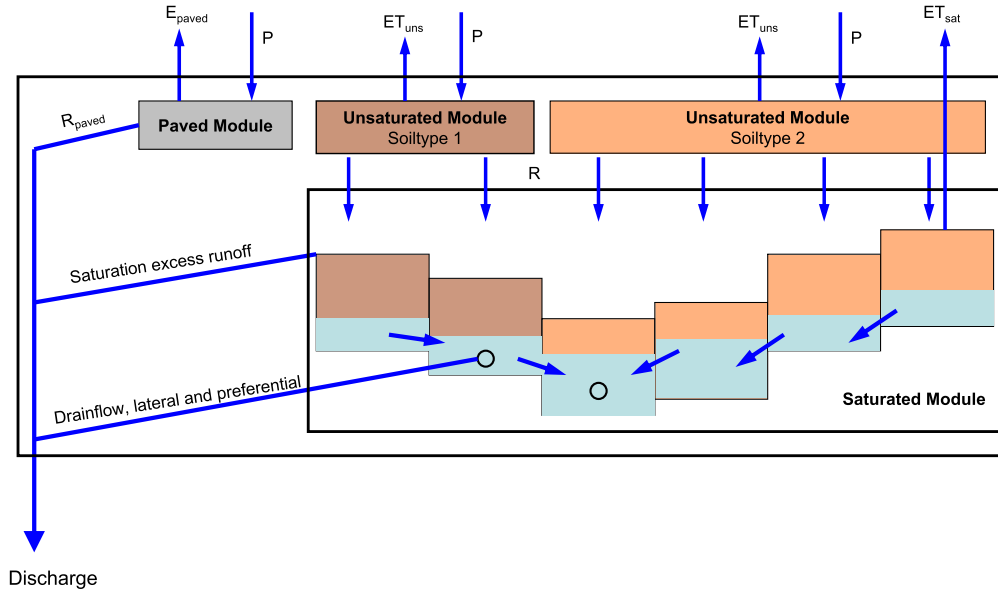
Figure 4.2: The model concept, see text.

Runoff from paved areas linearly depends on the paved storage.

$$
Q_{\mathrm{paved}} = \begin{cases} 0 & \text{if } S_{\mathrm{paved}} \leq S_{\mathrm{paved\_min}} \\ (S_{\mathrm{paved}} - S_{\mathrm{paved\_min}})k_{\mathrm{paved}} & \text{if } S_{\mathrm{paved}} > S_{\mathrm{paved\_min}} \end{cases} \tag{4.5}
$$

$S_{\mathrm{paved\_min}}$ [L] is the minimum storage that has to be filled to produce runoff and k_{paved} [T^{-1}] is the outflow rate.

If there is water in the paved storage, it can evaporate with the following rate

$$
E_{\mathrm{paved}} = ET_{\mathrm{ref}} \cdot m_{\mathrm{paved}} \tag{4.6}
$$

where ET_{ref} [$\mathrm{L\,T}^{-1}$] is the reference evapotranspiration calculated from meteorological data (see Sect.4.2.2), and m_{paved} [-] is a multiplier.

Unsaturated zone module

The water balance of the unsaturated zone is represented as follows:

$$
\frac{dS_{\mathrm{uns}}}{dt} = P - ET_{\mathrm{uns}} - R \tag{4.7}
$$

where S_uns [L] is the unsaturated storage, and R [L T^{-1}] is recharge to the saturated zone. R consists of a slow recharge component (R_slow) and preferential flow (R_pref).

$$R = R_\text{slow} + R_\text{pref} \tag{4.8}$$

R_slow linearly depends on the storage amount above field capacity. If the unsaturated storage is below field capacity, R_slow is assumed to be zero.

$$R_\text{slow} = \begin{cases} 0 & \text{if } S_\text{uns} < S_\text{fc} \\ (S_\text{uns} - S_\text{fc})k_\text{uns} & \text{if } S_\text{uns} \geq S_\text{fc} \end{cases} \tag{4.9}$$

S_fc [L] is the unsaturated store at field capacity and k_uns [T^{-1}] is the outflow rate.

A part of the precipitation bypasses the unsaturated zone as preferential flow and directly enters the saturated zone. This only occurs if the unsaturated zone is above field capacity, and it exponentially depends on the water content in the unsaturated zone.

$$R_\text{pref} = \begin{cases} 0 & \text{if } S_\text{uns} < S_\text{fc} \\ k_\text{pref} \left(\frac{S_\text{uns} - S_\text{fc}}{S_\text{uns\_max} - S_\text{fc}} \right)^{e_\text{pref}} \cdot P & \text{if } S_\text{uns} \geq S_\text{fc} \end{cases} \tag{4.10}$$

k_pref [-] and e_pref [-] are empirical parameters.

Above field capacity the evapotranspiration from the unsaturated module is at maximum, below field capacity it is reduced. The reference evapotranspiration calculated from meteorological data (ET_ref) refers to a reference grass surface. A time dependent multiplier (m_uns) was introduced to account for crops with different water requirements and the time dependence of the leaf area index (LAI) due to crop development.

$$ET_\text{uns} = \begin{cases} ET_\text{ref} \cdot m_\text{uns} & \text{if } S_\text{uns} \geq S_\text{fc} \\ ET_\text{ref} \cdot m_\text{uns} \left(\frac{\frac{S_\text{uns}}{S_\text{fc}}}{\frac{S_\text{uns}}{S_\text{fc}} + k_\text{et}} \right) (1 + k_\text{et}) & \text{if } S_\text{uns} < S_\text{fc} \end{cases} \tag{4.11}$$

with k_et [-] and m_uns [-] being parameters. The change of the LAI is coupled to air temperature and incorporated in the time dependent parameter m_uns.

$$\frac{dm_\text{uns}}{dt} = \begin{cases} m_\text{uns} \cdot \mu_0 (T_\text{air} - T_0) \left(1 - \frac{m_\text{uns}}{m_\text{uns,max}} \right) & \text{if } T_\text{air} \geq T_0 \\ m_\text{uns} \cdot k_\text{decay} (T_\text{air} - T_0) & \text{if } T_\text{air} < T_0 \\ 0 & \text{if } m_\text{uns} \leq m_\text{uns,min} \end{cases} \tag{4.12}$$

where μ_0 [T^{-1} Te^{-1}] and k_decay [T^{-1} Te^{-1}] are parameters, T_air [Te] is air temperature, T_0 [Te] is the minimum temperature above which LAI starts increasing, $m_\text{uns,min}$ [-] and $m_\text{uns,max}$ [-] are the minimum and maximum values for m_uns.

Saturated zone module

The saturated module is spatially distributed. The water balance within a grid-cell is calculated as follows:

$$\frac{dS_{\text{sat}}}{dt} = R - ET_{\text{sat}} + SF_{\text{lat}} - i \cdot D_{\text{lat}} - i \cdot D_{\text{pref}} - j \cdot Q_{\text{surf}} \qquad (4.13)$$

where S_{sat} [L] is the storage in the cell and SF_{lat} [L T^{-1}] is the lateral groundwater flow between cells.

$$i = \begin{cases} 1 & \text{for drained cells} \\ 0 & \text{for undrained cells} \end{cases} \qquad (4.14)$$

$$j = \begin{cases} 1 & \text{for cells with surface connectivity to the stream, see Sect. 4.2.3} \\ 0 & \text{for cells without surface connectivity to the stream} \end{cases} \qquad (4.15)$$

The change of the groundwater level in the cell is therefore calculated as follows

$$\frac{dh}{dt} = \frac{\frac{dS_{\text{sat}}}{dt}}{p_{\text{eff}}} \qquad (4.16)$$

where h [L] is the groundwater level and p_{eff} [-] is the effective porosity.

If the unsaturated zone is below field capacity and evapotranspiration from the unsaturated zone is therefore reduced, evapotranspiration can occur directly from the saturated zone.

$$ET_{\text{sat}} = \begin{cases} 0 & \text{if } S_{\text{uns}} \geq S_{\text{fc}} \\ m_{\text{sat}}(ET_{\text{ref}} \cdot m_{\text{uns}} - ET_{\text{uns}}) & \text{if } S_{\text{uns}} < S_{\text{fc}} \end{cases} \qquad (4.17)$$

At maximum, ET_{sat} accounts for the evapotranspiration deficit in the unsaturated zone, the multiplier m_{sat} [-] is between 0 and 1.

The lateral groundwater flow between cells is calculated based on the Dupuit-Forchheimer assumption. We furthermore assume isotropy in K_{sat}:

$$q_{\text{lat}} = K_{\text{sat}} \cdot \nabla h \qquad (4.18)$$

where q_{lat} [L T^{-1}] is the flux density, K_{sat} [L T^{-1}] is the saturated hydraulic conductivity, and h [L] is the groundwater head. The water flow between two neighboring cells can then be calculated as follows:

$$Q_{\text{lat}} = K_{\text{sat}} \cdot M_{\text{sat}} \cdot L_{\text{cell}} \frac{\Delta h}{L_{\text{cell}}} \qquad (4.19)$$

where Q_{lat} $[\text{L}^3\,\text{T}^{-1}]$ is the water flow between two cells, M_{sat} $[\text{L}]$ is the thickness of the saturated layer, and L_{cell} $[\text{L}]$ is the cell length. If we sum up the water flows to and from all neighboring cells and divide the sum by the cell area, we receive SF_{lat}.

In drained cells, the lateral groundwater flow into the drain is calculated based on the Hooghoudt equation as described by Beers (1976). We used an equation modified from Wittmer (2010) because the distance to single tiles is not considered explicitly. The flow depends on the water level above the drains.

$$D_{\text{lat}} = 4r_{\text{dr}} \cdot K_{\text{sat}} \left(\frac{m_{\text{dr}} \cdot H_{\text{dr}}}{Sp_{\text{dr}}} \right)^2 \tag{4.20}$$

D_{lat} $[\text{L}\,\text{T}^{-1}]$ is the drainflow, r_{dr} $[\text{-}]$ is a parameter that determines the entrance resistance to the tile drains, m_{dr} $[\text{-}]$ is a multiplier to obtain the water level in the middle between two drains from the modeled water level in the cell, H_{dr} $[\text{L}]$ is the water table height above the drain, and Sp_{dr} $[\text{L}]$ is the drain spacing.

If the groundwater level reaches the surface in a cell, three cases are distinguished:

1. The cell is directly connected to the stream on the surface (see Sect. 4.2.3). In this case all water above the surface is directly added to discharge (Q_{surf}).

2. The cell is not connected but it is drained. In this case, all water above the surface is added to drainflow as preferential flow (D_{pref}).

3. The cell is neither connected to the stream nor drained. The water remains in the cell.

The coupling between the saturated zone module and the unsaturated zone module is unidirectional from the unsaturated zone to the saturated zone. The fact that a cell is saturated to the surface does therefore not influence the unsaturated zone module above it. It is possible that the unsaturated zone above a saturated cell is not completely full. This concept was chosen to achieve a high computational efficiency.

The stream channel cells are incised to a mean water level in the stream. The surface topography in the stream cells is therefore represented by the mean water level and all the water above this level in the cell is directly converted to discharge. Lateral groundwater flow to stream cells is therefore also converted to Q_{surf}.

Model setup

We ran the model with homogeneous hydraulic properties in the saturated zone, only topography and the presence of tile drains where spatially distributed. The unsaturated

zone was divided into several classes according to land use (forest, settlement, agriculture) and, within agricultural landuse, according to the seven soil categories (see Sect. 4.2.4). We therefore ended up with nine unsaturated zone classes (forest, settlement and the seven soil categories). The reason for this setup was the assumption that the groundwater level in the catchment is mainly influenced by topography and artificial drainage and not by hydraulic soil properties (soil texture is rather homogeneous within the catchment (FAL, 1997)). However, to account for the spatial distribution of the unsaturated zone thickness (which also influences the other parameters of the unsaturated zone module), we divided the unsaturated zone into classes according to their soil water regime. The classification of soil water regimes was only used for the spatial division of the unsaturated zone (but not its parameterization).

The saturated zone was represented by a 16×16 m grid; the cells were 10 m thick. We assume that the soil and the moraine are the conducting layers while the Fresh water molasse is assumed to be impermeable (see Sect. 4.2.1). The calculations were run with hourly input time series; the model output was also in hourly steps.

Implementation

The model equations were implemented in a C++ program to achieve fast model simulations. The ordinary differential equations of the conceptual unsaturated zone modules and the paved area module were numerically integrated with the LSODA solver package (Hindmarsh, 1983; Petzold, 1983). The partial differential equations of the saturated zone module were integrated with an explicit Euler solution scheme with a computational time-step (20 minutes) that guaranteed numerical stability during the simulation period. The integration of the saturated zone module was sped up by parallelizing the explicit solution scheme with OpenMP threads (for the specification see `http://openmp.org`). Despite all these efforts the simulation of the 2D groundwater surface remained rather time consuming requiring 28 sec of computation time for 1 year of forward simulation on an Intel Core i7 – 3960X CPU (3.3 GHz).

Model implementation and model setup (e.g. spatial and temporal resolution) were chosen in a way that guaranteed simulations fast enough to allow a possible use for practical applications.

Calibration

The model was simultaneously calibrated to the discharge time series and the groundwater level time series in the eleven piezometers. A maximum likelihood approach was used.

Discharge was Box-Cox transformed before calibration with $\lambda = 1/3$ (Box and Cox, 1964, 1982). The transformation equation was as follows:

$$g(x) = \frac{x^{\lambda} - 1}{\lambda} \tag{4.21}$$

We assumed independent and normally distributed errors for the transformed discharge and the groundwater levels; the standard deviations for these were also calibrated. The likelihood function therefore looked as follows:

$$L(\boldsymbol{\theta}, \boldsymbol{\sigma}) \propto \prod_{i=1}^{11} \prod_{j=1}^{m} \frac{1}{\sigma_i \sqrt{2\pi}} \exp\left(-\frac{1}{2}\left(\frac{O_i^j - M_i^j(\boldsymbol{\theta})}{\sigma_i}\right)^2\right) \times \prod_{j=1}^{m} \frac{1}{\sigma_d \sqrt{2\pi}} \exp\left(-\frac{1}{2}\left(\frac{g(O_d^j) - g(M_d^j(\boldsymbol{\theta}))}{\sigma_d}\right)^2\right) \tag{4.22}$$

where L is the likelihood, $\boldsymbol{\theta}$ is the vector of model parameters, $\boldsymbol{\sigma}$ is the vector of the standard deviations, i are the 11 piezometer locations, j are the time–points, σ_i is the standard deviation at piezometer i, O_i^j is the observed groundwater level at piezometer i and time$j$, $M_i^j(\boldsymbol{\theta})$ is the modeled groundwater level at piezometer i and time$j$, σ_d is the standard deviation of the transformed discharge, $g(x)$ is the Box-Cox transformation (see above), O_d^j is the observed discharge at time j and $M_d^j(\boldsymbol{\theta})$ is the modeled discharge at time j.

During calibration the likelihood function was optimized with a coupled global-local algorithm. Optimization started with the Particle Swarm algorithm (Kennedy and Eberhart, 1995) and after reaching the stop criterion Nelder-Mead Simplex optimization (Nelder and Mead, 1965) was launched from the best parameter combination.

We chose a period in spring and summer 2009 as calibration period. It starts very wet in the beginning of spring, includes a long dry period, several rain events with varying magnitudes and intensities and it also contains the largest discharge event in the measurement period. We do not have continuous measurement time series from all the piezometers. For each piezometer we chose the calibration period so, that all the calibration time series (discharge and the 11 piezometers) contained the same number of observations. Most of the model parameters were calibrated to achieve the best possible model output with the given model structure. (The tables A.5 to A.8 in the Appendix indicate which of the parameters were calibrated and which were kept fixed during calibration. The tables also indicate the minimum and maximum values that were allowed in the calibration.) The initial state of the unsaturated zone was calibrated as well. The initial condition for the groundwater level is difficult to calibrate because the shape of the surface depends on the model parameters. The model run was started five months before the calibration period to adapt the groundwater surface to the model parameters. Additionally, we added a

parameter that allows a homogeneous shifting up or down of the groundwater initial state and chose an adaptive procedure. After a first calibration, we used a groundwater level map from the optimum parameter set as initial condition for a second calibration. In a first step we calibrated a model version with a homogeneous unsaturated zone. From the resulting optimum parameter set, we launched the calibration of the model version with the spatially distributed unsaturated zone. With this setup, one full optimization (global and local) took about one week depending on the speed of convergence.

4.3   Results

4.3.1   Saturation estimates

Figure 4.3 a) shows the map of the seven water regime classes from the reclassification of of the soil map. Class 1 is the driest, class 7 the wettest water regime class. In Fig. 4.4 the estimated saturation durations in the water regime classes are shown. To evaluate the map based estimates of the water regime we can compare the estimates with the measured groundwater levels from the piezometers (Fig. 4.4). In general, the estimated durations of soil saturation are in good agreement with the piezometers. There are some deviations at specific locations like the very wet piezometer in the driest soil class (piezometer 1 in Fig. 4.1 indicated by an arrow in Fig. 4.4). For a further evaluation of the spatial distribution of the water regime classes, we compared the water regime class map (Fig. 4.3 a)) with the topographic wetness index (Fig. 4.3 b)). The comparison reveals a generally good match between the two maps (high topoindex means wet soil). Even small scale features in the topoindex map are reflected in the soil map (e.g. in the NE of the catchment). For a quantitative comparison of the two maps, we classified the wettest two water regime classes (classes 6 and 7) as potential CSAs. This resulted in 20 % of the area classified as CSA. For the topoindex map we also classified the wettest 20 % as CSA. The areal overlap of the CSAs from the two methods is 52 %. Despite this reasonable agreement between the two maps there are some areas with rather high topoindices where the soils are classified in dry soil classes (e.g. in the west of the catchment).

The location of tile drains also contains information on the soil water regime. The tile drain map can therefore be used as additional comparison to plausibilize the soil map estimates. Tile drains are only present at locations with excess groundwater that has to be diverted. Drained areas are therefore good indicators of originally higher groundwater levels. Because the drains are installed between 1 and 1.5 m below the surface in the study catchment, groundwater levels are still expected to be rather high in drained areas.
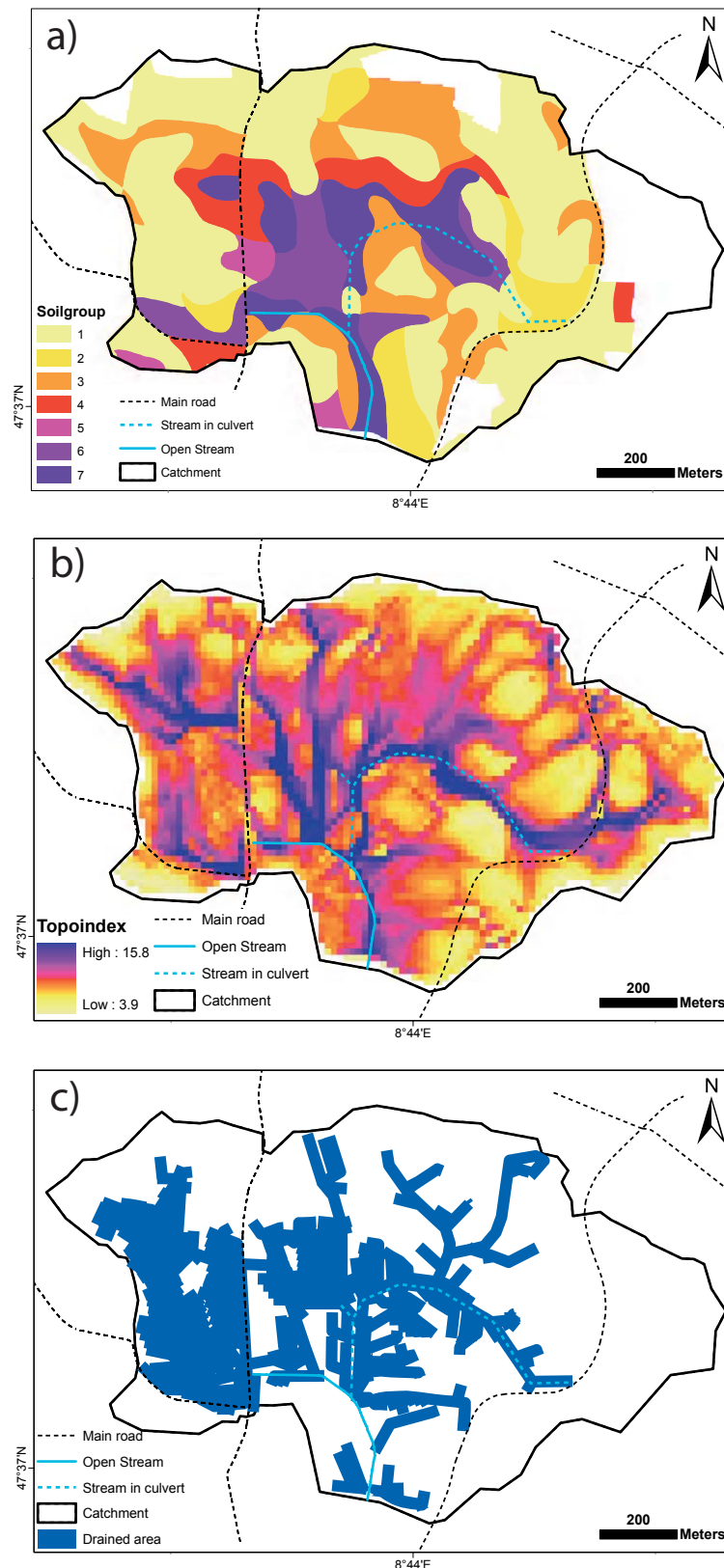
Figure 4.3: a) The reclassified soil map with the seven soil water regime classes (class 1 is the driest, class 7 the wettest), b) map of the topographic wetness index, c) map of the drained areas in the catchment. Sources: Gemeinde Ossingen (1995); Swisstopo (2008)
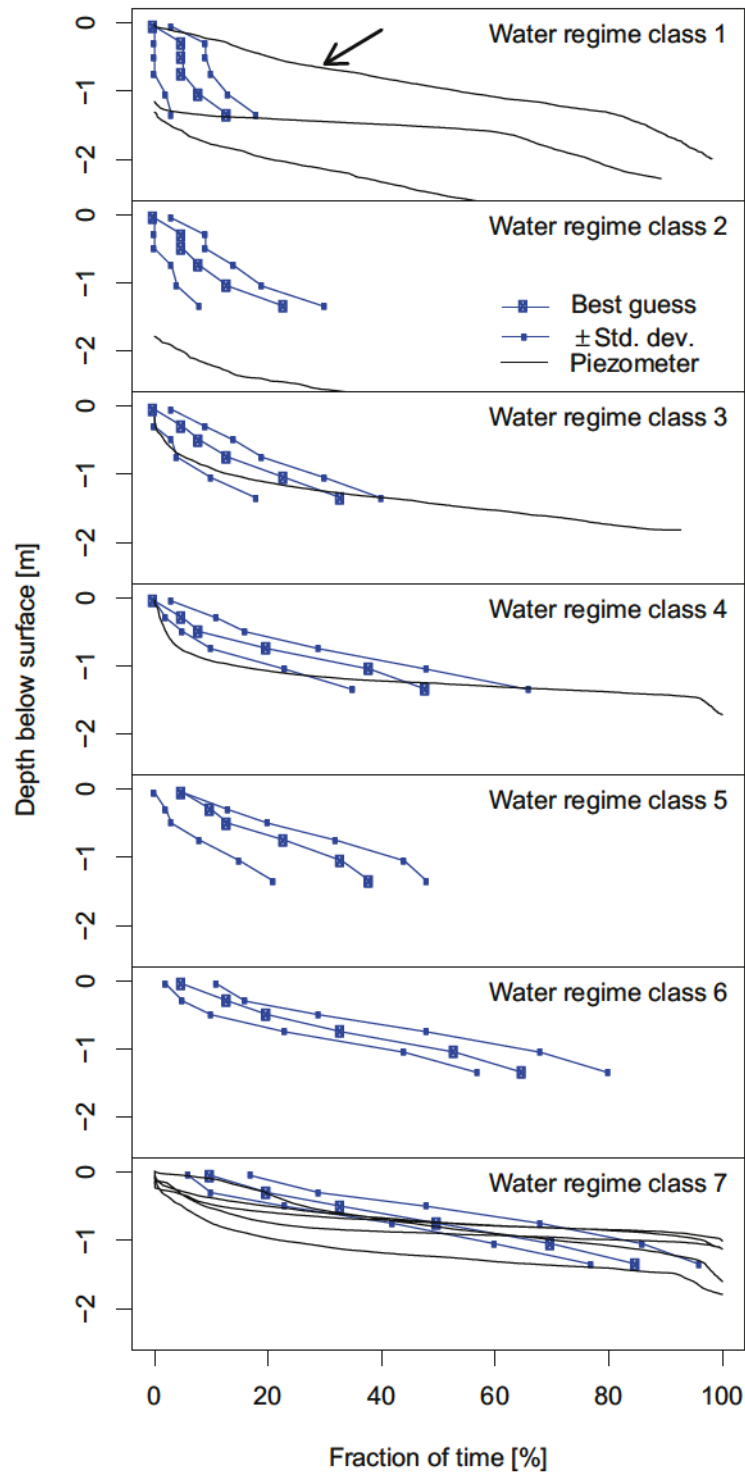
Figure 4.4: The estimated depth dependent saturation durations in the seven water regime classes with the expected variation within each class (blue) together with the measured saturation duration in the piezometers (black).

We therefore used the drainage map (Fig. 4.3 c)) as a further evaluation of the map of soil water regime classes. The comparison reveals that drained areas are areas with high topographic indices and that the drained soils are usually classified into a wet water regime class. However, the western part of the catchment is intensely drained and has rather high topographic wetness indices, but large areas are classified in the driest water regime class. Also the wet piezometer in water regime class 1 (Fig. 4.4, indicated by an arrow) is located in this area. The local assessment in the soil pit besides piezometer 1 (Fig. 4.1) supports the map based estimate. Only few small iron mottles were found below 1 m. The piezometric measurement therefore contradicts the local morphological interpretation in the soil pit and the map based estimate. This is the only soil pit location where this is the case, in the other three soil pits (Fig. 4.1) the piezometric measurement, the local morphological interpretation in the soil pit and the map based estimate corresponded well.

4.3.2   Calibration results and model validation

After calibration (the maximum likelihood parameter set can be found in Tables A.5 to A.8 in the Appendix), the model performed satisfactory with respect to discharge and absolute groundwater levels. Figure 4.5 shows the predicted and measured discharge time-series. The bad fit in the beginning stems from the difficulty to calibrate the initial groundwater level (see Sect. 4.2.5). After this initial phase, the discharge prediction is good with a Nash-Sutcliffe coefficient (Nash and Sutcliffe, 1970) of 0.91 for the calibration period. Also the predicted average groundwater levels at the piezometer locations are in good agreement with the measurements (Fig. 4.6). After the initial phase, the difference between modeled and measured groundwater level is usually less than one meter. The model was therefore able to reproduce the general hydrological behavior of the catchment. Also the modeled composition of the discharge, with most of the discharge originating from the drainage system, was in good agreement with the measurements (data not shown).

However, if the timeseries of the groundwater levels are plotted as depth below the soil surface (Fig. 4.7) it becomes obvious that there is a lack of groundwater level dynamics in the model. The observed groundwater levels are much more dynamic than the modeled ones. Additionally, Fig. 4.7 shows that the depth to groundwater in the model prediction is rather homogeneous throughout the area. The modeled average depth to groundwater does not vary much between the piezometer locations. In contrast, the measured depth to groundwater is more variable.

To further investigate the model performance with respect to the spatial distribution of groundwater levels we used the estimated saturation durations from the soil map (Fig. 4.8).
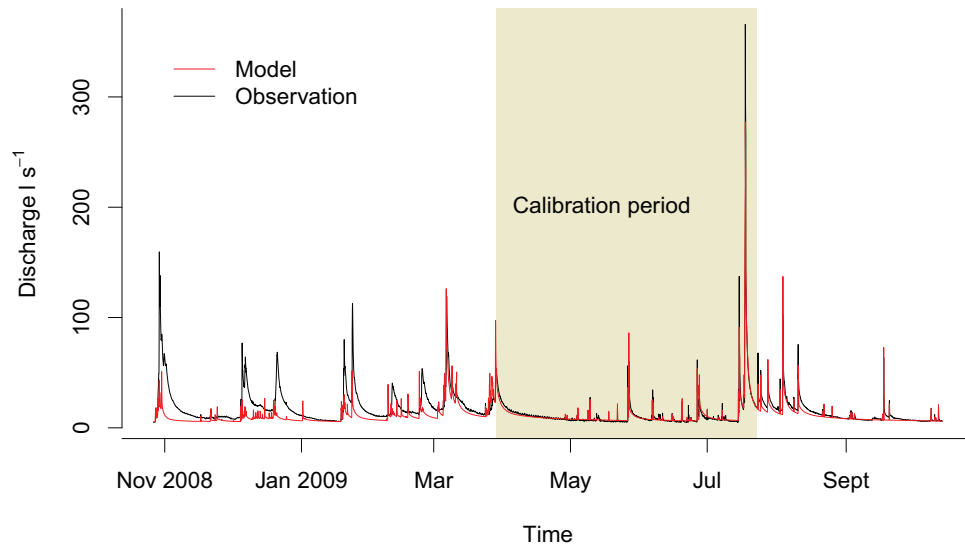
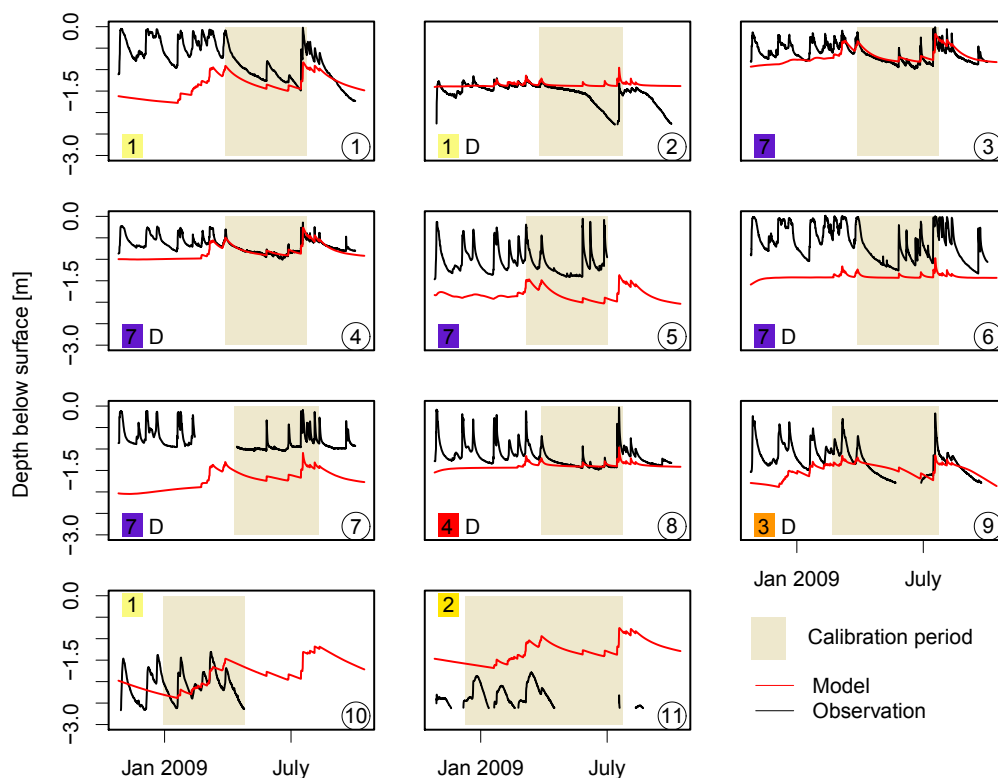**Figure 4.5:** The modeled and measured discharge time series.

This allowed a model evaluation at locations without measurements and at locations where the model was not calibrated to. Figure 4.8 shows that the model does not differentiate between the water regime classes. In all the classes, there are dry and wet model cells. As a general behavior, the model represents the dry locations (water regime class 1) too wet and the wet locations (water regime classes 6 and 7) too dry. However, the model was able to predict the areas with the lowest groundwater levels. Model cells where the modeled groundwater level is deeper than three meters below the surface are only located in water regime class one (Fig. 4.8). Hence, the model was not able to reproduce the spatial variability in saturation durations, except for the locations with the lowest groundwater levels, even though it was calibrated on measured groundwater levels distributed throughout the catchment.

For a more complete picture of the modeled spatial distribution of the depth to groundwater in the catchment Fig. 4.9 shows a map of the model output from 27 July 2009. This is a situation with high groundwater levels after the largest rain event in the modeled period. Figure 4.9 reveals a clear dominance of the drainage system in the determination of the modeled groundwater level (compare Fig. 4.9 with Fig. 4.3c)). This is also visible in Fig. 4.8. Most of the drained cells show a very similar behavior with stable groundwater levels around 1.5 m below the surface (the installation depth of the tile drains). A comparison of Fig. 4.9 with Fig. 4.3a) shows that the spatial pattern of the model output does not resemble the pattern observed in soil morphology. The spatial overlap between the CSAs
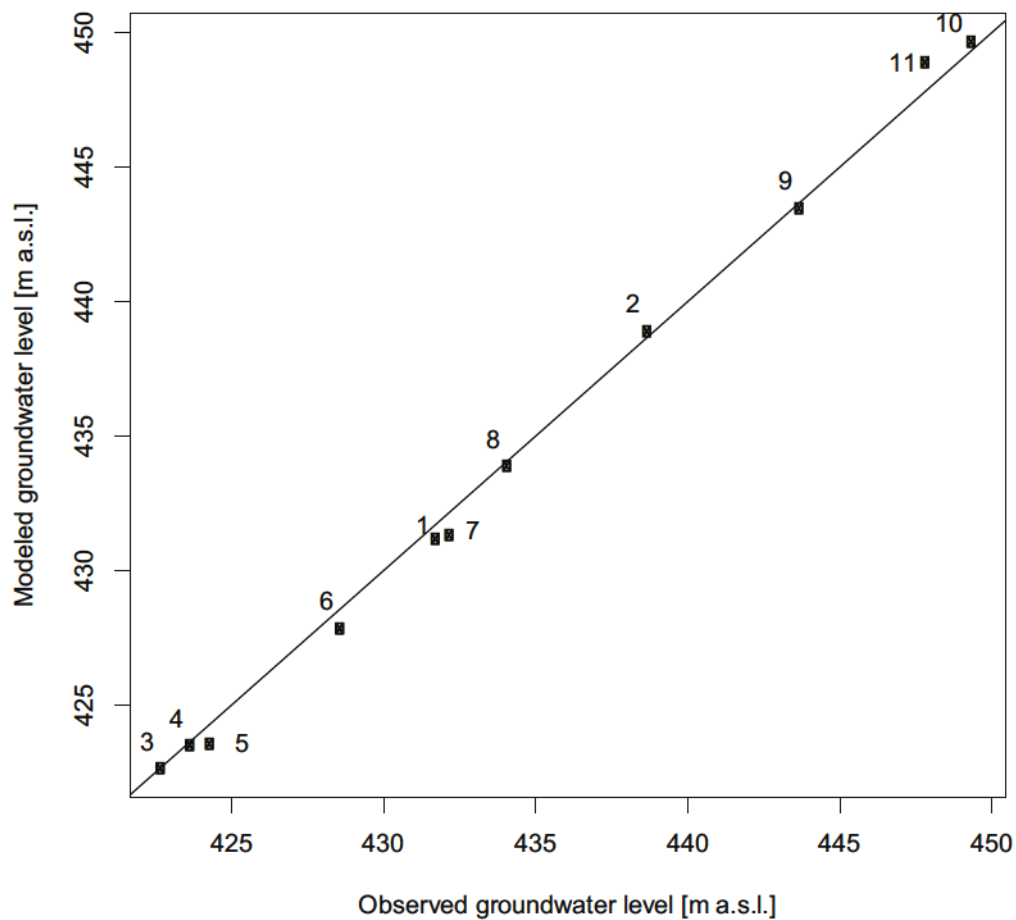
Figure 4.6: The observed average groundwater levels plotted against the modeled average groundwater levels at the piezometer locations together with the 1:1 line. The numbers indicate the piezometer location (see Fig. 2.1).

from the soil map (water regime classes 6 and 7) and the wettest 20 % of the cells in the modeled output is only 12 %. Model and soil map would therefore predict completely different locations as CSAs. The model predicts high water tables in areas where it should be dry. In the center of the catchment, where the area is drained but still wet in reality, the model predicts too low water levels (compare Fig. 4.9 with Fig. 4.3c)). It seems that the drainage system in the model is too efficient.

Figure 4.7: The modeled and measured groundwater levels at the piezometer locations as depth from the surface. The individual calibration periods are indicated (see Sect. 4.2.5). The circled number is the piezometer location (Fig. 4.1), the number in the colored box shows the water regime class, D indicates a drained model cell.

4.4   Discussion

4.4.1   Soil map translation

A meaningful validation of the saturation duration estimates from the soil map is not straight forward due to several difficulties. Fist, there are spatial aspects. The spatial coverage of the estimates corresponds to the soil map unit while piezometers are point measurements. Hence, deviations between soil map estimates and piezometer data may simply reflect local inhomogeneities. Furthermore, the soil map divides the area into units with sharp boundaries. Some of these boundaries are in reality gradual changes. The vicinity of a piezometer to a soil unit boundary can therefore hinder a meaningful evaluation. A second difficulty is that the estimates do not differ heavily; the saturation estimates change gradually from one class to the next. The piezometer measurements could therefore fit well in more than one class. Third, there are temporal aspects of the
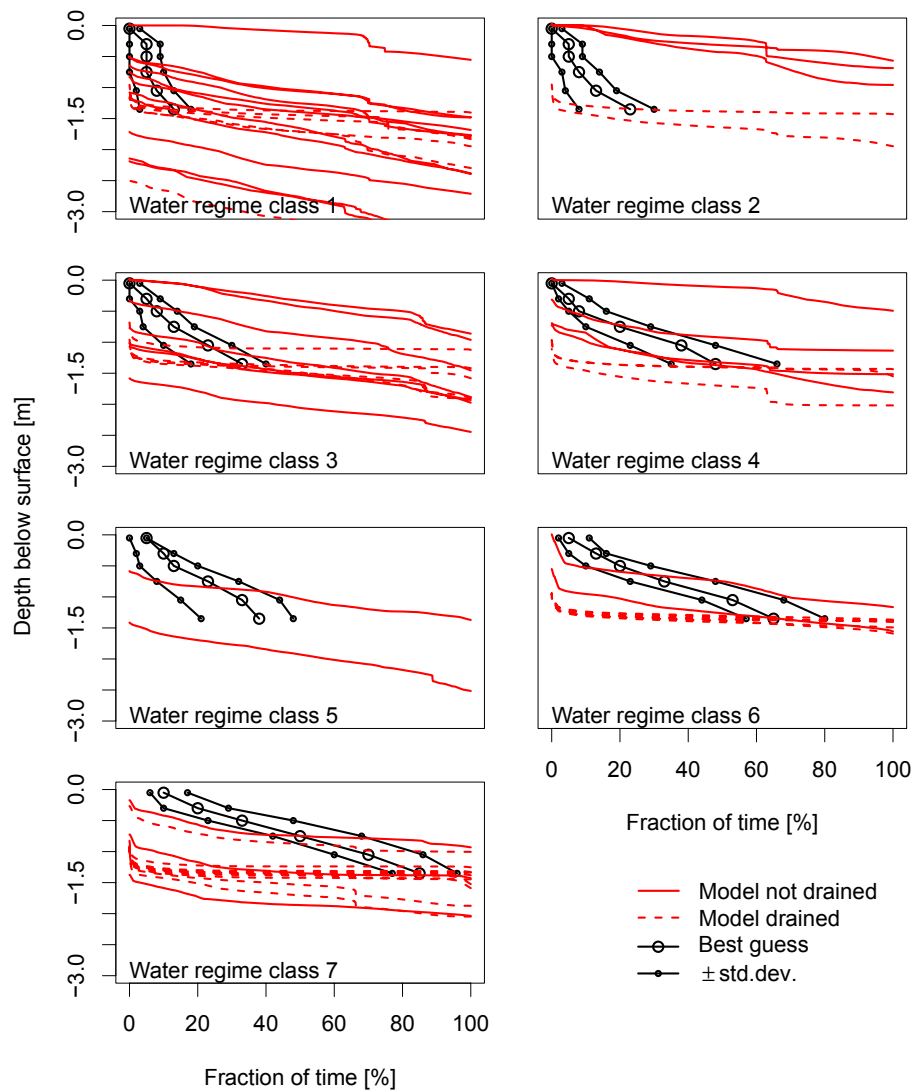
Figure 4.8: Comparison of the depth distribution of the saturation duration in selected model cells with the estimate from soil morphology. The model results are grouped into the respective water regime class and into drained and not drained cells.

validation. Soil morphology does not necessarily reflect the current water regime, especially when the water regime has recently changed because of artificial drainage. According to Hayes and Vepraskas (2000), soil drainage can alter morphology within decades. Finally, it is possible that the morphological signs of wetness do not evolve in a certain soil, even though the same water regime persists since a longer time. A possibility for this is soil saturation without oxygen depletion (e.g. frequent but short periods of saturation), which does not lead to morphological changes (Evans and Franzmeier, 1986; Pickering and
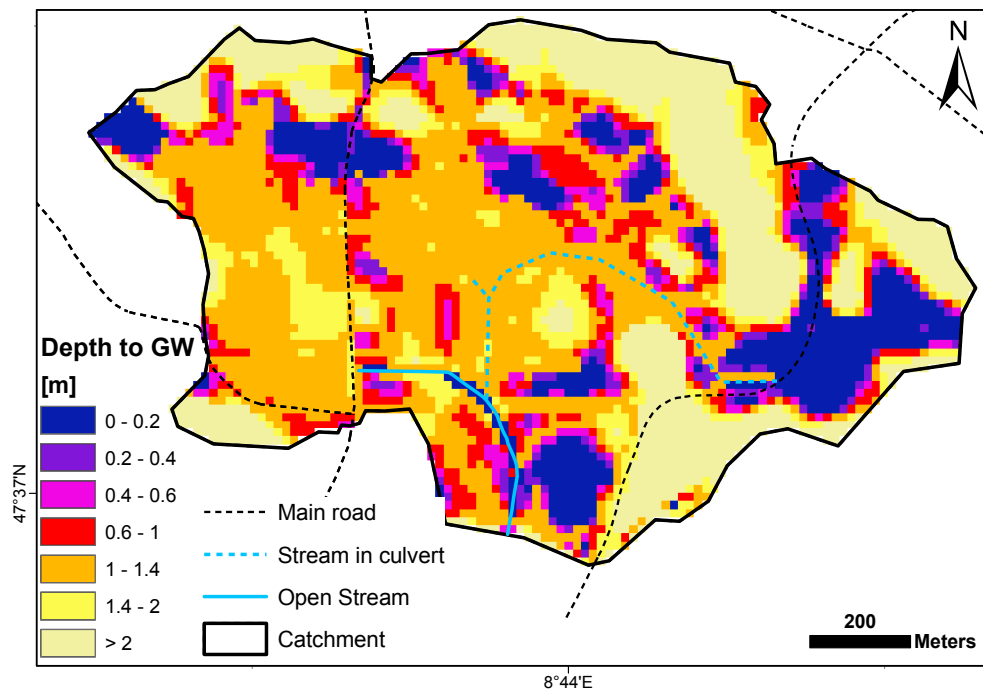
Figure 4.9: Map of the modeled depth to groundwater on 27 July 2009.

Veneman, 1984).

The main part of the drainage system in our study catchment was installed in the 1930ies, the soil map was produced between 1988 and 1997. It can therefore be expected that soil morphology reflects the current situation. However, the interpretation of drained soils will, in general, remain difficult.

The mismatch between the measured groundwater level and soil morphology at piezometer 1 shows the limitations of the approach. Soil morphology does not reflect the current water regime everywhere. The reasons for this can be manifold. As stated above, it is possible that the morphological signs of wetness did not evolve in this soil, even though the same water regime persists since a longer time. On the other hand, the current water regime as measured in the piezometer could have developed only few years ago, e.g. because of a poorly maintained and clogged part of the drainage system.

Despite these difficulties and limitations, the comparison of the estimates with the piezometric measurements shows a generally good agreement (Fig. 4.4). We are therefore confident that soil morphology in this region reflects the current water regime in most soils. The good agreement between the topographic wetness index and the map of the soil water regime classes indicates that the soil distribution with respect to soil saturation and soil water regime is mainly driven by topography in this catchment. In addition this

correspondence shows that the estimation of soil saturation from soil map information resulted in a reasonable spatial pattern of soil saturation in this catchment.

The quantitative interpretation of soil morphology will always remain uncertain to some degree. However, if the uncertainties can be quantified, such information can still be very valuable for model calibration and evaluation (Franks et al., 1998).

4.4.2   Model predictions

We chose a model setup with a homogeneous saturated zone where every cell in the saturated zone module had the same parameters. The only spatially variable attributes in the saturated zone module were topography, surface connectivity and tile drainage. However, with the spatially distributed unsaturated zone our setup resulted in 83 parameters to calibrate. The optimization was therefore a rather complex problem with the simultaneous calibration to discharge and groundwater levels at eleven locations. We started the calibration at the optimum parameter set of a model setup with a homogeneous unsaturated zone. Some of the parameters did not differentiate into the nine unsaturated zones but remained at the starting parameter value for all or some of the unsaturated zone modules. The likelihood function was therefore insensitive to a spatial distribution of these parameters (see Tables A.5 to A.8 in the Appendix for the maximum likelihood parameter set).

The model is able to reproduce the general hydrological behavior of the catchment (Figs. 3.2 and 4.6). The good match between observed and modeled groundwater levels (Fig. 4.6) with a model that assumes homogeneous soil properties indicates that groundwater levels in this catchment are mainly driven by topography and are not strongly influenced by the variability of hydraulic soil properties. However, if we focus on the top two meters below soil surface there are some deficiencies in the groundwater level predictions. This implies that other factors than just topography influence the depth to groundwater at this detailed scale.

The comparison with the estimates of soil saturation reveals a lack of differentiation between wet and dry areas (Fig 4.7) and wrong spatial patterns of soil saturation (Fig. 4.9). The main problems are i) the missing dynamics in the groundwater levels, ii) the dominance of the drainage system with respect to groundwater levels which leads to wrong spatial patterns of soil saturation and iii) the homogeneity within the drained part of the catchment. These deficiencies are problematic if one wants to use such a model to predict critical source areas. Saturation excess overland flow only occurs in situations with high groundwater levels. A prediction model therefore needs to be able to adequately

reproduce groundwater dynamics especially in situations with high groundwater levels. Furthermore, large parts of the intensively cultivated cropping areas in Switzerland are artificially drained; the model should therefore be able to predict groundwater levels and their dynamics in drained areas. The prediction of saturation excess areas requires a very high accuracy in groundwater level prediction. A difference of 50 cm or less in the depth to groundwater is already crucial, because it decides weather an area often produces saturation excess overland flow. When the absolute groundwater level range within the catchment is more than 30 m, the prediction of 50 cm difference is a difficult task. Even though the model captured the general hydrological behavior of the catchment with respect to discharge and absolute groundwater levels, it was far from being useful as a prediction tool for saturated areas. It did not achieve the accuracy that is needed for practical applications.

Some of the deficiencies were possibly caused by the chosen model setup of decoupled unsaturated and saturated zone modules. The groundwater level dynamics could probably be improved with a fully coupled saturated – unsaturated model where the effective porosity could vary with depth and with the status of the unsaturated zone. In addition, the unsaturated zone module does not react to changes in the groundwater level, even though in reality the unsaturated zone storage shrinks with a rising groundwater level. (Water that was counted to the unsaturated zone storage before belongs to the saturated storage when the water level rises. The unsaturated zone becomes thinner and therefore contains less water.) (Seibert et al., 2003). A further problem is the areal representation of the drainage system which is, in reality, a linear feature. The areal representation in the model prevents the buildup of high groundwater levels between drainage tubes and the corresponding high gradients between drainage tube and the undrained space between drainage tubes. If the tile drains should be implemented as linear features in a model, this would require a much higher spatial resolution. The rather low spatial resolution of our model setup (16 m) generally prevents the reproduction of very steep gradients on short distances which also influences the groundwater level dynamics.

These possible improvements of the model structure would lead to a three dimensional fully coupled saturated – unsaturated model with a high spatial resolution and a linear representation of the drainage system. It seems that such a detailed model would be necessary to achieve the accuracy which is necessary for the prediction of CSAs. A closer look at the piezometer data in Fig. 4.7 reveals that the groundwater level fluctuations are rather complex. Every piezometer reacts individually to the different rain events. Moreover, the dynamics of piezometers within the same water regime class differ substantially. Even if we consider weather a piezometer location is drained or not, it is impossible to explain the differences and similarities of the groundwater dynamics. It would have been

possible that the model can explain the spatial variability of groundwater level dynamics if these dynamics are determined by a combination of topographic position, the soil water regime class and the drained areas. However, the discrepancy between modeled and measured groundwater levels indicates that other processes influence the groundwater levels to a degree that can not be neglected. Even in the rather simple and homogeneous study catchment the fluctuations of the shallow groundwater seem to be complex. From a scientific point of view it would be interesting to dig deeper into these processes, trying to understand the influencing factors of the groundwater level dynamics with the help of a more complex model and a better spatial resolution. However, such a model would require very detailed information on the drainage system and its maintenance status. Besides, the computational demand for such a model would be very high when it is applied to the area of a whole catchment.

In the light of the above discussion about a more complex model it seems surprising that the prediction of CSAs by the topographic wetness index is in better agreement with the soil map than the predictions of the much more complex and realistic model. The assuptions behind the topographic wetness index are a grondwater level surface that is parallel to surface topography and the topo index totally ignores the tile drains. The added process understanding in our model where we included the tile drains, the unsaturated zone and a more realistic groundwater level surface calculation did not result in better spatial predictions. In contrast, the spatial predictions became worse. However, the topographic wetness index does not allow a quantitative analysis. Still, the rather good performance of the topographic wetness index with respect to spatial predictions indicates that a model of similar complexity and computational demand as ours might possibly be able to better predict CSAs and still have the advantages of a quantitative model prediction. Possibly we added model complexity at the wrong processes.

So far we discussed identification of CSAs caused by saturation excess overland flow. However, it was shown that areas that produce infiltration excess overland flow can be CSA on arable land (Doppler et al., 2012). These areas depend strongly on the actual land management and they can change with crop rotation or when the management practices are changing. Therefore, their identification requires knowledge on the current local site conditions. As an example, Srinivasan and McDowell (2009) found that small trampled areas beside fences were relevant in the occurrence of infiltration excess overland flow and the transport of phosphorus to the stream. Such features can not be captured by models based on generally available information and once they are identified in the field there is no need to implement them into a prediction model.

The focus of this study was to use a model that would be applicable for practical purposes.

Besides model based predictions, critical source areas can also be directly identified in the field by experts. This requires interviews with the local farmers and detailed site inspections. If a prediction model for CSAs should serve as basis for pollution mitigation measures, it must have advantages as compared to field visits by experts. An advantage of model predictions would be that predictions can be based on existing knowledge, so that field visits would not be necessary. However, the need for very detailed knowledge (e.g. on the drainage system and on the actual land management) undoes this advantage. Additionally, the demanding setup of a very detailed model, its calibration and test in every small catchment (not to talk about uncertainty analysis) would not lead to a time gain compared to field visits by experts to directly identify CSAs in the field.

4.5 Conclusions and outlook

Our case study has shown that the estimation of saturation durations from morphological soil map information is possible and these estimates have proven to be useful for model validation even though the resulting map of duration of soil saturation remains uncertain to some degree because the estimates do not always represent the current water regime. The additional data source provides quantitative spatial information on the soil water regime that can be used as validation data for the predicted spatial patterns. In a further step such estimates could also be used to calibrate spatially distributed hydrological models, so that no groundwater level measurements are needed for model calibration.

The model was able to reproduce the general hydrological behavior of the catchment. However, the desired accuracy of the groundwater level predictions - which is needed for the identification of CSAs - could not be achieved. The processes that determine the groundwater level dynamics in this catchment seem to be more complex than the used model. It seems that a high spatial resolution and very detailed process representations are needed for a groundwater level prediction that is accurate enough for the identification of CSAs in practical situations. Drained areas are especially challenging for the following reasons: limited data availability on tile drain locations and maintenance status; difficult integration in catchment models (concept and spatial resolution) and finally the estimation of soil saturation duration is much more difficult in drained areas.

Our results indicate that dynamic, spatially distributed hydrological models to predict CSAs are still far from being useful for management decisions. If a model should be accurate enough and should also include infiltration excess areas, it would require information that is not generally available. Furthermore, the setup and test of such a complex model would need more resources than direct observations of CSAs in the field by experts and the

local farmers. If site specific management of CSAs should be achieved, we recommend to identify these areas in the field and not solely by model predictions. However, predictions by simple models like the topographic wetness index can be helpful for the identification of CSAs in the field. It would also be intersting to test the predictive capabilities of different modeling concepts under real world conditions.

Acknowledgements

Chapter 5

Conclusion

The goal of this work was to assess and improve the predictability of critical source areas for herbicides. A particular focus was set on herbicide transport through subsurface pathways like tile drains and storm sewers. Three subgoals were defined:

1. To improve the process understanding of herbicide mobilization and transport from the field to the stream. A detailed understanding of how mobilization and transport processes influence the overall herbicide loss of a field is required if one aims at predictions in areas where no field data is available.

2. To quantify the spatial variability of herbicide losses in a test catchment at the scale of individual fields. Such data sets are needed to validate predictions and to test hypotheses about site properties that determine the spatial variability.

3. To test the predictability of critical source areas with a spatially distributed hydrological model. The prediction test should show if, at the current state of research and data availability, models can be used for management decisions. To increase the spatial data availability, we tested how one can make use of spatial data on the soil water regime that is contained in conventional soil maps to improve the prediction of CSAs.

The chosen approach to achieve these goals was a combination of field experiment and modeling. We present the results of a controlled herbicide application experiment where we could quantify the spatial variability of herbicide losses without beeing influenced by different weather conditions or different substance properties. We followed the herbicide transport with samples along the whole transport pathway from the treated fields to overland flow and drainflow and finally to the receiving stream. At the same time we investigated soil hydrological state variables and processes in the the catchment to link herbicide

transport to the hydrological processes. The challenge with this field experiment were the different scales that were involved. On the one hand, there was the need for observations at catchment and subcatchment scale to understand the whole systems behaviour. On the other hand, very detailed and well resolved oberservations were required to improve the process understanding. The resulting data set is very detailed and valuable to understand herbicide transport at catchment scale.

The simultaneous work in the field and with the model was fruitful for both sides. The work on the model helped to structure the field observations, while the field observations showed which processes are relevant and need to be modeled adequately. However, the detailed observations in the field also reveald the limits of what is possible to represent in a model.

5.1   Processes affecting herbicide mobilization and transport

Due to the detailed investigations in the field experiment, insights into relevant processes affecting herbicide mobilization and transport could be gained.

Relevance of infiltation excess overland flow for herbicide mobilization

Based on previous studies, it was assumed that saturation excess overland flow is the dominant mechanism of herbicide mobilization and transport under the conditions prevailing in the Swiss Plateau. Due to the detailed investigations in the field experiment we could show that infiltration excess overland flow can also be a crucial process. In this study, the major part of herbicides transported to the stream was mobilized by infiltration excess overland flow. Important reasons for this were the high intensity rainfall events after herbicide application and the limited soil coverage on the corn fields. Thunderstorms with high intensity rainfall are common during summer in Switzerland. It can therefore be assumed that the finding of infiltration excess overland flow being important is not a particularity of this study but that, under Swiss conditions, infiltation excess overland flow can be an important herbicide mobilization process in general. This is especially true for crops and crop stages with little soil coverage.

Manholes and storm drains as herbicide pathways to the stream

In areas where the topography is such that overland flow from the fields can not directly flow into the stream because it is retained in topographic sinks, the subsurface drainage system is the main input pathway for herbicides. The subsurface pipe network encompasses tile drains as well as storm sewers for roads and farmyards. Besides the preferential flow to tile drains, maintenance manholes of the drainage system and road and farmyard storm drains can be relevant input pathways. Maintenance manholes are distributed throughout the drained areas, often they are in the middle of fields. Even though they have closed lids and are not intended to collect surface runoff, they can collect relevant amounts of overland flow which then directly enters the drainage system and therefore the stream. Storm drains on roads and farmyards are intended to collect runoff from these paved areas. However, if overland flow from the fields reaches such paved areas, the storm drains also collect the overland flow with herbicides. Often these storm drains are directly connected to streams. Because of the dense road network in rural areas of Switzerland, such situations are rather common.

Influence of sorption on herbicide mobilization and transport

So far, it has been assumed that sorption has only a small influence on herbicide transport once the compounds have been mobilized into the fast flowing water. However, our data give a more differentiated picture of how chemical interactions between compounds and soil influence the transport processes. First, the sorption properties of the herbicides influence their mobilization. Desorption kinetics and the apparent distribution coefficient both play a role. However, their interplay is not yet clarified. Furthermore, we could show that sorption does influence the herbicide transport through macropores where stronger sorbing compounds were retained more than less sorbing compounds. This was in contrast to the expectations since the travel times through macropores are short.

5.2 Critical source areas

5.2.1 Do critical source areas exist everywhere?

The results of this study show that critical source areas are a useful heuristic concept to understand herbicide losses to the stream. However, the findings also demonstrate the limits of the applicability of the concept. The observed spatial variability of herbicide loss rates in the test catchment was not as large as it was expected due to the large

variability of soil water regimes. Moreover, the ranking of the fields with regard to herbicide lossrates was not the same in all the rain events. This means that critical source areas are not temporally stable and can therefore not be considered as a site property. Thus, in conditions of similar loss behavior, a management that only focuses on the most critical source areas would not lead to a significant reduction of diffuse pollution.

In contrast to the findings of this study, earlier studies in a different region of the Swiss Plateau found extreme spatial variability in the herbicide lossrates. Therefore, it can be concluded that the magnitude of the spatial variability of herbicide losses is obviously not the same in all regions. In areas where the spatial variability is large, site specific management on critical source areas makes sense. In areas with little spatial variability rather area-wide measures should be considered.

5.2.2   Identification of critical source areas

A simple but accurate and reliable method for the identification of CSAs is required for the support of management decisions. The model that was used in this study captured the general hydrological behavior of the catchment well. However, the model results were not accurate enough for the predction of CSAs caused by saturation excess overland flow. Groundwater level dynamics and the spatial pattern of soil saturation were not correctly reproduced by the model.

The results of the modeling study indicate that the use of soil morphology information for model testing is promising. The estimation of the duration of soil saturation was reasonable in our case. In addition, it was possible to quantify the uncertainty of the saturation duration estimates. This is crucial if the estimates should be used for model validation and / or calibration. The resulting map of soil saturation durations (and their uncertainty) could be used as validation data for the model predictions and revealed some deficiencies in the model. The use of this additional spatial database is not only of interest for the prediction of critical source areas, but it can be used for distributed hydrological modeling in general where usually spatial data for model calibration and validation are rare.

There are indications that with a more complex and detailed model it might be possible to predict CSAs more accurately. Especially the representation of the coupling between the unsaturated and the saturated zone seems to be a critical part for the prediction of shallow groundwater tables. Furthermore, a high spatial resolution is important and the way how the drainage system is represented in the model seems to be crucial for an accurate groundwater level prediction especially in drained areas.

The rather good performance of the topographic wetness index with respect to spatial predictions however indicates that very simple models can be useful tools to get first ideas on possible locations of critical source areas.

5.3   Practical implications

The findings of this study have implications for the practical implementation of mitigation strategies against diffuse pollution of surface waters with herbicides:

1. The fact that infiltration excess overland flow can be an important herbicide mobilization and transport process offers mitigation options. The areas where infiltration excess overland flow occurs in crop production regions strongly depend on the crop, the crop stage and on land management. There are options to reduce the occurrence of infiltation excess overland flow by adapted land management (e.g. plowing direction, type of harrowing, addition of organic material to stabilize soil aggregates,...). The same measures are also used to prevent soil erosion. Measures to prevent soil erosion could therefore also mitigate diffuse pollution.

2. The connectivity of fast flow paths from the fields to the stream is crucial for diffuse pollution. Preventing overland flow from directly entering the stream or a shortcut to the stream (manholes, stormdrains) is a promising way of reducing diffuse pollution. Land management should therefore aim at a soil passage for all water before it enters the stream.

3. If CSAs exist in a certain area and if they are correctly identified, this offers the opportunity of taking action only on the CSAs to efficiently reduce diffuse pollution. However, the study results suggest that the identification of CSAs with complex and detailed models may not be a feasable way for practical applications. Even if a model would be able to correctly predict CSAs, there are reasons that prevent a reasonable use of such models in routine applications:

   (a) The main reason is the extensive data requirement for such models. Data are needed in a degree of detail that is not commonly available. Examples for such data are: information on the drainage system and its maintenace status or the plowing direction and the surface roughness on the fields. Futhermore in some cases, small scale features in the landscape like field edges etc. dominate the loss behavior. Such data can only be obtained by field visits which is not within

the scope of a model that should make predictions solely based on available information.

(b) The time demand for model setup and testing is high for very detailed models.

(c) The computational demand for reasonable model calibrations and uncertainty analyses is very high.

(d) If field visits are necessary anyway, the time gain of model based identification of CSAs as compared to identification in the field is questionable.

Based on the above argumentats, we recommend to identify CSAs by experts' field visists and interviews with local farmers. Nevertheless, maps that display important influencing factors could support the work of experts in the field. Maps that could be used for this purpose include i) an erosion risk map, ii) a drainage map (including manhole and storm drain locations), iii) a soil map (possibly with the soil saturation duration estimates), iv) a map of connectivity (including connectivity to drained roads and manholes of the drainage system), and v) a map of the topographic wetness index.

Bibliography

Abbott, M. B., Bathurst, J. C., Cunge, J. A., O'Connell, P. E., and Rasmussen, J.: An introduction to the European Hydrological System - Systeme Hydrologique Européen, "SHE", 1: History and philosophy of a physically-based, distributed modelling system, Journal of Hydrology, 87, 45–59, 1986.

Agnew, L. J., Lyon S., Gérard-Marchant, P., Collins, V. B., Lembo, A. J., Steenhuis, T. S., Walter, M. T.: Identifying hydrologically sensitive areas: Bridging the gap between science and application, Journal of Environmental Management, 78, 63–76, 2006.

Allen, R. G., Pereira, L. S., Raes, D., and Smith, M.: Crop evapotranspiration – Guidelines for computing crop water requirements – FAO Irrigation and drainage paper 56, FAO – Food and Agriculture Organization of the United Nations, Rome, 1998.

Altfelder, S., Streck, T., and Richter, J.: Nonsingular sorption of organic compounds in soil: The role of slow kinetics, J. Environ. Qual., 29, 917–925, 2000.

Anderson, M. G. and Burt, T. P.: Toward more detailed field monitoring of variable source areas, Water Resour. Res., 14, 1123–1131, 1978.

Aurousseau, P., Gascuel-Odoux, C., Squividant, H., Trepos, R., Tortrat, F., and Cordier, M. O.: A plot drainage network as a conceptual tool for the spatial representation of surface flow pathways in agricultural catchments, Comput. Geosci., 35, 276–288, 2009.

Barron, O. V., Pollock, D., and Dawes, W.: Evaluation of catchment contributing areas and storm runoff in flat terrain subject to urbanisation, Hydrol. Earth Syst. Sci., 15, 547–559, 2011.

Beers, W. F .J.: Computing drain spacings, Wageningen, International institute for land reclamation and improvement, 1976.

Béguin, J., and Smola, S.: Stand der Draingen in der Schweiz, Bilanz der Umfrage 2008, Bundesamt fü Landwirtschaft BLW, Abteilung Melioration, Bern, 2010.

Betson, R. P.: What is watershed runoff, J. Geophys. Res., 69, 1541–1552, 1964.

Blazkova, S., Beven, K. J., Kulasova, A.: On constraining TOPMODEL hydrograph simulations using partial saturated area information, Hydrological Processes, 16, 441–458, 2002.

Boorman, D. B., Hollis, J. M., and Lilly, A.: Hydrology of soil types: a hydrologically-based classification of the soils of the United Kingdom, Inst. Hydrol., Wallingford, http://www.ceh.ac. uk/products/publications/hydrology.html, 1995.

Borah, D. K. and Bera, M.: Watershed–scale hydrologic and nonpoint–source pollution models: Review of mathematical bases, Transactions of the Asae, 46, 1553–1566, 2003.

Box, G.E.P. and Cox, D.R.: An analysis of transformations, Journal of the royal statistical society, series B – statistical methodology, 26, 211 – 252, 1964.

Box, G.E.P. and Cox, D.R.: An analysis of transformations revisited, rebutted, Journal of the americal statistical association, 77, 209 – 210, 1982.

Brown, C. D. and van Beinum, W.: Pesticide transport via sub-surface drains in Europe, Environ. Pollut., 157, 3314–3324, 2009.

Brusseau, M. L. and Rao, P. S. C.: The influence of sorbate-organic matter interactions on sorption nonequilibrium, Chemosphere, 18, 1691–1706, 1989.

Camenzuli, L.: Degradation of herbicides in soils, kinetics and limiting factors in field and laboratory, Master Thesis, Swiss Federal Institute of Technology (ETH), Zürich, Switzerland, 2010.

Capel, P. D., and Larson, S. J.: Effect of Scale on the Behavior of Atrazine in Surface Waters, Environmental Science & Technology, 35, 648–657, 2001.

Carluer, N. and De Marsily, G.: Assessment and modelling of the influence of man-made networks on the hydrology of a small watershed: implications for fast flow components, water quality and landscape management, J. Hydrol., 285, 76–95, 2004.

Chèvre, N., Loepfe, C., Fenner, K., Singer, H., Escher, B., and Stamm, C.: Pestizide in Schweizer Oberflächengewässern, wirkungsbasierte Qualitätskriterien, GWA, 4, 297 – 307, 2006.

Church, M. and Woo, M. K.: Geography of surface runoff: some lessons for research, in: Process studies in hillsope hydrology, edited by: Anderson, M. G. and Burt, T. P., Wiley, Chichester, 299–326, 1990.

Deasy, C., Baxendale, S. A., Heathwaite, A. L., Ridall, G., Hodgkinson, R., and Brazier, R. E.: Advancing understanding of runoff and sediment transfers in agricultural catchments through simultaneous observations across scales, Earth Surf. Proc. Land., 36, 1749–1760, 2011.

Descroix, L., Viramontes, D., Estrada, J., Barrios, J. L. G., and Asseline, J.: Investigating the spatial and temporal boundaries of Hortonian and Hewlettian runoff in Northern Mexico, J. Hydrol., 346, 144–158, 2007.

Domagalski, J. L., Ator, S., Coupe, R., McCarthy, K., Lampe, D., Sandstrom, M., and Baker, N.: Comparative Study of Transport Processes of Nitrogen, Phosphorus, and Herbicides to Streams in Five Agricultural Basins, USA, J. Environ. Qual., 37, 1158–1169, 2008.

Doppler, T., Camenzuli, L., Hirzel, G., Krauss, M., Lück, A., and Stamm, C.: Spatial variability of herbicide mobilisation and transport at catchment scale: insights from a field experiment, Hydrol. Earth Syst. Sci., 16, 1947–1967, 2012.

Dunne, T. and Black, R. D.: Partial area contributions to storm runoff in a small New-England watershed, Water Resour. Res., 6, 1296–1311, 1970.

Easton, Z. M., Fuka, D. R., Walter, M. T., Cowan, D. M., Schneiderman, E. M., and Steenhuis, T. S.: Re-conceptualizing the soil and water assessment tool (SWAT) model to predict runoff from variable source areas, J. Hydrol., 348, 279–291, 2008.

Einsele, G: Sedimentary Basins: Evolution, Facies, and Sediment Budget. 2nd ed. Springer, Berlin, 2000.

ESRI, ArcGIS Desktop 9.3.1, Redlands, CA, USA, 2009.

Evans, C. V. and Franzmeier, D. P.: Saturation, Aeration, and Color Patterns in a Toposequence of Soils in North-Central Indiana, Soil Science Society of America Journal, 50, 975–980, 1986.

FAL: Bodenkarte Kanton Zürich 1:5000, Eidgenössische Forschungsanstalt für Agrarökologie und Landbau Zürich, 1997.

Flühler, H., Durner, W., and Flury, M.: Lateral solute mixing processes – a key for understanding field-scale transport of water and solutes, Geoderma, 70, 165–183, 1996.

Franks, S. W., Gineste, P., Beven, K. J., and Merot, P.: On constraining the predictions of a distributed model: The incorporation of fuzzy estimates of saturated areas into the calibration process, Water Resources Research, 34, 787–797, 1998.

Franzmeier, D. P., Yahner, J. E., Steinhardt, G. C., Sinclair, H. R.: Color Patterns and Water-Table Levels in Some Indiana Soils, Soil Science Society of America Journal, 47, 1196–1202, 1983.

Freer, J. E., McMillan, H., McDonnell, J. J., Beven, K. J.: Constraining dynamic TOP-MODEL responses for imprecise water table information using fuzzy rule based performance measures, Journal of Hydrology, 291, 254–277, 2004.

Freeze, R. A.: Streamflow generation, Rev. Geophys., 12, 627–647, 1974.

Frey, M. P., Schneider, M. K., Dietzel, A., Reichert, P., and Stamm, C.: Predicting critical source areas for diffuse herbicide losses to surface waters: role of connectivity and boundary conditions, J. Hydrol., 365, 23–36, 2009.

Frey, M. P., Stamm, C., Schneider, M. K., and Reichert, P.: Using discharge data to reduce structural deficits in a hydrological model with a Bayesian inference approach and the implications for the prediction of critical source areas, Water Resources Research, 47, W12529, 2011.

Gallart, F., Latron, J., Llorens, P., and Beven, K.: Using internal catchment information to reduce the uncertainty of discharge and baseflow predictions, Advances in Water Resources, 30, 808–823, 2007.

Gburek, W. J. and Sharpley, A. N.: Hydrologic controls on phosphorus loss from upland agricultural watersheds, J. Environ. Qual., 2, 267–277, 1998.

Gemeinde Ossingen: Drainagenkarte 1:1000, Flurgenossenschaft Gemeinde Ossingen, 1995.

Gemeinde Ossingen: Entwässerungsplan der Gemeinde Ossingen, 2008.

Gerecke, A. C., Schärer, M., Singer, H. P., Müller, S. R., Schwarzenbach, R. P., Sägesser, M., Ochsenbein, U., and Popow, G.: Sources of pesticides in surface waters in Switzerland: pesticide load through waste water treatment plants – current situation and reduction potential, Chemosphere, 48, 307–315, 2002.

Gerits, J. J. P., de Lima, J. L. M. P., and van den Broek, T. M. W.: Overland flow and erosion, in: Process studies in hillsope hydrology, edited by: Anderson, M. G. and Burt, T. P., Wiley, Chichester, 173–214, 1990.

Ghafoor, A., Jarvis, N.J., Thierfelder, T., and Stenström J.: Measurements and modeling of pesticide persistence in soil at the catchment scale, Science of the Total Environment, 409, 1900–1908, 2011a

Ghafoor, A., Moeys, J., Stenström, J., Tranter, G., and Jarvis N.J.: Modeling spatial vari-
    ation in microbial degradation of pesticides in soil, Environmental Science & Technology,
    45, 6411–6419, 2011b

Gomides Freitas, L.: Herbicide losses to surface waters in a small agricultural catchment,
    Ph.D. thesis, Swiss Federal Institute of Technology, Zürich (ETH), 2005.

Gomides Freitas, L., Singer, H., Müller, S. R., Schwarzenbach, R. P., and Stamm, C.:
    Source area effects on herbicide losses to surface waters – a case study in the Swiss
    Plateau, Agr. Ecosyst. Environ., 128, 177–184, 2008.

Goodrich, D. C., Lane, L. J., Shillito, R. M., Miller, S. N., Syed, K. H., and Wool-
    hiser, D. A.: Linearity of basin response as a function of scale in a semiarid watershed,
    Water Resour. Res., 33, 2951–2965, 1997.

Grabs, T., Seibert, J., Bishop, K., and Laudon, H.: Modeling spatial patterns of saturated
    areas: A comparison of the topographic wetness index and a dynamic distributed model,
    Journal of Hydrology, 373, 15–23, 2009.

Grayson, R. B., Moore, I. D., and McMahon, T. A.: Physically based hydrologic modeling
    1. A terrain-based model for investigative purposes, Water Resources Research, 26,
    2639–2658, 1992a.

Grayson, R. B., Moore, I. D., and McMahon, T. A.: Physically based hydrologic modeling
    2. Is the concept realistic?, Water Resources Research, 26, 2659–2666, 1992b.

Grayson, R. B., Blöschl, G., Western, A. W., and McMahon, T. A.: Advances in the
    use of observed spatial patterns of catchment hydrological response, Advances in Water
    Resources, 25, 1313–1334, 2002.

Groupe diagnostic du CORPEN: Qualité des eaux et produits phytosanitaires: Propo-
    sitions pour une demarche de diagnostic, Republique Francaise, Ministere de
    l'Environnement et Ministere de l'Agriculture, de la Peche et de l'Alimentation. 1996.

GschV, Gewässerschutz Verordnung SR-814.201, Swiss water protection ordinance, 2005

Güntner, A., Seibert, J., and Uhlenbrook, S.: Modeling spatial patterns of saturated areas:
    An evaluation of different terrain indices, Water Resour. Res., 40, W05114, 2004.

Hahn, C., Prasuhn, V., Stamm, C., and Schulin, R.: Phosphorus losses in runoff from
    manured grassland of different soil P status at two rainfall intensities, Agr. Ecosyst.
    Environ., 153, 65–74, 2012.

Hayes, W. A. and Vepraskas, M. J.: Morphological changes in soils produced when hy-drology is altered by ditching, Soil Science Society of America Journal, 64, 1893–1904, 2000.

Heathwaite, A. L., Quinn, P. F., and Hewett, C. J. M.: Modelling and managing critical source areas of diffuse pollution from agricultural land using flow connectivity simula-tion, J. Hydrol., 304, 446–461, 2005.

Herschy, R. W.: Streamflow measurement, 2nd Edn., E&FN Spon, London, 1995.

Hindmarsh, A. C.: A Systematized Collection of ODE Solvers, in: IMACS Transactions on Scientific Computation, Stepleman, R. S., Scientific Computing, Amsterdam, 55 – 64, 1983.

Hirzel, G.: Detecting and measuring overland flow in the "Eschibach" catchment, Ossin-gen, Switzerland, Master Thesis, Swiss Federal Institute of Technology (ETH), Zürich, Switzerland, 2009.

Horton, R. E.: The role of infiltration in the hydrologic cycle, EOS T. Am. Geophys. Un., 14, 446–460, 1933.

Hrachowitz, M., Savenije, H. H. G., Blöschl, G., McDonnell, J. J., Sivapalan, M., Pomeroy, J. W., Arheimer, B., Blume, T., Clark, M. P., Ehret, U., Fenicia, F., Freer, J. E., Gelfan, A., Gupta, H. V., Hughes, D. A., Hut, R. W., Montanari, A., Pande, S., Tetzlaff, D., Troch, P. A., Uhlenbrook, S., Wagener, T., Winsemius, H. C., Woods, R. A., Zehe, E., and Cudennec, C.: A decade of Predictions in Ungauged Basins (PUB) – a review, Hydrological Sciences Journal, 58, 1198–1255, 2013.

Jacobs, P. M., West, L. T. and Shaw, J. N.: Redoximorphic features as indicators of seasonal saturation, Lowndes County, Georgia, Soil Science Society of America Journal, 66, 315–323, 2002.

Jarvis, N. J.: A review of non-equilibrium water flow and solute transport in soil macrop-ores: Principles, controlling factors and consequences for water quality, Eur. J. Soil Sci., 58, 523–546, 2007.

Kennedy, J. and Eberhart, R.: Particle swarm optimization, in: Proceedings of the Inter-national Conference on Neural Networks (IEEE), vol. 4, 1942 – 1948, 1995.

Kiesel, J., Fohrer, N., Schmalz, B., and White, M. J.: Incorporating landscape depressions and tile drainages of a Northern German lowland catchment into a semi-distributed model, Hydrol. Process., 24, 1472–1486, 2010.

Kirkby, M. J., Callan, J., Weyman, D., and Wood, J.: Measurement and modeling of dynamic contributing areas in very small catchments, Working paper 167, School of Geography, University of Leeds, Leeds, England, 1976.

Kladivko, E. J., Brown, L. C., and Baker, J. L.: Pesticide transport to subsurface tile drains in humid regions of North America, Crit. Rev. Env. Sci. Tec., 31, 1–62, 2001.

Lamb, R., Beven, K., and Myrabø, S.: Use of spatially distributed water table observations to constrain uncertainty in a rainfall-runoff model, Advances in Water Resources, 22, 305–317, 1998.

Larson, S. J., Capel, P. D., Goolsby, A. G., Zaugg, S. D., and Sandstrom, M. W.: Relations between pesticide use and riverine flux in the Mississippi River basin, Chemosphere, 31, 3305–3321, 1995.

Ledermann, T., Herweg, K., Liniger, H. P., Schneider, F., Hurni, H., and Prasuhn, V.: Applying erosion damage mapping to assess and quantify off-site effects of soil erosion in Switzerland, Land Degrad. Dev., 21, 353–366, 2010.

Leu, C., Singer, H., Stamm, C., Müller, S. R., and Schwarzenbach, R. P.: Simultaneous assessment of sources, processes, and factors influencing herbicide losses to surface waters in a small agricultural catchment, Environ. Sci. Technol., 38, 3827–3834, 2004a.

Leu, C., Singer, H., Stamm, C., Müller, S. R., and Schwarzenbach, R. P.: Variability of herbicide losses from 13 fields to surface water within a small catchment after a controlled herbicide application, Environ. Sci. Technol., 38, 3835–3841, 2004b.

Leu, C., Singer, H., Müller, S. R., Schwarzenbach, R. P., and Stamm, C.: Comparison of atrazine losses in three small headwater catchments, J. Environ. Qual., 34, 1873–1882, 2005.

Leu, C., Schneider, M. K., and Stamm, C.: Estimating catchment vulnerability to diffuse herbicide losses from hydrograph statistics, J. Environ. Qual., 39, 1441–1450, 2010.

Liess, M. and Schulz, R.: Linking insecticide contamination and population response in an agricultural stream, Environ. Toxicol. Chem., 18, 1948–1955, 1999.

Louchart, X., Voltz, M., Andrieux, P., and Moussa, R.: Herbicide transport to surface waters at field and watershed scales in a Mediterranean vineyard area, J. Environ. Qual., 30, 982–991, 2001.

Lyon, S. W., McHale, M. R., Walter, M. T., and Steenhuis, T. S.: The impact of runoff generation mechanisms on the location of critical source areas, J. Am. Water Resour. As., 42, 793–804, 2006.

Mamy, L. and Barriuso, E.: Desorption and time-dependent sorption of herbicides in soils, Eur. J. Soil Sci., 58, 174–187, 2007.

Maréchal, D., and Holman, I. P.: Development and application of a soil classification-based conceptual catchment-scale hydrological model, Journal of Hydrology, 312, 277–293, 2005.

Montagne, D., Cornu, S., Le Forestier, L. and Cousin, I.: Soil Drainage as an Active Agent of Recent Soil Evolution: A Review, Pedosphere, 19, 1–13, 2009.

Moore, T. R., Dunne, T., and Taylor, C. H.: Mapping runoff-producing zones in humid regions, J. Soil Water Conserv., 31, 160–164, 1976.

Morgan, C. P. and Stolt, M. H.: Soil morphology–water table cumulative duration relationships in southern New England, Soil Science Society of America Journal, 70, 816–824, 2006.

Müller, K., Bach, M., Hartmann, H., Spiteller, M., Frede H.-G.: Point- and Nonpoint-Source Pesticide Contamination in the Zwester Ohm Catchment, Germany, J. Environ. Qual., 31, 309–318, 2002.

Munz, N., Leu, C., and Wittmer, I.: Pestizidmessungen in Fliessgewässern, Schweizweite Auswertung, Aqua & Gas, 11, 32–41, 2012.

Nash, J.E. and Sutcliffe, J.V.: River flow forcasting through conceptual models, part 1 – a discussion of principles. 10, 282 – 290, 1970.

Neitsch, S., Arnold, J., Kiniry, J., and Williams, J.: Soil and water assessment tool theoretical documentation. Version 2005, Tech. Rep., Texas Water Resource Institute, Temple, Texas, 2005.

Nelder, J. A. and Mead, R.: A Simplex Method for Function Minimization, The Computer Journal, 7, 308 – 313, 1965.

Noll, M. R. and Magee, E. A.: Quantification of phosphorus sources to a small watershed: a case study of Graywood Gully, Conesus Lake, NY, J. Great Lakes Res., 35, 50–55, 2009.

Payraudeau, S., Junker, P., Imfeld, G., and Gregoire, C.: Characterizing hydrological connectivity to identify critical source areas for pesticides losses, 18th World Imacs Congress and Modsim09 International Congress on Modelling and Simulation, 13 to 17 July 2009, Cairns, Australia, 1879–1885, 2009.

Petzold, L.: Automatic Selection of Methods for Solving Stiff and Nonstiff Systems of Ordinary Differential Equations, SIAM Journal on Scientific and Statistical Computing, 4, 136 – 148, 1983.

Pickering, E. W. and Veneman, P. L. M.: Moisture Regimes and Morphological-Characteristics in a Hydrosequence in Central Massachusetts, Soil Science Society of America Journal, 48, 113–118, 1984.

Pionke, H. B., Gburek, W. J., Sharpley, A. N., and Schnabel, R. R.: Flow and nutrient export patterns for an agricultural hill-land watershed, Water Resour. Res., 32, 1795–1804, 1996.

Pionke, H. B., Gburek, W. J., and Sharpley, A. N.: Critical source area controls on water quality in an agricultural watershed located in the Chesapeake Basin, Ecol. Eng., 14, 325–335, 2000.

PPDB: The PPDB (Pesticide Properties DataBase), collated by the University of Hertfordshire, 2010.

Rabiet, M., Margoum, C., Gouy, V., Carluer, N., and Coquery, M.: Assessing pesticide concentrations and fluxes in the stream of a small vineyard catchment - Effect of sampling frequency, Environmental Pollution, 158, 737–748, 2010.

Refsgaard, J. C., Storm, B., and Clausen, T.: Système Hydrologique Européen (SHE): review and perspectives after 30 years development in distributed physically-based hydrological modelling. Hydrology Research, 41, 355–377, 2010.

Reichenberger S., Hollis J.M., Jarvis N.J., Lewis, K.A., Tzilivakis J., Mardhel V., François O., Cerdan O., Dubus I.G., Réal B., Højberg A.L., Nolan B.T.: Report on the identification of landscape features and contamination pathways at different scales. Report DL25 of the FP6 EU-funded FOOTPRINT project [www.eu-footprint.org], 2008.

Schneider, M. K., Brunner, F., Hollis, J. M., and Stamm, C.: Towards a hydrological classification of European soils: preliminary test of its predictive power for the base flow index using river discharge data, Hydrol. Earth Syst. Sci., 11, 1501–1513, 2007.

Seibert, J., Rodhe, A., and Bishop, K.: Simulating interactions between saturated and unsaturated storage in a conceptual runoff model, Hydrological Processes, 17, 379–390, 2003.

Siber, R., Stamm, C., and Reichert, P.: Modeling potential herbicide loss to surface waters on the Swiss plateau, Journal of Environmental Management, 91, 290–302, 2009.

Simonson, G. H. and Boersma, L.: Soil Morphology and Water Table Relations .2. Correlation between Annual Water Table Fluctuations and Profile Features, Soil Science Society of America Proceedings, 36, 649–653, 1972.

Singer, H., Jaus, S., Hanke, I., Lück, A., Hollender, J., and Alder, A. C.: Determination of biocides and pesticides by on-line solid phase extraction coupled with mass spectrometry and their behaviour in wastewater and surface water, Environ. Pollut., 158, 3054–3064, 2010.

Srinivasan, M. S., Wittman, M. A., Hamlett, J. M., and Gburek, W. J.: Surface and subsurface sensors to record variable runoff generation areas, T. ASAE, 43, 651–660, 2000.

Srinivasan, M. S., Gburek, W. J., and Hamlett, J. M.: Dynamics of stormflow generation – a hillslope-scale field study in east-central Pennsylvania, USA, Hydrol. Process., 16, 649–665, 2002.

Srinivasan, M. S. and McDowell, R. W.: Identifying critical source areas for water quality: 1. Mapping and validating transport areas in three headwater catchments in Otago, New Zealand, Journal of Hydrology, 379, 54–67, 2009.

Stamm, C., Sermet, R., Leuenberger, J., Wunderli, H., Wydler, H., Flühler, H., and Gehre, M.: Multiple tracing of fast solute transport in a drained grassland soil, Geoderma, 109, 245–268, 2002.

Stamm, C., Waul, C., Leu, C., Freitas, L. G., Popow, G., Singer, H., and Müller, S.: Sorption effects on herbicide losses to surface waters in a small catchment of the Swiss Plateau, Zeitschrift für Pflanzenkrankheiten und Pflanzenschutz, J. Plant Dis. Protect, 19, 951–958, 2004.

Stehle, S., Elsaesser, D., Gregoire, C., Imfeld, G. l., Niehaus, E., Passeport, E., Payraudeau, S., Schäfer, R. B., Tournebize, J., and Schulz, R.: Pesticide Risk Mitigation by Vegetated Treatment Systems: A Meta-Analysis, J. Environ. Qual., 40, 1068–1080, 2011.

Streck, T., Poletika, N. N., Jury, W. A., and Farmer, W. J.: Description of simazine transport with rate-limited, two-stage, linear and nonlinear sorption, Water Resour. Res., 31, 811–822, 1995.

Swisstopo: DTM$^{©}$, reproduced with permission of swisstopo, Wabern, Switzerland, JA100119, 2003.

Swisstopo: Geologischer Atlas der Schweiz$^{©}$, reproduced with permission of swisstopo, Wabern, Switzerland, JA100119, 2007.

Swisstopo: Vector25$^{©}$, reproduced with permission of swisstopo, Wabern, Switzerland, JA100119, 2008.

Terribile, F. and Coppola, A. and Langella, G. and Martina, M. and Basile, A.: Potential and limitations of using soil mapping information to understand landscape hydrology, Hydrology and Earth System Sciences, 15, 3895–3933, 2011.

Thurman, E. M., Goolsby, D. A., Meyer, M. T., and Kolpin, D. W.: Herbicides in surface waters of the Midwestern United-States – the effect of spring flush, Environ. Sci. Technol., 25, 1794–1796, 1991.

Vepraskas, M. J. and Wilding, L. P.: Aquic Moisture Regimes in Soils with and without Low Chroma Colors, Soil Science Society of America Journal, 47, 280–285, 1983.

Vereecken, H., Vanderborght, J., Kasteel, R., Spiteller, M., Schäffer, A. and Close, M.: Do lab-derived distribution coefficient values of pesticides match distribution coefficient values determined from column and field-scale experiments? A critical analysis of relevant literature, J. Environ. Qual., 40, 879–898, 2011.

Villaverde, J., Van Beinum, W., Beulke, S., and Brown, C. D.: The kinetics of sorption by retarded diffusion into soil aggregate pores, Environ. Sci. Technol., 43, 8227–8232, 2009.

Weiler, M. and McDonnell J.: Virtual experiments: a new approach for improving process conceptualization in hillslope hydrology, Journal of Hydrology, 285, 3–18, 2004.

Weiler, M. and Naef, F.: Simulating surface and subsurface initiation of macropore flow, J. Hydrol., 273, 139–154, 2003.

Wittmer, I. K.: Influence of agricultural pesticide and urban biocide use on load dynamics in surface waters, Ph.D. thesis, Swiss Federal Institute of Technology, Zürich (ETH), 2010.

Wittmer, I. K., Bader, H. P., Scheidegger, R., Singer, H., Lück, A., Hanke, I., Carlsson, C., and Stamm, C.: Significance of urban and agricultural land use for biocide and pesticide dynamics in surface waters, Water Resour. Res., 44, 2850–2862, 2010.

Zhu, H. X. and Selim, H. M.: Hysteretic behavior of metolachlor adsorption-desorption in soils, Soil Sci., 165, 632–645, 2000.

Appendix

Supporting information for chapter 2
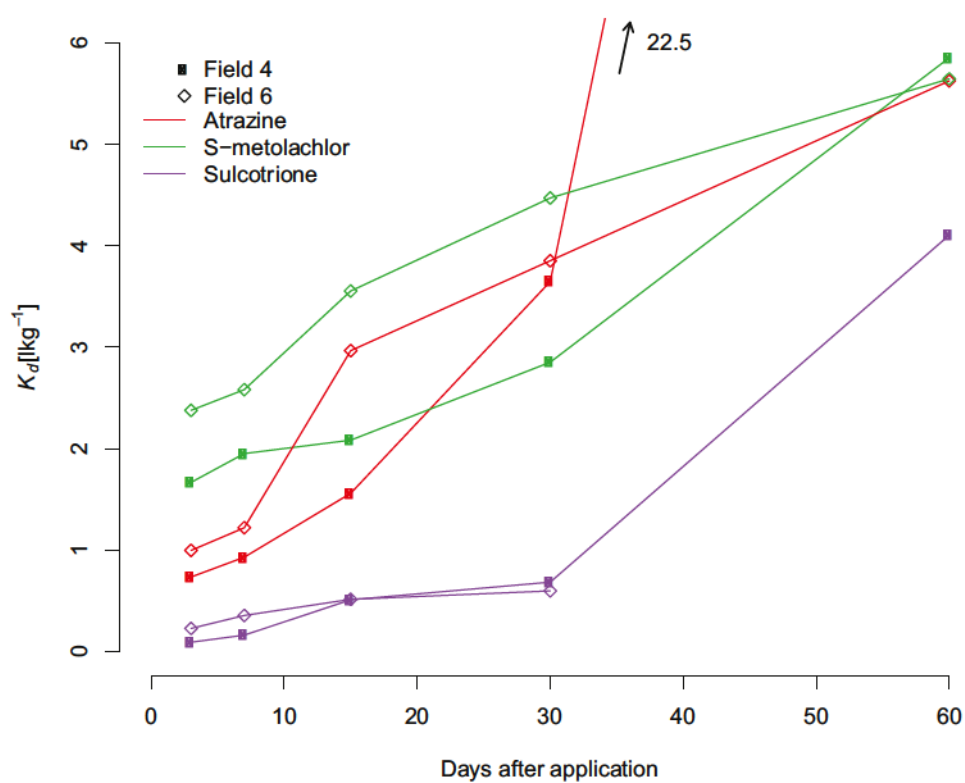
Figure A.1: K_d values for three substances on two experimental fields over two month after application. K_d of atrazine on field 4 at day 60 is 22.5 l kg^{-1}; pore water concentration of sulcotrione on field 6 at day 60 was below detection limit.
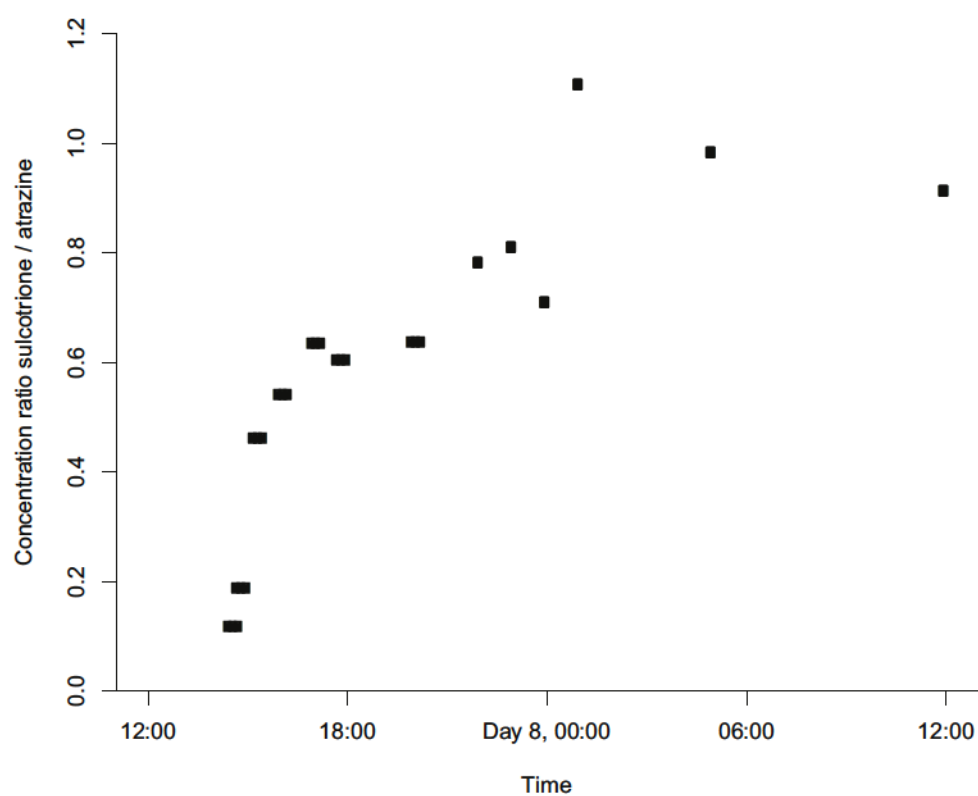
Figure A.2: Concentration ratio sulcotrione / atrazine at station O_u during event E2 (26 June 2009, seven days after application).

Supporting information for chapter 3

Calculation of field specific loads from the subcatchment loads

$$
\begin{aligned}
L_1 &= L_{O_u} \\
L_4 &= L_{S_u} \\
L_2 &= L_{O_m} - L_{O_u} \\
L_3 &= L_{S_d} - L_{S_u} \\
L_{5,6} &= L_{O_d} - L_{O_m} - L_{S_d}
\end{aligned} \tag{A.1}
$$

with L_1, L_2, L_3 and L_4 being the loads from fields 1 to 4, $L_{5,6}$ is the combined load from fields 5 and 6 which can not be separated. L_{O_u}, L_{O_m}, L_{O_d}, L_{S_u} and L_{S_d} are the subcatchment loads at the specified sampling stations (see Fig. 3.1).

Spatial variability of loss rates of S-metolachlor and sulcotrione
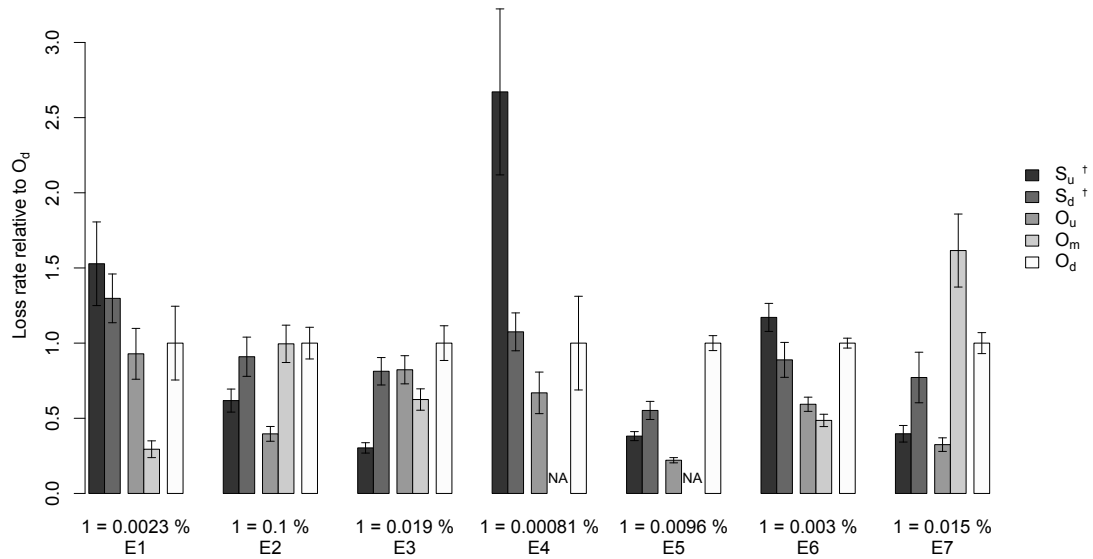
Figure A.3: Spatial variability of S-metolachlor loss rates in the seven sampled events. The loss rates of the subcatchments in each event are normalized to the loss rate of the full catchment (Station O_d) in the respective event (absolute values above event number). NA = no samples from station O_m. † The values at stations S_u and S_d are strongly influenced by the accidental application of S-metolachlor on a sugar beet field.
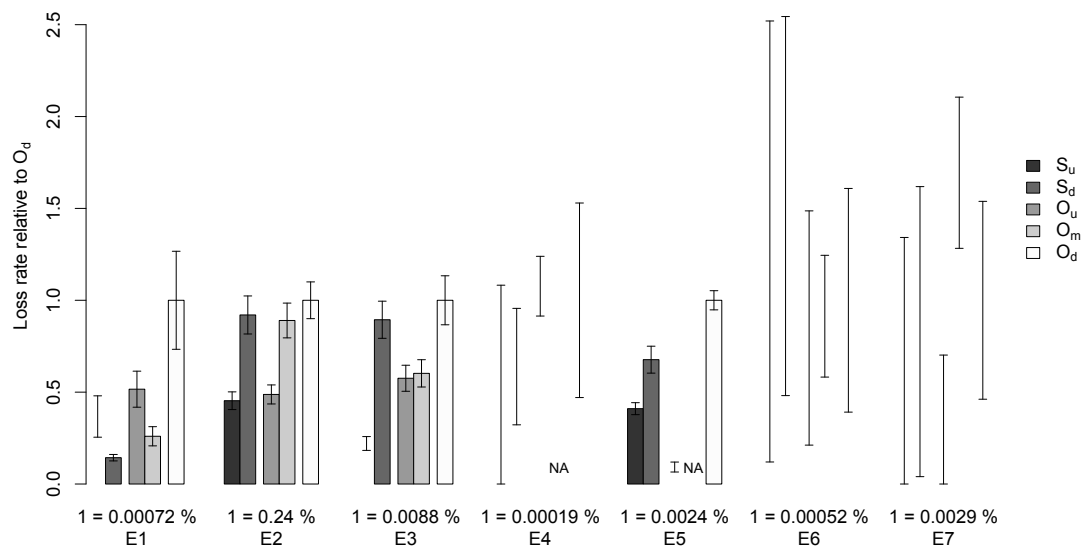
Figure A.4: Spatial variability of sulcotrione loss rates in the seven sampled events. The loss rates of the subcatchments in each event are normalized to the loss rate of the full catchment (Station O_d) in the respective event (absolute values above event number). (NA = no samples from station O_m). For situations with too many concentrations below the limit of quantification the possible ranges of loss rates are shown (see section 3.2.8)
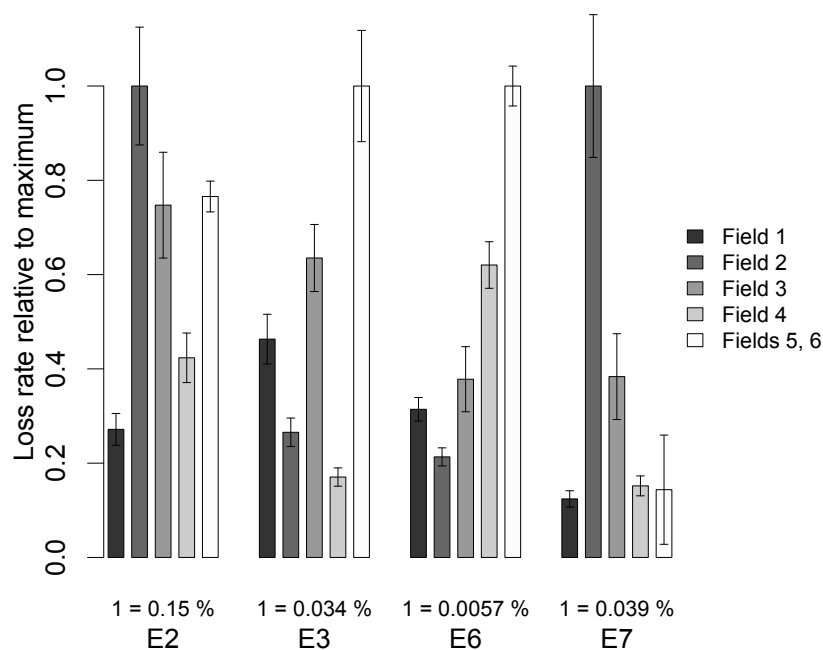
Figure A.5: Spatial variability of S-metolachlor loss rates in four events at field scale. The loss rates of the experimental fields are normalized to the loss rate of the field with the highest loss rate in the respective event (absolute values given above event number, in events E2 and E7 normalization to field 2, in E3 and E6, normalization to fields 5,6).
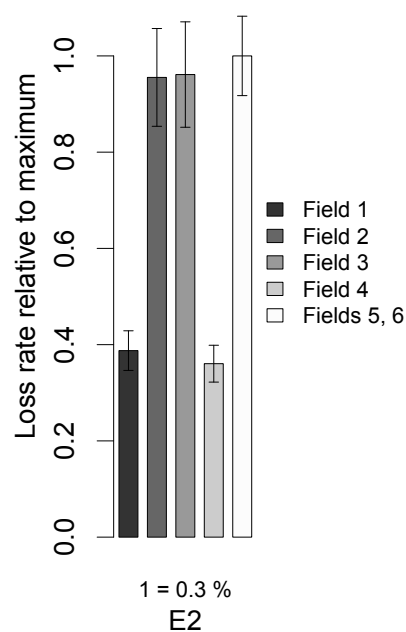
Figure A.6: Spatial variability of sulcotione loss rates in event E2 at field scale. The loss rates of the experimental fields are normalized to the loss rate of the field with the highest loss rate (fields 5, 6).

Field specific half-lives and distribution coefficients

Table A.1: Field-specific dissipation half-lives of the PLE-extractable content of the three herbicides atrazine, S-metolachlor, and sulcotrione.

Field Nr.	DT_{50} [d]		
	Atrazine	S-metolachlor	Sulcotrione
Field 1	10.7	12.7	5.6
Field 2	6.8	9.5	4.6
Field 3	9.5	12.3	5.4
Field 4	10.2	14.3	5.9
Field 5	12.2	19.4	6.5
Field 6	7.8	14.5	4.9

Table A.2: Temporal changes of field-specific apparent distribution coefficients of atrazine.

Day	K_d [L kg^{-1}]					
	Field 1	Field 2	Field 3	Field 4	Field 5	Field 6
0	0.92	1.37	0.65	1.55	1.27	1.04
3	0.88	0.47	0.60	0.63	1.00	0.91
7	1.06	0.93	0.90	1.33	1.22	0.60
15	1.82	1.56	2.20	2.21	2.97	1.41
30	5.23	3.65	6.54	5.30	3.85	1.32
60	20.67	22.52	23.22	23.05	5.63	4.04

Table A.3: Temporal changes of field-specific apparent distribution coefficients of S-metolachlor.

Day	K_d [L kg^{-1}]					
	Field 1	Field 2	Field 3	Field 4	Field 5	Field 6
0	1.84	2.21	1.37	2.60	2.30	1.79
3	2.19	1.67	1.86	1.73	2.38	2.12
7	2.30	1.95	2.00	2.64	2.58	1.38
15	2.22	2.08	2.23	2.98	3.55	2.18
30	3.94	2.85	3.51	4.23	4.47	2.30
60	7.58	5.85	9.53	8.53	5.65	4.27

Table A.4: Temporal changes of field-specific apparent distribution coefficients of sulcotrione.

Day	K_d [L kg^{-1}]					
	Field 1	Field 2	Field 3	Field 4	Field 5	Field 6
0	0.10	0.21	-0.10 †	0.07	0.19	0.14
3	0.18	0.09	-0.09 †	-0.01 †	0.23	0.19
7	0.19	0.16	0.09	0.19	0.36	0.07
15	0.46	0.51	0.30	0.63	0.52	0.49
30	1.06	0.68	0.70	1.03	0.60	0.51
60	2.51	4.11	2.60	2.50	< LOQ	0.01

†: The negative values are artifacts of the measurement uncertainties: with little sorption occurring the concentrations measured in the PLE extracts (C_{PLE}) and in the pore water ($C_{porewater}$) are very similar. Due to the uncertainty of the analytical procedure, it may happen that experimental $C_{PLE} < C_{porewater}$ resulting in negative values for K_d according to Eq. 3.3. These negative values have not been used for further analysis of the data. LOQ: Limit of quantification.

Relationships between loss rates and field properties
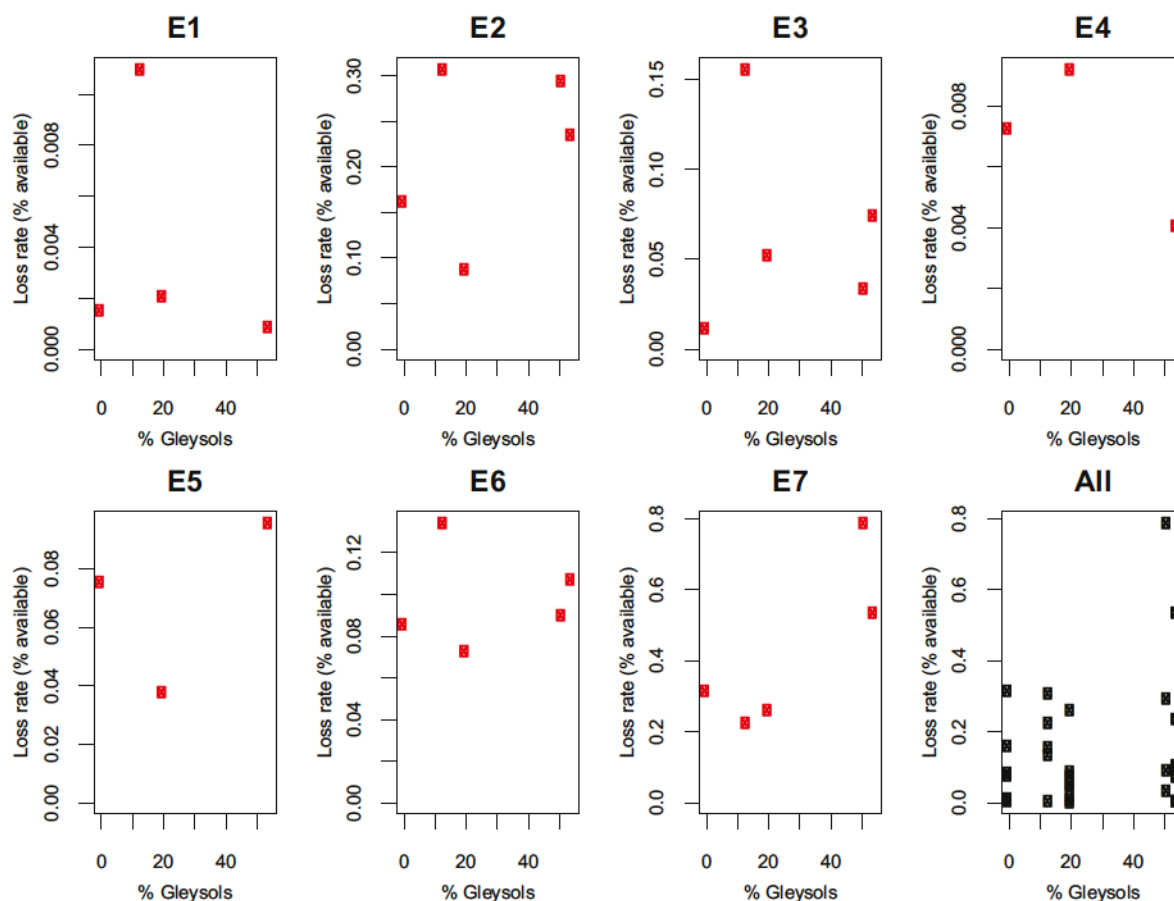
Figure A.7: Relationship between the percentage of Gleysols of each field and the observed loss rates of atrazine (expressed in percent of the available amounts) during the seven events (E1 - E7) for all fields. The black dots combine all data for all events into a single plot.
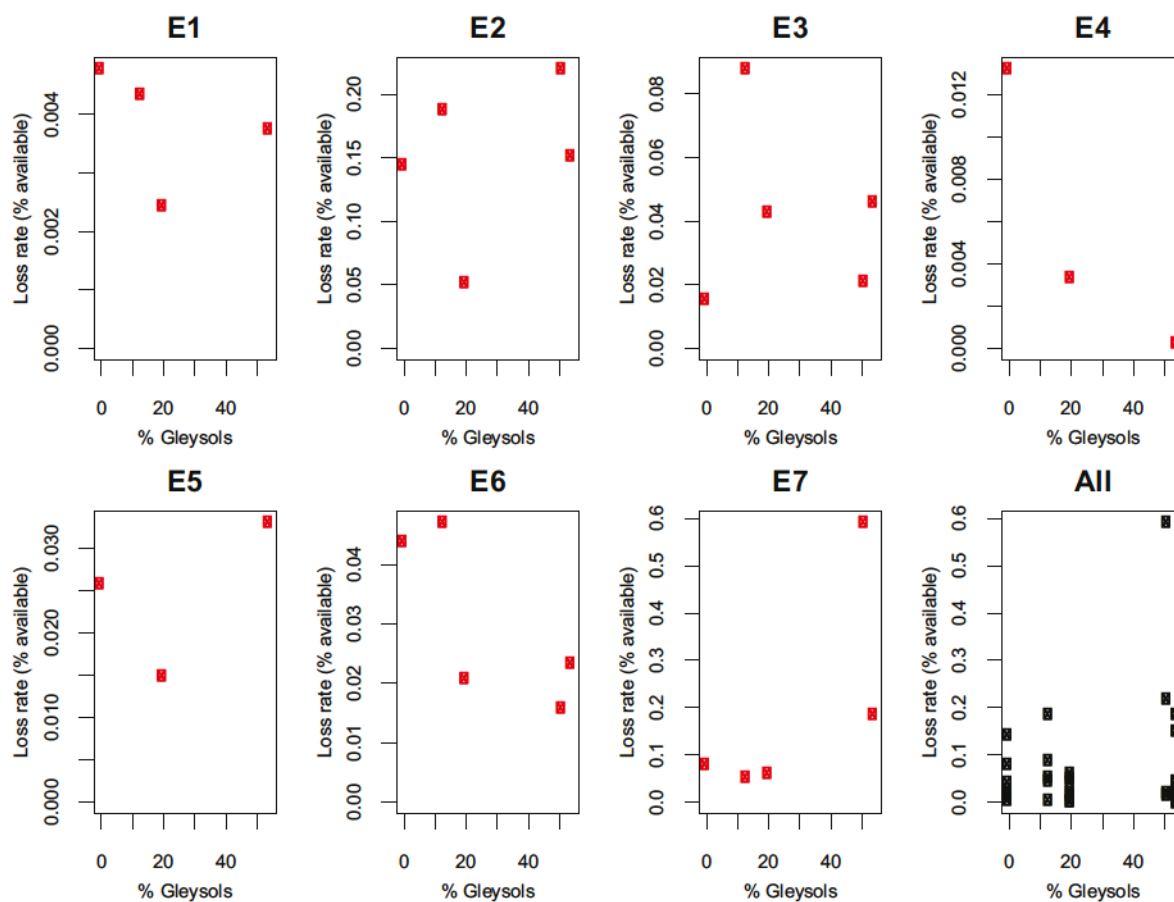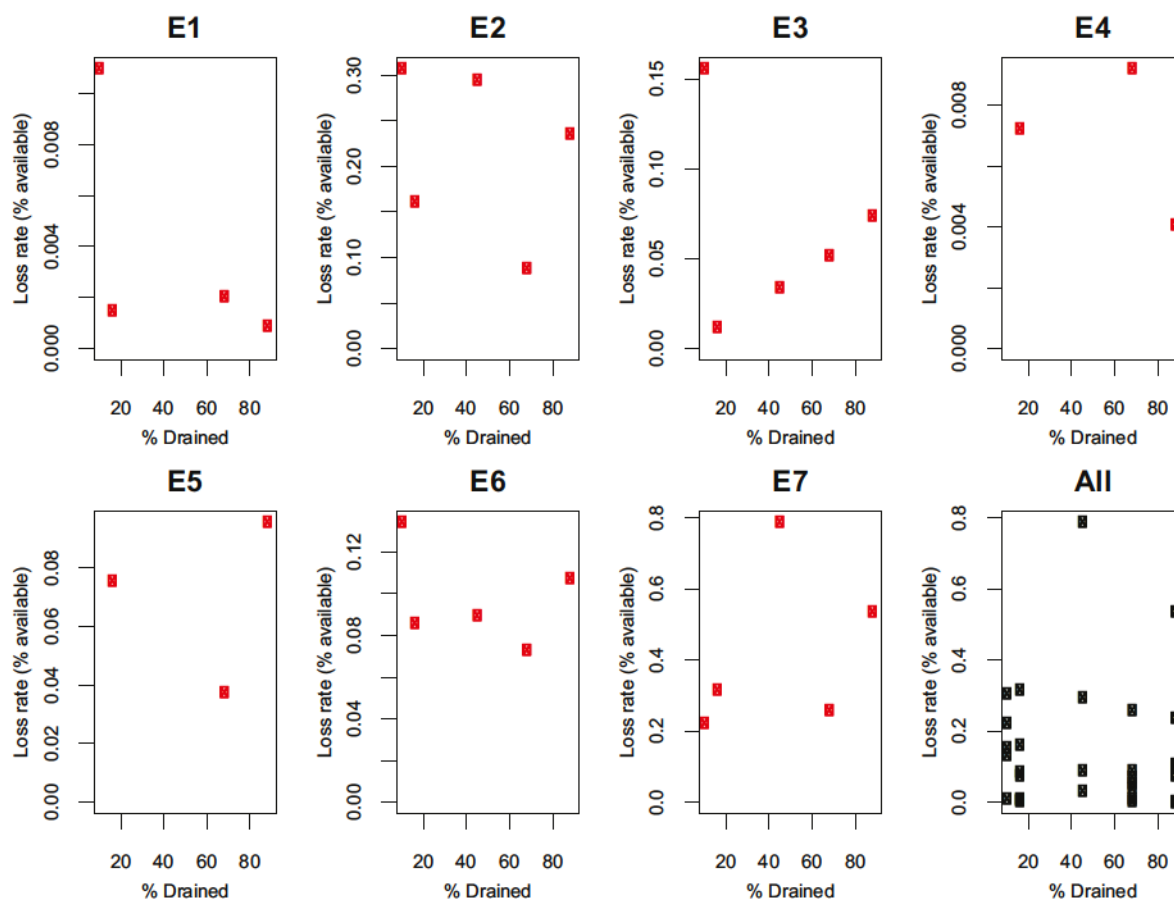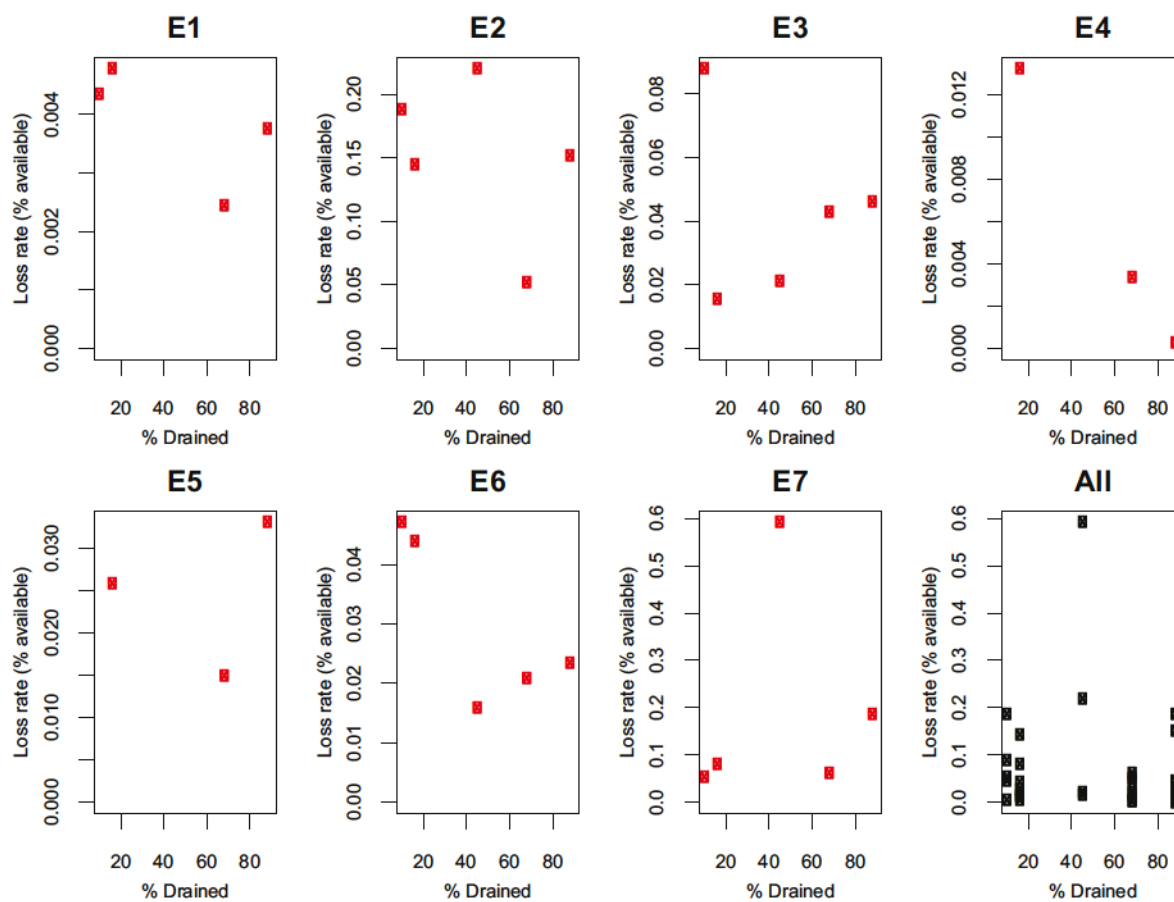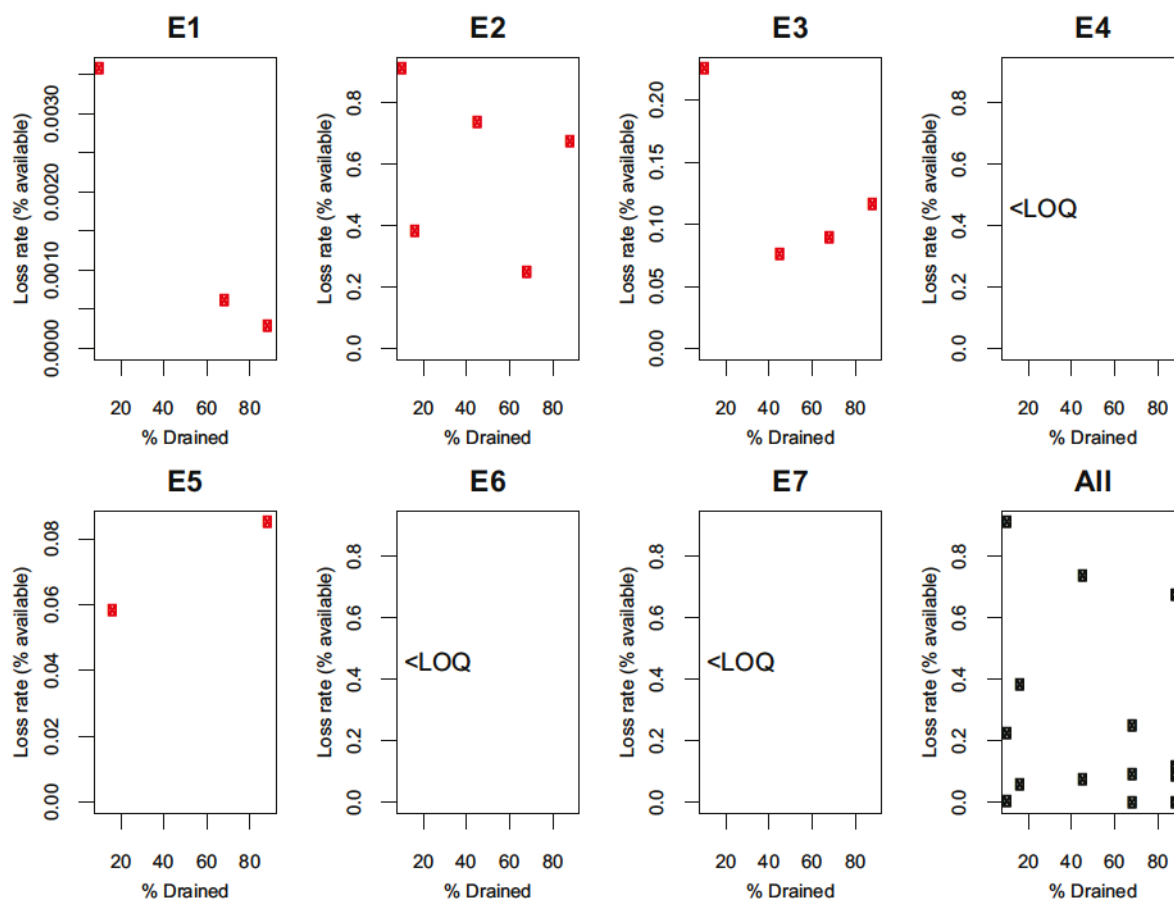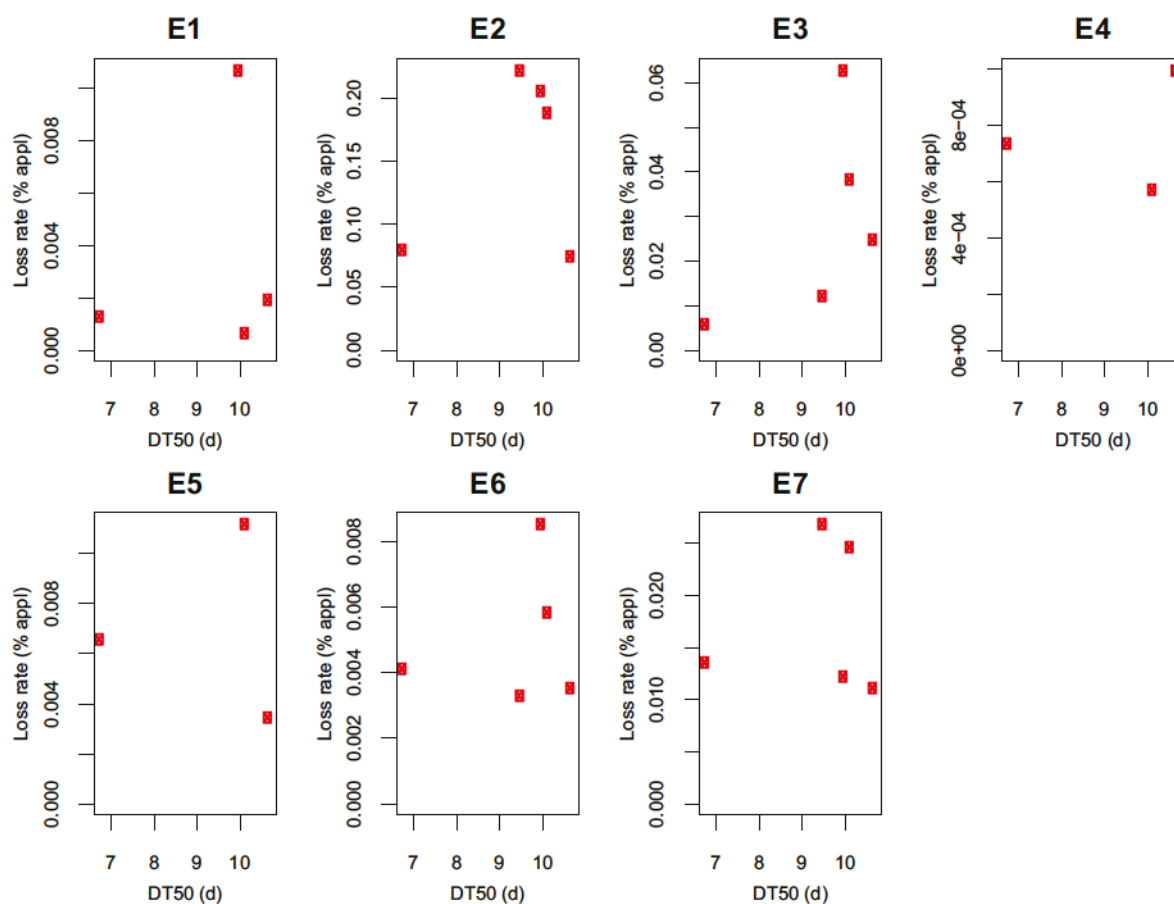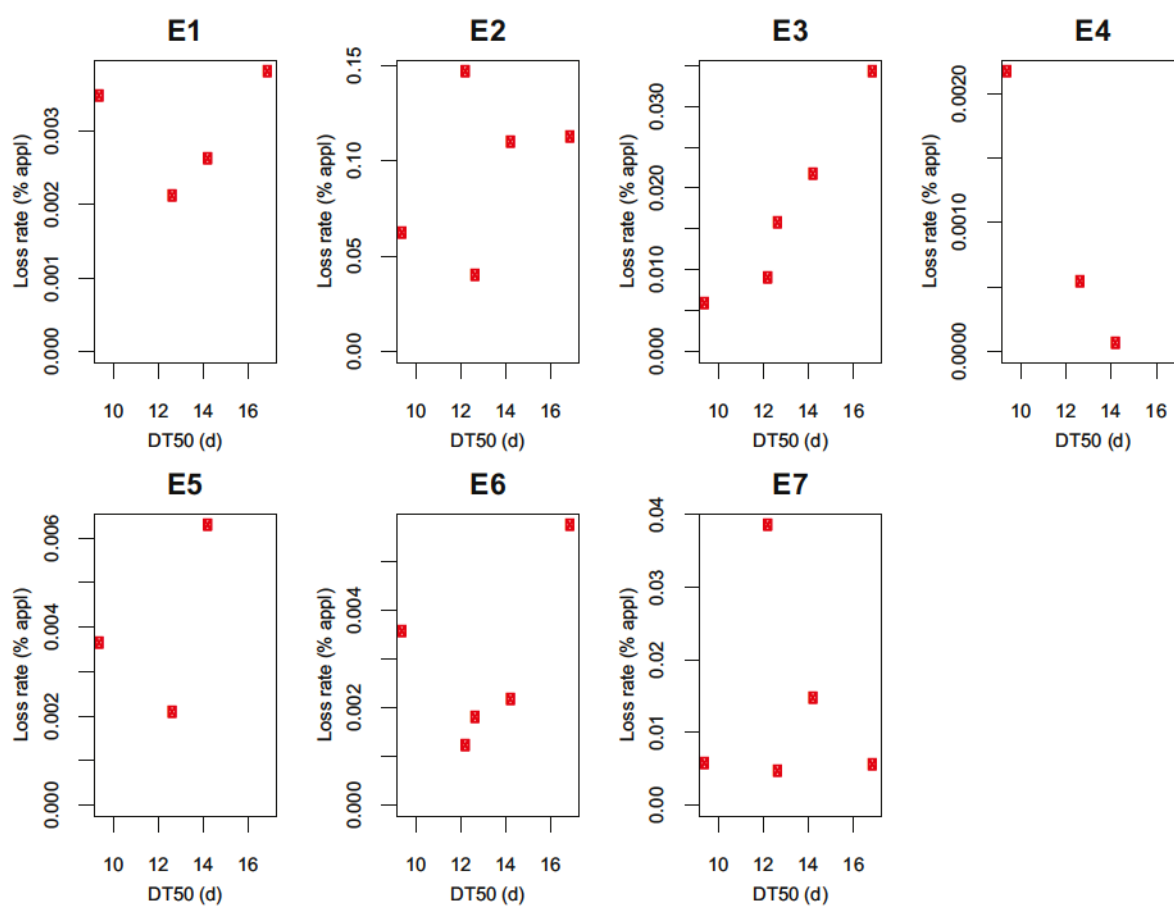
Figure A.8: Relationship between the percentage of Gleysols of each field and the observed loss rates of S-metolachlor (expressed in percent of the available amounts) during the seven events (E1 - E7) for all fields. The black dots combine all data for all events into a single plot.
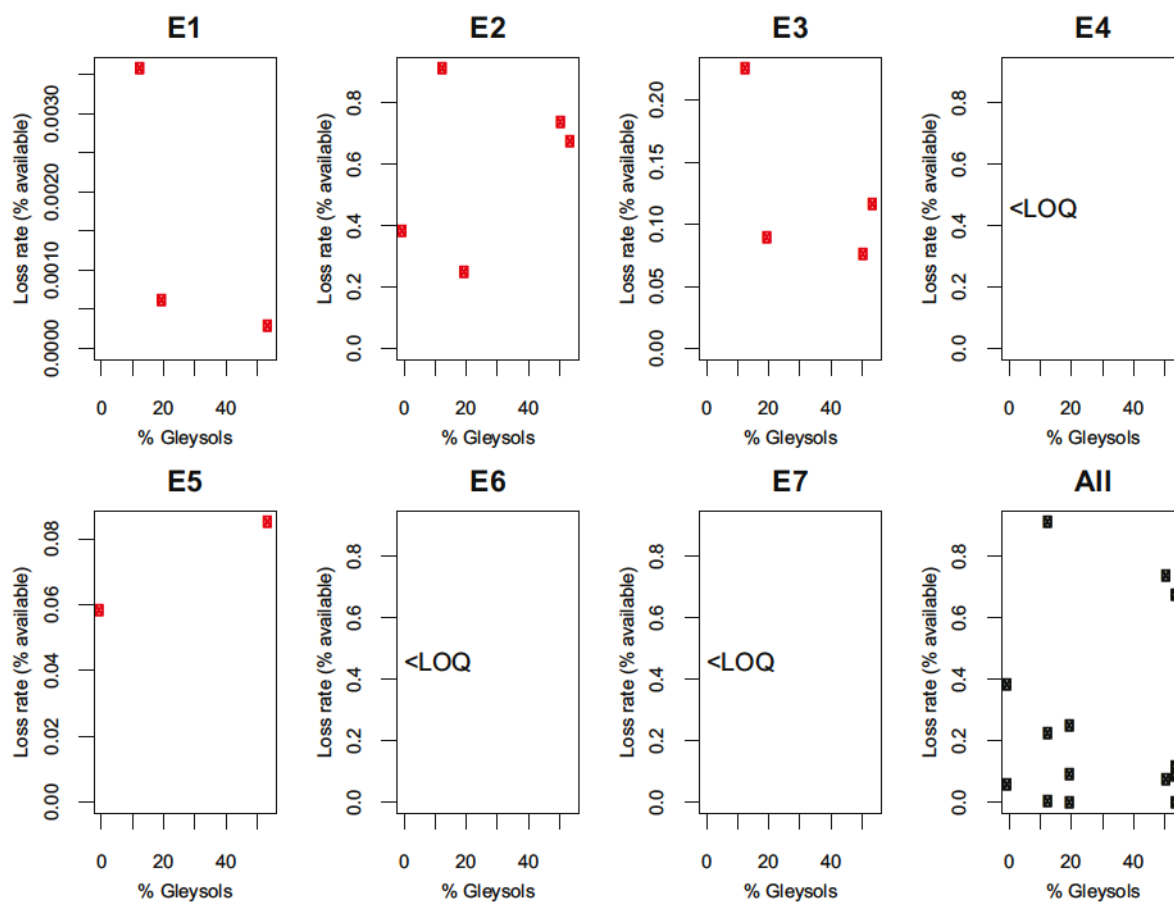
Figure A.9: Relationship between the percentage of Gleysols of each field and the observed loss rates of sulcotrione (expressed in percent of the available amounts) during the seven events (E1 - E7) for all fields. The black dots combine all data for all events into a single plot. <LOQ: no loss data because concentrations were below LOQ.
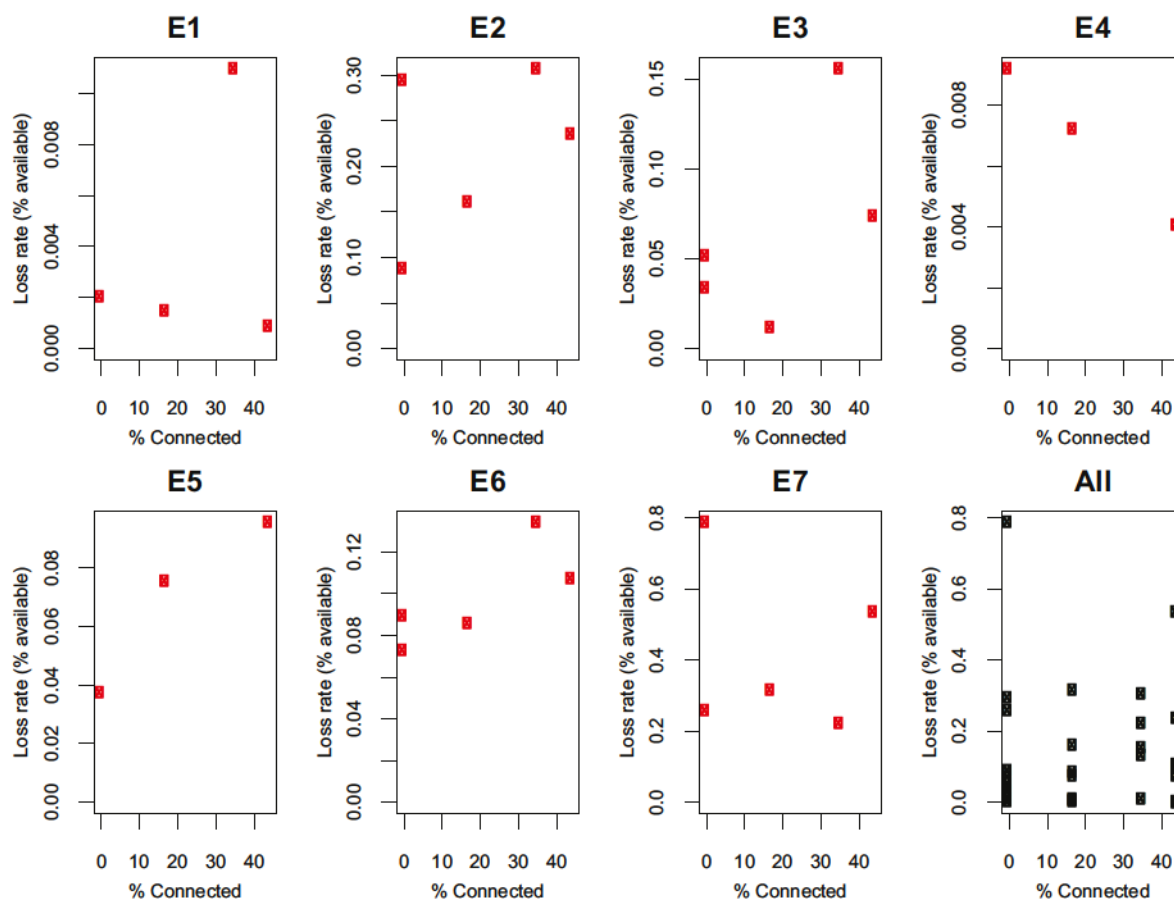
Figure A.10: Relationship between the fraction of each field that is directly (on the surface or via shortcuts) connected to the stream network and the observed loss rates of atrazine (expressed in percent of the available amounts) during the seven events (E1 - E7) for all fields. The black dots reveal the superposition of all events.
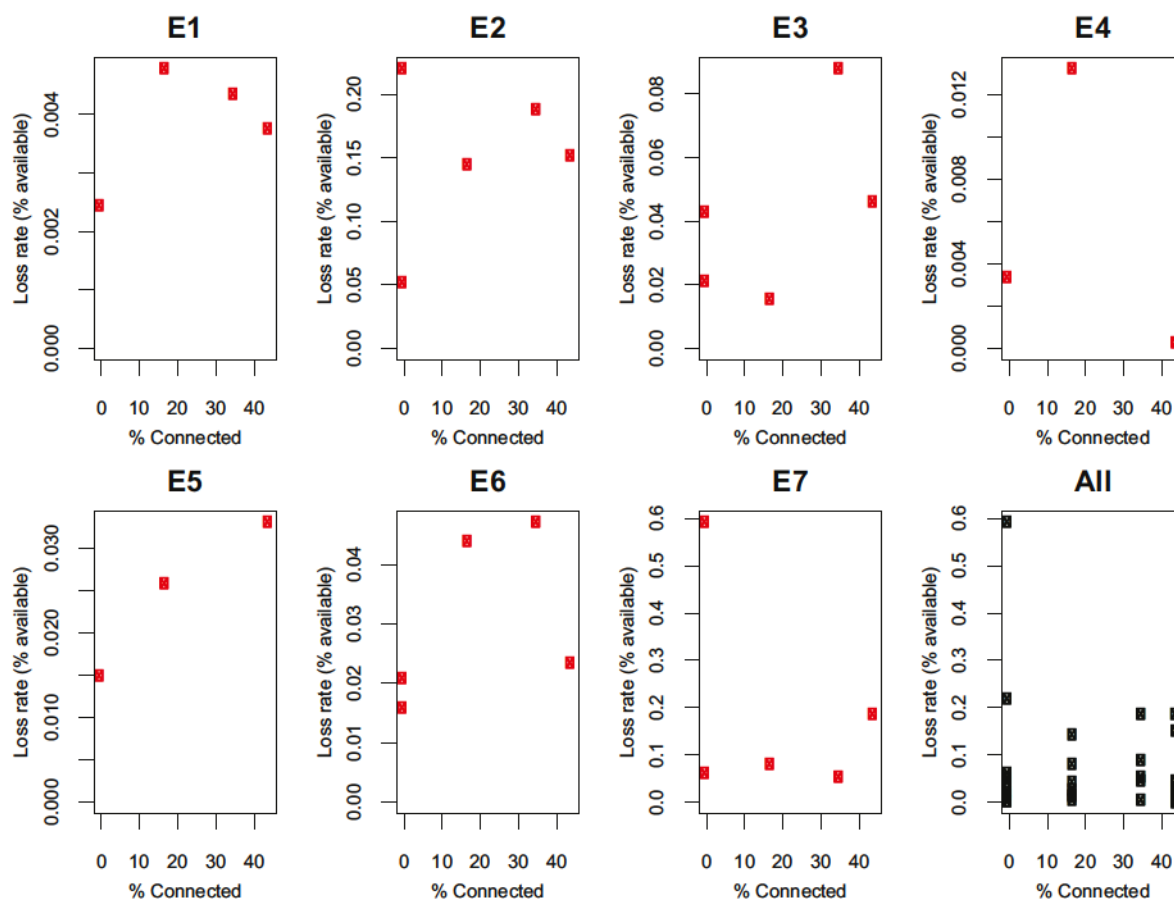
Figure A.11: Relationship between the fraction of each field that is directly (on the surface or via shortcuts) connected to the stream network and the observed loss rates of S-metolachlor (expressed in percent of the available amounts) during the seven events (E1 - E7) for all fields. The black dots reveal the superposition of all events.
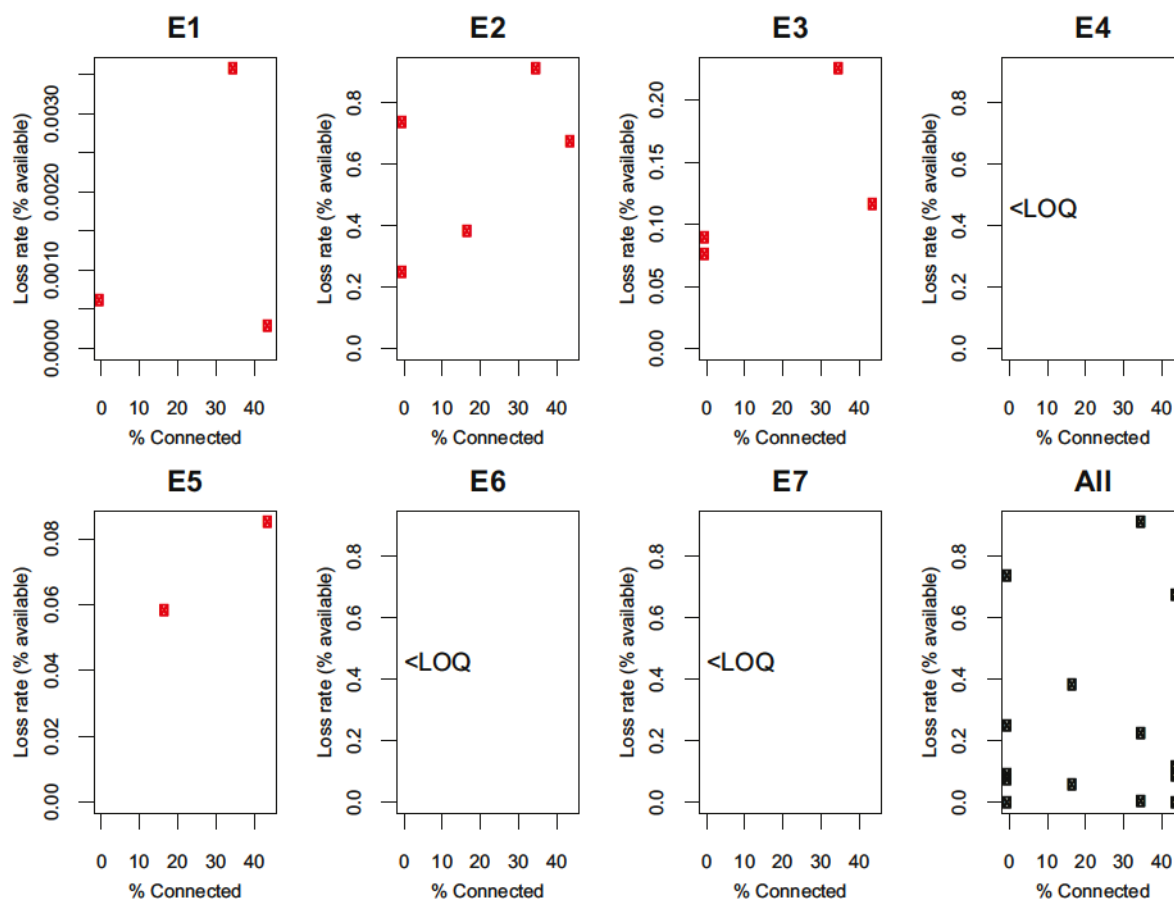
Figure A.12: Relationship between the fraction of each field that is directly (on the surface or via shortcuts) connected to the stream network and the observed loss rates of sulcotrione (expressed in percent of the available amounts) during the seven events (E1 - E7) for all fields. The black dots reveal the superposition of all events. <LOQ: no loss data because concentrations were below LOQ.

Figure A.13: Relationship between the fraction of each field that is artificially drained and the observed loss rates of atrazine (expressed in percent of the available amounts) during the seven events (E1 - E7) for all fields. The black dots reveal the superposition of all events.

Figure A.14: Relationship between the fraction of each field that is artificially drained and the observed loss rates of S-metolachlor (expressed in percent of the available amounts) during the seven events (E1 - E7) for all fields. The black dots reveal the superposition of all events.

Figure A.15: Relationship between the fraction of each field that is artificially drained and the observed loss rates of sulcotrione (expressed in percent of the available amounts) during the seven events (E1 - E7) for all fields. The black dots reveal the superposition of all events. <LOQ: no loss data because concentrations were below LOQ.

Relationships between loss rates and substance properties

Figure A.16: Relationship between the atrazin half life (DT_{50}) of each field and the observed loss rates (expressed in percent of the applied amounts) during the seven events for all fields.

Figure A.17: Relationship between the S-metolachlor half life (DT_{50}) of each field and the observed loss rates (expressed in percent of the applied amounts) during the seven events for all fields.
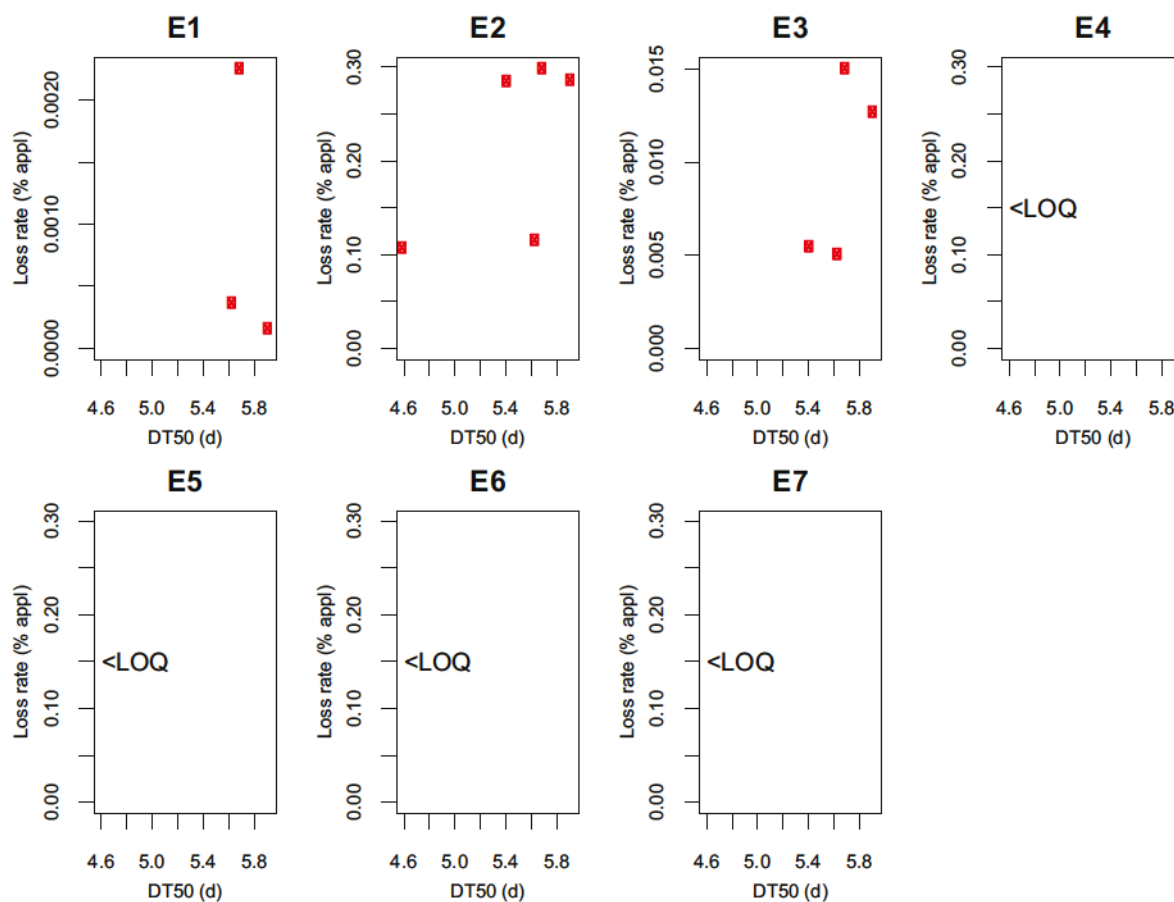
Figure A.18: Relationship between the sulcotrione half life (DT_{50}) of each field and the observed loss rates (expressed in percent of the applied amounts) during the seven events for all fields. <LOQ: loads could not be determined because the concentrations in the stream were below the limit of quantification.
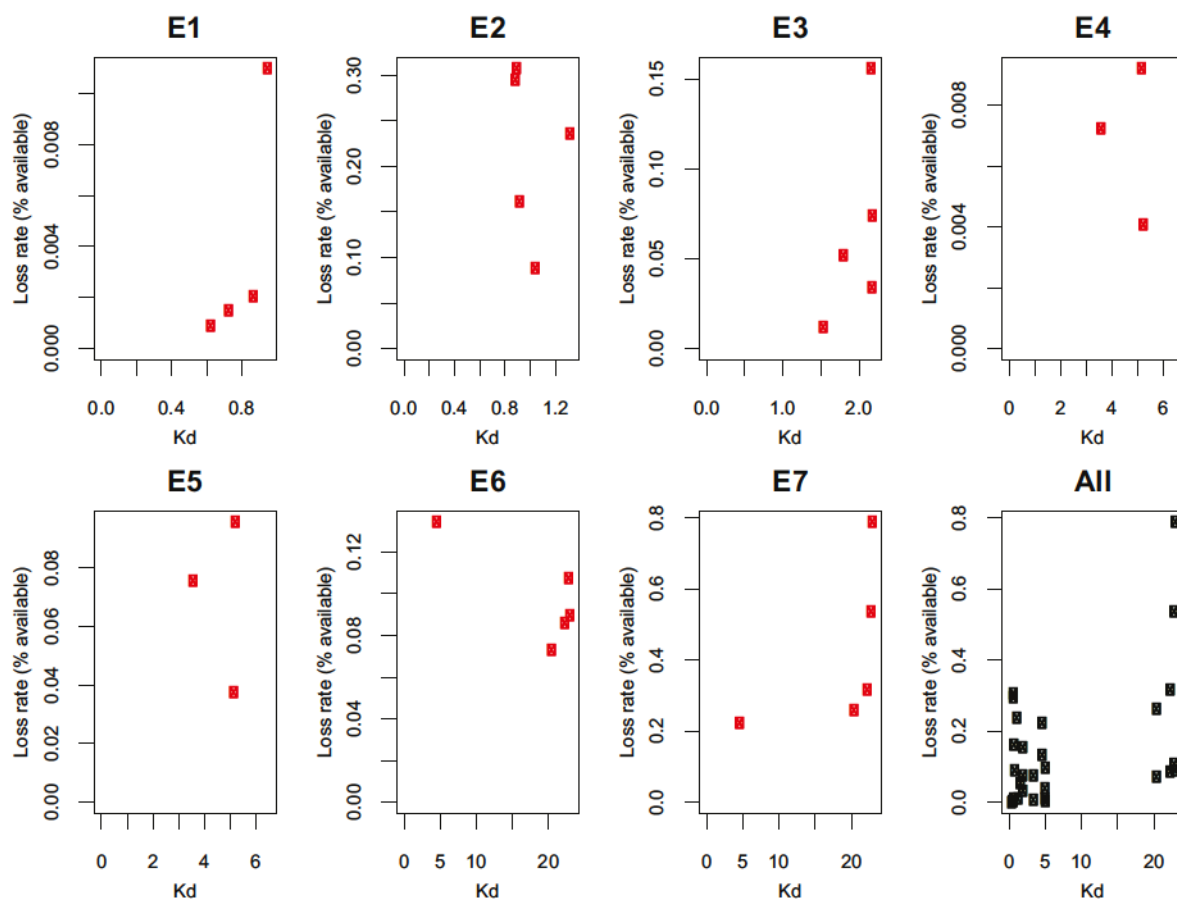
Figure A.19: Relationship between K_d values of each field for atrazine at the time of an event and the observed loss rates (expressed in percent of the available amounts) during the seven events (E1 - E7) for all fields. The black dots combine all data for all events into a single plot.
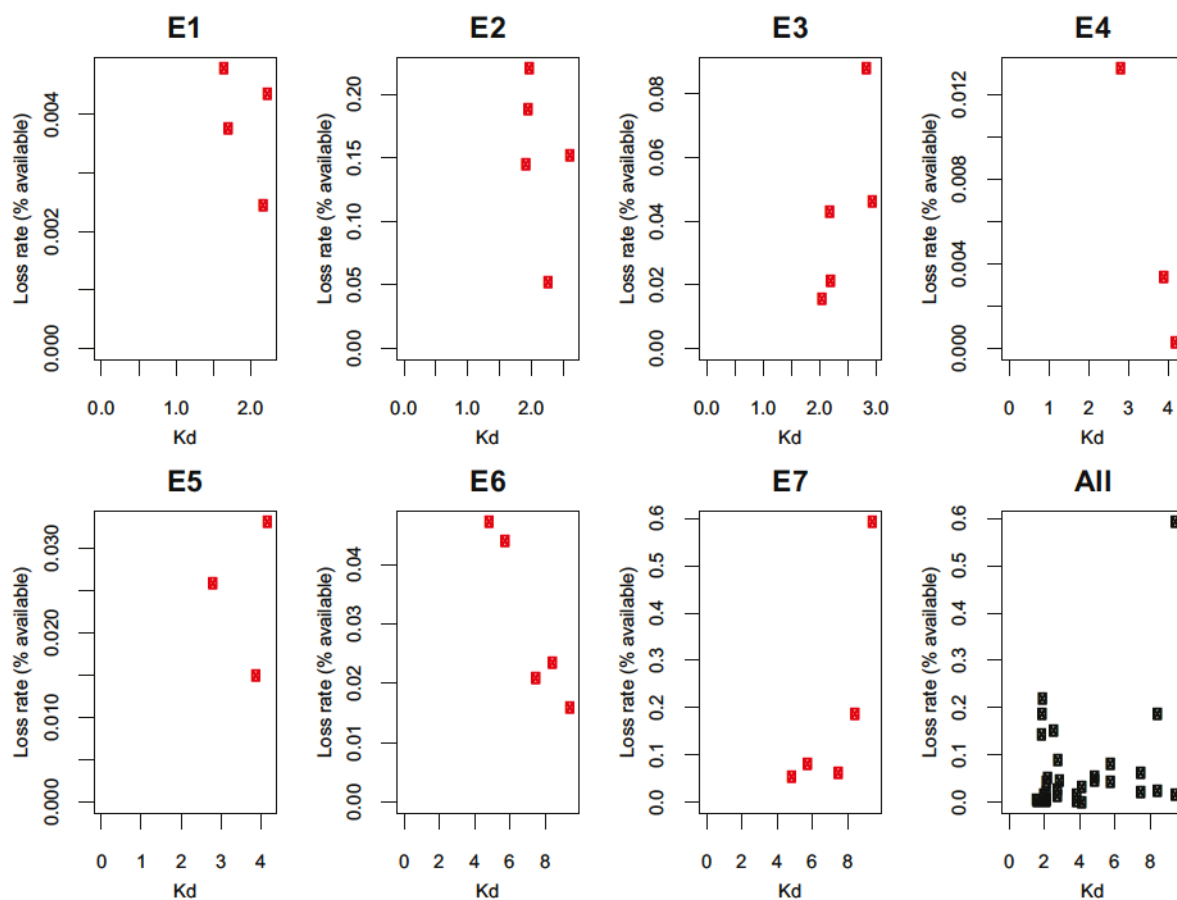
Figure A.20: Relationship between K_d values of each field for S-metolachlor at the time of an event and the observed loss rates (expressed in percent of the available amounts) during the seven events (E1 - E7) for all fields. The black dots combine all data for all events into a single plot.
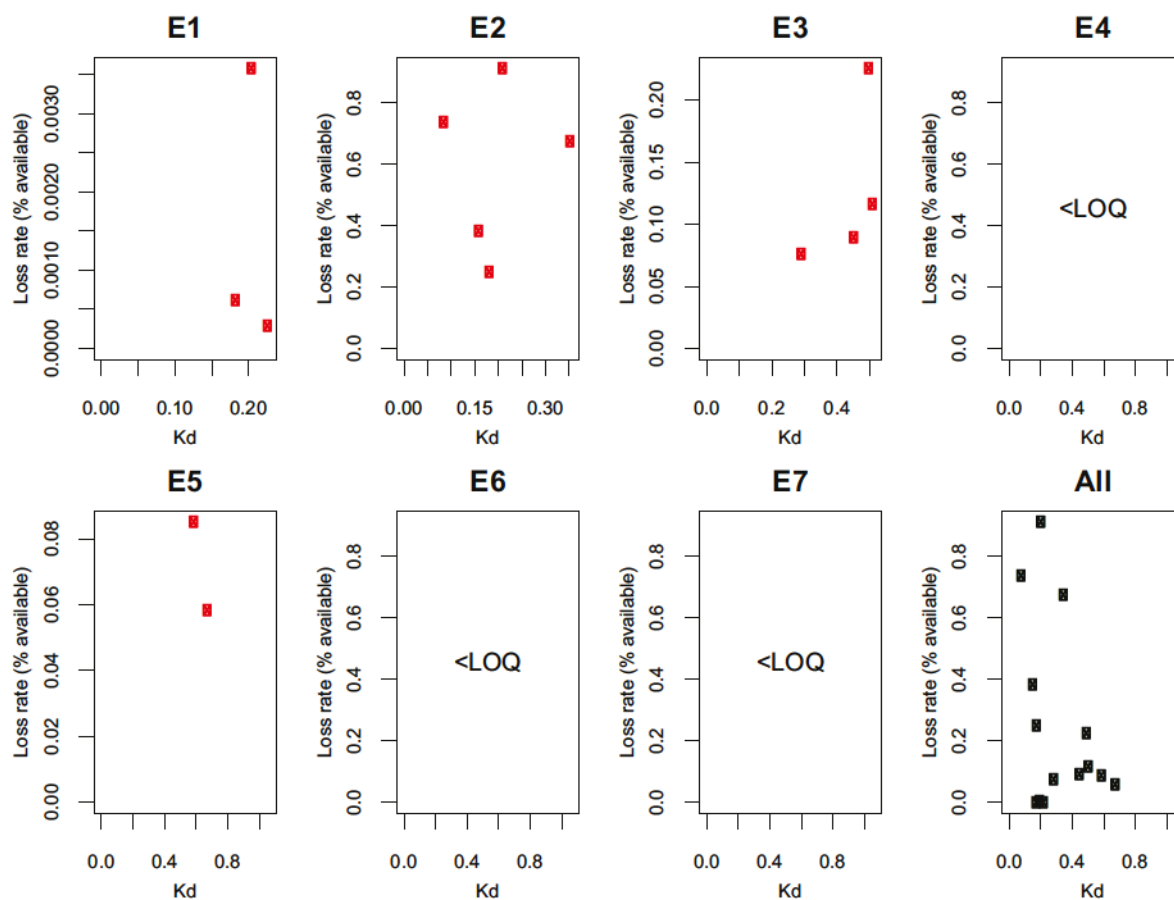
Figure A.21: Relationship between K_d values of each field for sulcotrione at the time of an event and the observed loss rates (expressed in percent of the available amounts) during the seven events (E1 - E7) for all fields. The black dots combine all data for all events into a single plot. <LOQ: no loss data because concentrations were below LOQ.

Supporting information for chapter 4

The following tables show the values of the maximum likelihood parameters. We are aware that these are effective parameters. Some of them are outside a physically meaningful range because they compensate for structural deficits in the model. The column "Calibration" indicates if a parameter was calibrated or kept fixed at a given value. The columns "min" and "max" show the minimum and maximum values of the parameters that were allowed during calibration.

Table A.5: Parameters of the paved area module.

Parameter name	Unit	Value	Calibration	min	max
$S_{\text{paved\_min}}$	mm	1.5	no	-	-
k_{paved}	h^{-1}	3.0	no	-	-
m_{paved}	-	3.5	no	-	-
paved area	m^2	18'888.5	yes	2'000	∞

Table A.6: Parameters of the unsaturated zone module. Some of the parameters of the unsaturated zone module did not differentiate into the spatially distributed unsaturated zones but remained at the value of the optimum from the calibration with the homogeneous unsaturated zone (see Sect. 4.2.5). These parameters are indicated with † in the Calibration column. The brackets indicate to which unsaturated zone the parameter belongs. [s1] to [s7] are the seven soil water regime classes, [sett] refers to settlement areas and [forest] to forested areas. [lw] indicates that all seven water regime classes share the same parameter, no indication in brackets means the same parameter for the whole unsaturated zone.

Parameter name	Unit	Value	Calibration	min	max
$S_{\text{uns\_max}}[s1]$	mm	1400.99	yes	10	5000
$S_{\text{uns\_max}}[s2]$	mm	814.819	yes †	10	5000
$S_{\text{uns\_max}}[s3]$	mm	1106.35	yes	10	5000
$S_{\text{uns\_max}}[s4]$	mm	814.819	yes †	10	5000
$S_{\text{uns\_max}}[s5]$	mm	1546.85	yes	10	5000
$S_{\text{uns\_max}}[s6]$	mm	814.819	yes †	10	5000
$S_{\text{uns\_max}}[s7]$	mm	814.819	yes †	10	5000
$S_{\text{uns\_max}}[sett]$	mm	4875.22	yes	10	5000
$S_{\text{uns\_max}}[forest]$	mm	1104.93	yes	10	5000
$fc[s1]$	-	0.670762	yes	0	1
$fc[s2]$	-	0.796285	yes	0	1
$fc[s3]$	-	0.797603	yes	0	1

Parameter name	Unit	Value	Calibration	min	max
$fc[s4]$	-	0.793688	yes	0	1
$fc[s5]$	-	0.665779	yes †	0	1
$fc[s6]$	-	0.665779	yes †	0	1
$fc[s7]$	-	0.787419	yes	0	1
$fc[sett]$	-	0.664554	yes	0	1
$fc[forest]$	-	0.781458	yes	0	1
$k_{\mathrm{uns}}[s1]$	h^{-1}	0.717911	yes †	0	1
$k_{\mathrm{uns}}[s2]$	h^{-1}	0.717911	yes †	0	1
$k_{\mathrm{uns}}[s3]$	h^{-1}	0.717911	yes †	0	1
$k_{\mathrm{uns}}[s4]$	h^{-1}	0.717911	yes †	0	1
$k_{\mathrm{uns}}[s5]$	h^{-1}	0.717911	yes †	0	1
$k_{\mathrm{uns}}[s6]$	h^{-1}	0.717911	yes †	0	1
$k_{\mathrm{uns}}[s7]$	h^{-1}	0.989107	yes	0	1
$k_{\mathrm{uns}}[sett]$	h^{-1}	0.717911	yes †	0	1
$k_{\mathrm{uns}}[forest]$	h^{-1}	0.717911	yes †	0	1
$k_{\mathrm{pref}}[s1]$	-	0.880871	yes †	0	1
$k_{\mathrm{pref}}[s2]$	-	0.880871	yes †	0	1
$k_{\mathrm{pref}}[s3]$	-	0.880871	yes †	0	1
$k_{\mathrm{pref}}[s4]$	-	0.880871	yes †	0	1
$k_{\mathrm{pref}}[s5]$	-	0.880871	yes †	0	1
$k_{\mathrm{pref}}[s6]$	-	0.880871	yes †	0	1
$k_{\mathrm{pref}}[s7]$	-	0.880871	yes †	0	1
$k_{\mathrm{pref}}[sett]$	-	0.880871	yes †	0	1
$k_{\mathrm{pref}}[forest]$	-	0.880871	yes †	0	1
$e_{\mathrm{pref}}[s1]$	-	2.43903	yes	1	5
$e_{\mathrm{pref}}[s2]$	-	4.90072	yes	1	5
$e_{\mathrm{pref}}[s3]$	-	2.70257	yes	1	5
$e_{\mathrm{pref}}[s4]$	-	1.99827	yes †	1	5
$e_{\mathrm{pref}}[s5]$	-	1.99827	yes †	1	5
$e_{\mathrm{pref}}[s6]$	-	1.99827	yes †	1	5
$e_{\mathrm{pref}}[s7]$	-	1.99827	yes †	1	5
$e_{\mathrm{pref}}[sett]$	-	4.73838	yes	1	5
$e_{\mathrm{pref}}[forest]$	-	4.99867	yes	1	5

Parameter name	Unit	Value	Calibration	min	max
$k_{\mathrm{et}}[s1]$	-	0.87514	yes †	0	1
$k_{\mathrm{et}}[s2]$	-	0.87514	yes †	0	1
$k_{\mathrm{et}}[s3]$	-	0.87514	yes †	0	1
$k_{\mathrm{et}}[s4]$	-	0.87514	yes †	0	1
$k_{\mathrm{et}}[s5]$	-	0.87514	yes †	0	1
$k_{\mathrm{et}}[s6]$	-	0.87514	yes †	0	1
$k_{\mathrm{et}}[s7]$	-	0.963509	yes	0	1
$k_{\mathrm{et}}[sett]$	-	0.87514	yes †	0	1
$k_{\mathrm{et}}[forest]$	-	0.87514	yes †	0	1
$\mu_0[lw]$	$h^{-1}K^{-1}$	0.000824	yes †	10^{-7}	1
$\mu_0[sett]$	$h^{-1}K^{-1}$	0.0001	no	-	-
$\mu_0[forest]$	$h^{-1}K^{-1}$	0.000824	yes †	10^{-7}	1
$T_0[lw]$	K	10.425	yes	0	15
$T_0[sett]$	K	5.0	no	-	-
$T_0[forest]$	K	12.1983	yes	0	15
$m_{\mathrm{uns\_max}}[lw]$	-	1.01632	yes	1	20
$m_{\mathrm{uns\_max}}[sett]$	-	3.0	no	-	-
$m_{\mathrm{uns\_max}}[forest]$	-	1.42395	yes	1	20
k_{decay}	$h^{-1}K^{-1}$	0.00001	no	-	-
$m_{\mathrm{uns\_min}}$	-	0.5	no	-	-
Initial state of S_{uns}					
$S_{\mathrm{uns\_init}}[s1]$	-	0.498083	yes	0	1
$S_{\mathrm{uns\_init}}[s2]$	-	0.415475	yes	0	1
$S_{\mathrm{uns\_init}}[s3]$	-	0.654671	yes	0	1
$S_{\mathrm{uns\_init}}[s4]$	-	0.414843	yes †	0	1
$S_{\mathrm{uns\_init}}[s5]$	-	0.593526	yes	0	1
$S_{\mathrm{uns\_init}}[s6]$	-	0.891386	yes	0	1
$S_{\mathrm{uns\_init}}[s7]$	-	0.414843	yes †	0	1
$S_{\mathrm{uns\_init}}[sett]$	-	0.965453	yes	0	1
$S_{\mathrm{uns\_init}}[forest]$	-	0.63688	yes	0	1

Table A.7: Parameters of the saturated zone module.

Parameter name	Unit	Value	Calibration	min	max
m_{sat}	-	1.0	no	-	-
K_{sat}	$m\,h^{-1}$	0.002386	yes	0	∞
r_{dr}	-	4.32867	yes	0	7
m_{dr}	-	4.32867	yes	1	6
p_{eff}	-	0.1089	yes	0	1
Sp_{dr}	m	17	no	-	-
Draindepth	m	1.5	no	-	-
Initial state of groundwater level					
Shift from initial groundwater map	m	-0.47762	yes	-2	2

Table A.8: Parameters of the calibration. These are the standard deviations at the measurement locations used for calibration (see Sect. 4.2.5). Theoretically these are measurement errors. However in reality they certainly include model errors.

Parameter name	Unit	Value	Calibration	min	max
$\sigma[Piezo1]$	m	0.371875	yes	0.05	2.5
$\sigma[Piezo2]$	m	0.406586	yes	0.05	2.5
$\sigma[Piezo3]$	m	0.107557	yes	0.05	2.5
$\sigma[Piezo4]$	m	0.059275	yes	0.05	2.5
$\sigma[Piezo5]$	m	0.757373	yes	0.05	2.5
$\sigma[Piezo6]$	m	0.668431	yes	0.05	2.5
$\sigma[Piezo7]$	m	0.736764	yes	0.05	2.5
$\sigma[Piezo8]$	m	0.159669	yes	0.05	2.5
$\sigma[Piezo9]$	m	0.411092	yes	0.05	2.5
$\sigma[Piezo10]$	m	0.94531	yes	0.05	2.5
$\sigma[Piezo11]$	m	1.40036	yes	0.05	2.5
$\sigma[Qtransformed]$	$(l\,s^{-1})^{1/3}$	0.411153	yes	0.05	2.5

Acknowledgement